National Development Plan 2007 - 2013

Environmental Protection Agency
An Ghníomhaireacht um Chaomhnú Comhshaoil

Environmental Research Centre
Report Series No. 18

Water Quality and the Water Framework Directive – Neuro-Fuzzy Models for Use in River Basin Direct Management

STRIVE

Environmental Protection Agency Programme

2007-2013

Strategy for Science, Technology and Innovation

Comhshaol, Oidhreacht agus Rialtas Áitiúil
Environment, Heritage and Local Government

Environmental Protection Agency

The Environmental Protection Agency (EPA) is a statutory body responsible for protecting the environment in Ireland. We regulate and police activities that might otherwise cause pollution. We ensure there is solid information on environmental trends so that necessary actions are taken. Our priorities are protecting the Irish environment and ensuring that development is sustainable.

The EPA is an independent public body established in July 1993 under the Environmental Protection Agency Act, 1992. Its sponsor in Government is the Department of the Environment, Heritage and Local Government.

OUR RESPONSIBILITIES

LICENSING

We license the following to ensure that their emissions do not endanger human health or harm the environment:

- waste facilities (e.g., landfills, incinerators, waste transfer stations);
- large scale industrial activities (e.g., pharmaceutical manufacturing, cement manufacturing, power plants);
- intensive agriculture;
- the contained use and controlled release of Genetically Modified Organisms (GMOs);
- large petrol storage facilities.
- Waste water discharges

NATIONAL ENVIRONMENTAL ENFORCEMENT

- Conducting over 2,000 audits and inspections of EPA licensed facilities every year.
- Overseeing local authorities' environmental protection responsibilities in the areas of - air, noise, waste, waste-water and water quality.
- Working with local authorities and the Gardaí to stamp out illegal waste activity by co-ordinating a national enforcement network, targeting offenders, conducting investigations and overseeing remediation.
- Prosecuting those who flout environmental law and damage the environment as a result of their actions.

MONITORING, ANALYSING AND REPORTING ON THE ENVIRONMENT

- Monitoring air quality and the quality of rivers, lakes, tidal waters and ground waters; measuring water levels and river flows.
- Independent reporting to inform decision making by national and local government.

REGULATING IRELAND'S GREENHOUSE GAS EMISSIONS

- Quantifying Ireland's emissions of greenhouse gases in the context of our Kyoto commitments.
- Implementing the Emissions Trading Directive, involving over 100 companies who are major generators of carbon dioxide in Ireland.

ENVIRONMENTAL RESEARCH AND DEVELOPMENT

- Co-ordinating research on environmental issues (including air and water quality, climate change, biodiversity, environmental technologies).

STRATEGIC ENVIRONMENTAL ASSESSMENT

- Assessing the impact of plans and programmes on the Irish environment (such as waste management and development plans).

ENVIRONMENTAL PLANNING, EDUCATION AND GUIDANCE

- Providing guidance to the public and to industry on various environmental topics (including licence applications, waste prevention and environmental regulations).
- Generating greater environmental awareness (through environmental television programmes and primary and secondary schools' resource packs).

PROACTIVE WASTE MANAGEMENT

- Promoting waste prevention and minimisation projects through the co-ordination of the National Waste Prevention Programme, including input into the implementation of Producer Responsibility Initiatives.
- Enforcing Regulations such as Waste Electrical and Electronic Equipment (WEEE) and Restriction of Hazardous Substances (RoHS) and substances that deplete the ozone layer.
- Developing a National Hazardous Waste Management Plan to prevent and manage hazardous waste.

MANAGEMENT AND STRUCTURE OF THE EPA

The organisation is managed by a full time Board, consisting of a Director General and four Directors.

The work of the EPA is carried out across four offices:

- Office of Climate, Licensing and Resource Use
- Office of Environmental Enforcement
- Office of Environmental Assessment
- Office of Communications and Corporate Services

The EPA is assisted by an Advisory Committee of twelve members who meet several times a year to discuss issues of concern and offer advice to the Board.

Environmental Research Centre 2007–2013

Water Quality and The Water Framework Directive – Neuro-Fuzzy Models for Use in River Basin District Management

(2005-FS5-GIS-7)

Environmental Research Centre Report

Prepared for the Environmental Protection Agency

by

Centre for Water Resources Research, University College Dublin

Authors:

Ahmed Elssidig Nasr and Michael Bruen

ENVIRONMENTAL PROTECTION AGENCY
An Ghníomhaireacht um Chaomhnú Comhshaoil
PO Box 3000, Johnstown Castle, Co.Wexford, Ireland

Telephone: +353 53 916 0600 Fax: +353 53 916 0699 LoCall: 1890 33 55 99
Email: info@epa.ie Website: www.epa.ie

ACKNOWLEDGEMENTS

This report is published as part of the Science, Technology, Research and Innovation for the Environment (STRIVE) Programme 2007–2013. The programme is financed by the Irish Government under the National Development Plan 2007–2013. It is administered on behalf of the Department of the Environment, Heritage and Local Government by the Environmental Protection Agency which has the statutory function of co-ordinating and promoting environmental research.

The authors would like to acknowledge the EPA for the financial support and for making its GIS database available to the study. Mrs Fiona O'Rourke of the Reporting and Information Section in Office of Environmental Assessment of the EPA is particularly acknowledged for facilitating the delivery of the GIS data. A number of organisations are also acknowledged for providing the data of the catchments used in the study. These include Teagasc, the Three Rivers Project, and the Lough Derg/ Lough Ree project for providing data from the 84 catchments used in testing the neuro-fuzzy national P mode. The data of the 11 catchments from around the world used in testing the ANFISP model was collected by the Department of Engineering Hydrology of University College Galway through a series of International Flood Forecasting Workshops organised by the department and funded by the Department of Foreign Affairs in Ireland. The Oona Catchment data was collected by Dr Phil Jordan of the University of Ulster in Northern Ireland as part of the LS 2.2. EPA-funded project.

The contribution of Dr Karen Daly of Teagasc in providing data to test the neuro-fuzzy approach to developing a national P model is gratefully acknowledged.

ENVIRONMENTAL RESEARCH CENTRE PROGRAMME 2007-2013

Published by the Environmental Protection Agency, Ireland

ISBN: 978-1-84095-389-3
Price: Free **Online version**

Details of Project Partners

Ahmed Elssidig Nasr
(1) Centre for Water Resources Research
School of Architecture, Landscape, and Civil Engineering
University College Dublin
Newstead Building
Belfield
Dublin 4
Ireland
Tel.: +353 1 716 3228
Email: Ahmed.Nasr@ucd.ie

(2) School of Civil and Building Services Engineering
College Of Engineering and Built Environment
Dublin Institute of Technology
Bolton Street
Dublin 1
Tel.: +353 1 402 2933
Email: ahmed.nasr@dit.ie

Michael Bruen
Centre for Water Resources Research
School of Architecture, Landscape, and Civil Engineering
University College Dublin
Newstead Building
Belfield
Dublin 4
Tel.: +353 1 716 3212
Email: Michael.Bruen@ucd.ie

Table of Contents

Acknowledgements **ii**

Disclaimer **ii**

Details of Project Partners **iii**

Executive Summary **vii**

1 Introduction **1**

1.1 Background 1

1.2 Water Framework Directive Modelling Efforts 1

1.3 Objectives of the Study 3

1.4 Methodology 3

1.5 Organisation of the Report 4

2 Fuzzy Logic Modelling Approach **5**

2.1 Introduction 5

2.2 Background on Fuzzy Set Theory 5

2.3 Fuzzy Modelling 7

2.4 Partitioning of the Input and Output Variables Space 7

2.5 Neuro-Fuzzy Model 8

2.6 Adaptive Neuro-Fuzzy Inference System (ANFIS) 9

2.7 Review of Previous Applications of Fuzzy Methods in Hydrologic-Related Studies 10

2.8 Conclusions 14

3 Adapative Neuro-Fuzzy Inference System Phosphorus (ANFISP) Model **15**

3.1 Introduction 15

3.2 Conceptual Representation of the ANFISP Model 16

3.3 The ANFISP Model 18

3.4 The Soil Moisture Accounting and Routing Model 18

3.5 The Simple Linear Reservoir Model 20

3.6 The Grid Oriented Phosphorus Component Model 21

3.7 The SWAT Model 23

3.8 Application of the ANFISP Model 24

3.9 Hydrological Component of the ANFISP Model 24
3.10 Phosphorus Component of the ANFISP Model 39
3.11 Conclusion 47

4 Neuro-Fuzzy National Phosphorus Model 49

4.1 Introduction 49
4.2 Literature Review 49
4.3 Estimation of Nutrients Loads using Catchment Characteristics 51
4.4 Newly Developed Neuro-Fuzzy National Phosphorus Model 52
4.5 ***k***-Means Clustering Algorithm 53
4.6 Application of the Neuro-Fuzzy National Phosphorus Model 54
4.7 Variables of the Neuro-Fuzzy National Phosphorus Model 56
4.8 Formulation of Different Neuro-Fuzzy National Phosphorus Models 57
4.9 Results 58
4.10 Discussion 65
4.11 Conclusions 68

5 Conclusions and Recommendations 69

5.1 Overview 69
5.2 ANFISP Model 69
5.3 The Neuro-Fuzzy National Phosphorus Model 70
5.4 Future Work 71

References 72

Acronyms and Annotations 76

Appendix: Published Papers or in Preparation 78

Executive Summary

Tackling the problem of eutrophication in fresh waters is at the top of the agenda for the implementation of the Water Framework Directive (WFD) in Ireland. One major pressure is phosphorus loading from diffuse sources. Therefore, there is a need to apply appropriate measures to reduce the diffuse phosphorus pollution at a catchment scale in many river basin districts (RBDs). As implementing these measures disturbs the existing system in the catchment, it is important to be able to predict their impact. This requires the use of a *reliable* mathematical model to represent the system. Catchment models have become an essential component of sustainable ecosystems modelling and are now used in a much wider range of socio-economic ecologic applications. This study contributes to this subject by developing a state-of-the-art adaptive neuro-fuzzy inference system (ANFIS) based on a suite of two new diffuse phosphorus (P) models: (i) the adaptive neuro-fuzzy inference system phosphorus (ANFISP) model and (ii) the neuro-fuzzy national P model.

ANFISP Model

The ANFISP model simulates the hydrological and water-quality variables involved in diffuse-source P modelling using the soil moisture accounting and routing (SMAR) model for discharges and the grid oriented phosphorus component (GOPC) model for the mobilisation and transport processes of diffuse-source P. The development of the ANFISP model was conducted in two stages: (i) flow modelling and (ii) phosphorus modelling.

Flow Modelling of ANFISP Model

First, the hydrological component was developed and its performance was assessed. It accounts for the effects of changes in flows with location and time. To examine changes with time, rainfall and evaporation in 11 catchments around the world (including the Brosna catchment in Ireland) were investigated. Changes with location were modelled by first dividing the catchments into smaller sub-units and then determining the flows in each. In all cases, the performance of the SMAR model within the ANFISP model was assessed by comparing it with alternative models. There was a significant improvement as a result of adopting a fuzzy logic (FL) modelling. The improvements were mostly due to improved modelling of changes with time; and the remainder of the work concentrated on this aspect of the model.

Phosphorus Modelling of ANFISP Model

The hydrological component used in the temporal scenario of the ANFISP model was extended by incorporating the GOPC model to simulate total P (TP) loads. The application of this model to the Oona Water catchment in Northern Ireland was used to assess its performance. Again, the strength of the FL modelling approach was shown clearly in the good results obtained. The ANFISP model can be applied to any gauged river catchment.

Neuro-Fuzzy National Phosphorus Model

In the second modelling approach, a neuro-fuzzy national phosphorus model was developed to provide annual estimates of the average annual orthoP concentrations, using only physical variables as inputs. This type of model can be applied to ungauged catchments where no river flow discharge and phosphorus concentrations are available. Data from 84 catchments where diffuse phosphorus pollution is dominant were used in testing the model. Six different split-sample scenarios were used to partition the total number of catchments into two parts, one to calibrate and the other to validate the model. In developing the model, the catchments were divided into two or three groups using the *k*-means clustering algorithm. This new approach produced improved results for all cases, when compared with existing empirical models. In addition, the model has benefited considerably from the inclusion of a phosphorus desorption index (PDI) and a runoff risk index (RRI) as explanatory variables.

While these models were not used in developing management plans in the first development cycle of river basin management plans for the WFD, they are now available for use as required. Typically, the national P model might be used as a screening tool to identify high-risk areas, while the ANFISP model may be used to quantify the effects of some physical variables, and their uncertainty, on the export of phosphorus from a single catchment.

1 Introduction

1.1 Background

The main activities for the implementation of the Water Framework Directive (WFD) (EEC, 2000) in Ireland are taking place in the context of river basin management projects led by local authorities. The overall objective of these projects is to develop a river basin management system, which will include a programme of measures designed to maintain and/or achieve at least good water-quality status for all waters, and to facilitate the preparations of river basin management plans.

Water quality in Ireland is generally good – it compares very favourably with other European Union (EU) member states. However, the main challenge for water quality is to deal with eutrophication arising from excess inputs of nutrients, particularly phosphorous, from point and diffuse sources. The extent of eutrophication in the river system has been increasing steadily since the 1970s and has been identified by the Environmental Protection Agency (EPA) as probably the most serious current environmental pollution problem (Lucey, 2009; Clabby et al., 2008). Therefore, a catchment-based national strategy to combat eutrophication in rivers and lakes had been adopted even before the initiation of the WFD. For instance, major catchment-based initiatives, linked to a major programme of investment in sewage infrastructure in these catchments, were carried out in respect of Loughs Derg, Ree and Leane and the Suir, Boyne and Liffey rivers. The improvements achieved in the context of these projects should be carried forward and developed in the context of river basin management projects during the implementation of the WFD.

The resources available to the local authorities to implement the proposed measures will be limited. Therefore, before implementing any measure it is vital to investigate its efficiency by predicting its expected impacts. The cost effectiveness of each measure can also be determined, helping to prioritise the measures. Mathematical models are required for this task (Irvine et al., 2005) because simulation models can apply best-available scientific knowledge, conditioned by historical evidence to predict water-quality responses to management measures. In addition, the value of a model as a simulator of the water-quality system is defined largely by the relevance, precision and quantity of the available data.

1.2 Water Framework Directive Modelling Efforts

The way in which a model is used to solve any 'real-life' problem is not unique and depends on various factors. However, Scholten et al. (2000) set guidelines for using models in the implementation of the WFD. According to these guidelines, the modellers' tasks consist of:

(i) starting with a logbook; (ii) defining the modelling project; (iii) building the model; (iv) analysing the model; (v) using the model; (vi) interpreting the results; and (vii) reporting and archiving. It is obvious that implementing these steps in river basin district (RBD) management poses a huge challenge for the water authorities. Furthermore, additional challenges come from the complexity of the ecological systems being managed and the necessity for multidisciplinary models to represent the physical, chemical, biological, geological and socio-economic subsystems in the natural river basin.

Saloranta et al. (2003) defined the WFD modelling requirements:

- Plan for actions and measures needed to obtain or maintain the good chemical and ecological status in water bodies;
- Set critical limits for parameters – for example, nutrient concentration, reflecting the good ecological status in a water body;
- Estimate the cost-effectiveness of alternative water management options or control programmes;
- Analyse the anthropogenic impact on water bodies, that is, determine the undisturbed reference conditions;
- Propose key areas where monitoring should be intensified;
- Help the process of negotiation among relevant stakeholders.

Similarly, Lindenschmidt et al. (2007) categorised these requirements into the three areas shown in Fig. 1.1. The first area of modelling is mainly concerned with defining the reference conditions for good water-quality status based on biological, physico-chemical and morphological indicators. The second is devoted to the relationship between pressures (diffuse and point-source pollution) from the land and the impact on the water-quality parameters. Finally, decision support systems are the third modelling area, which facilitate the assessment of various alternative measures and assist in making decisions about them. Up to now most modelling attempts have followed a common path – starting from area 1, passing to area 2 and then ending at area 3. However, Lindenschmidt et al. (2007) recommended the reverse path for achieving the WFD objectives more efficiently. In any of the paths, the second modelling area (which deals with the pressure-impact modelling) is common, and thus it has been the focus of most of the previous modelling work as well as the present study.

1.2.1 Pressure-Impact Modelling

The pressure-impact modelling related to eutrophication consists of two phases. The first phase is mainly concerned with estimating the nutrient loads from diffuse and point pollution sources and the second phase estimates their impact. In Ireland, nutrient loads from the latter have been reduced as a result of significant upgrading to many waste water treatment plants. However, the relative contribution of diffuse pollution sources has increased dramatically and therefore it becomes the focus of modelling attempts (e.g. Nasr and Bruen, 2006; Daly and Mills, 2006) and the current study. The estimated nutrient loads from the first phase represent inputs to the second phase of modelling where the impacts of eutrophication, such as excessive growth of planktonic algae, benthic and filamentous algae, and aquatic macrophytes, etc., are the targets. Nevertheless, ecological models dealing with the impacts of eutrophication are not well developed (Irvine et al., 2005), and further research is required to improve these models; however, this is beyond the scope of the current study.

Generally, the nutrient load from diffuse pollution sources is influenced by the anthropogenic pressures in the catchment, including excessive application of fertilisers and any of the agricultural activities which generate significant amounts of nutrients. In addition, the hydrological pathways are also important since they define the mechanisms of transporting the nutrients. Therefore, to ensure a proper estimation of diffuse nutrients loads, any model used should have components for estimating the water flows and the concentrations of chemicals in these flows. It is possible

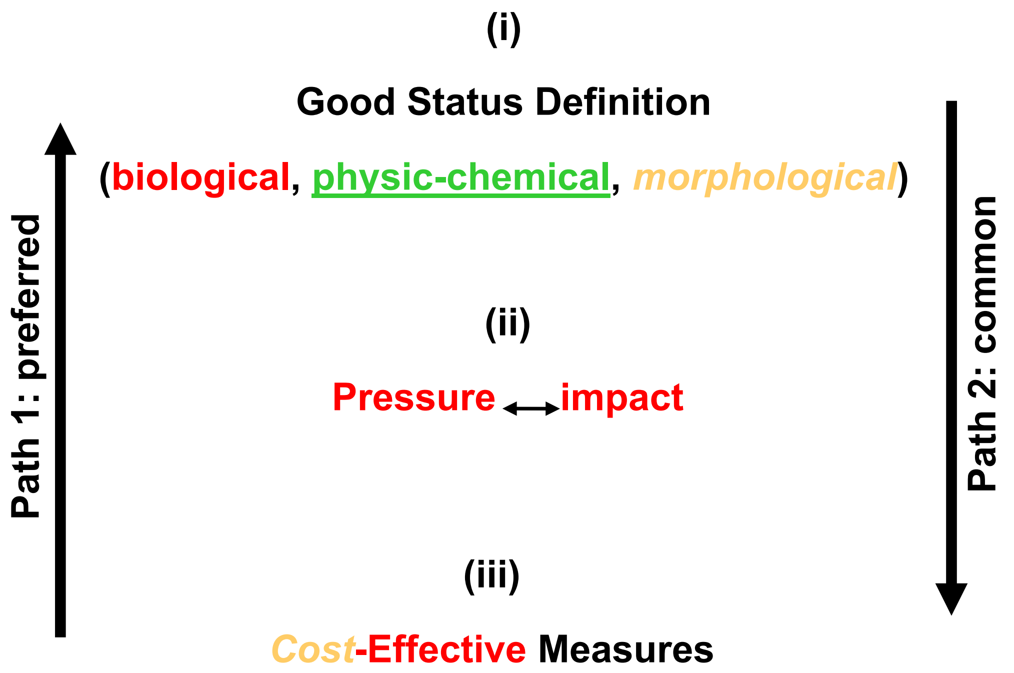

Figure 1.1. The Water Framework Directive modelling requirement.

to distinguish between two different types of model, based on the time step being used in the simulation. The first type of model provides continuous simulation, and the time step in such a model varies from one minute up to one month. On the other hand, discrete outputs can be obtained from the second (empirical, regression) types of model. Such models are often used to estimate annual loads of nutrients.

A variety of modelling techniques has been used in developing either continuous or discrete diffuse nutrient models with different degrees of spatial and physical complexity. Among these techniques are the artificial intelligence (AI) and geographic information systems (GISs), both of which have gained wide publicity among the scientific community since the 1990s. Owing to its efficiency in storing, analysing and allowing user-friendly access to spatial data, the GIS becomes an essential part of most catchment-modelling efforts. The importance of GISs has been realised since the onset of the WFD implementation, and arrangements have been put in place to build the required databases and make them available. Two main types have been used in relation to AI techniques: (i) the artificial neural networks (ANN) and (ii) fuzzy logic (FL). Most recently, the two techniques have been coupled together to form a new powerful technique called 'neuro-fuzzy modelling'. The use of neuro-fuzzy models in environmental modelling is relatively new, as can be seen from the literature review in Section 2. The approach is used here to model diffuse phosphorus pollution.

1.3 Objectives of the Study

Ireland is putting a considerable amount of effort into the current crucial phase in the WFD. The tasks in this phase are devoted to achieving two main aims: (i) identifying the measures required to restore and maintain the water-quality standards in all water bodies; and (ii) predicting the effects of applying such measures. The current study was motivated by the second aim. Hence, its main objective is to develop state-of-the-art neuro-fuzzy models for use in predicting the future impact of applying measures required by the WFD to manage diffuse phosphorus pollution.

Two separate models have been developed in the current project. The first is a physically based dynamic model of diffuse-source phosphorus contamination that can take account of input data uncertainties. This uses the adaptive neuro-fuzzy inference system (ANFIS) to represent the input variables as 'fuzzy numbers' while treating the outputs as 'crisp variables'. The resulting model is called the 'adaptive neuro-fuzzy inference system phosphorus (ANFISP)' model.

A daily time step is employed in the ANFISP model to simulate both the hydrological and water-quality processes involved in the diffuse phosphorus modelling. Two other models are used in ANFISP – (i) the soil moisture accounting and routing (SMAR) model (O'Connell et al., 1970) to simulate the hydrological processes and (ii) the grid oriented phosphorus component (GOPC) model (Nasr et al., 2005) for the phosphorus processes.

The second model uses an empirical relationship to provide estimates of average annual phosphorus concentrations using some easily measured catchment characteristics as explanatory variables. Unlike the national phosphorus model developed by Daly and Mills (2006) where a single empirical relationship is derived for the whole country, the 'neuro-fuzzy national phosphorus, (P) model'' developed in this study can classify catchments into different 'types' or 'clusters' and can have a different sub-model to represent the different behaviour typical of each cluster. The *k*-means clustering algorithm (Hartigan and Wong, 1979) is used to derive a specified number of clusters, each of which represents catchments with similar spatial characteristics. A cluster in this sense can represent a homogenous land patch which has unique catchment behaviour with respect to the diffuse transport of phosphorus and hence a separate sub-model is used to determine the amount of diffuse phosphorus loss contributed by this cluster. Then all sub-models are integrated in a neuro-fuzzy model which is built to obtain the final estimate of the average annual phosphorus concentrations.

1.4 Methodology

The ANFISP and the neuro-fuzzy national P models were developed and tested separately. For each model all computations involved were written in a FORTRAN program code, which also read the required input data and produced the targeted outputs from the model (Table 1.1).

Table 1.1. Features of the ANFISP and neuro-fuzzy national phosphorus models.

	ANFISP model	Neuro-fuzzy national phosphorus model
Time step of simulation	**Daily**	**Annual**
Input data	Rainfall Evaporation Estimated phosphorus loads to soil	Digital elevation model (DEM) Land-use map Soil map Desorption index Runoff index
Output data	Discharge Total phosphorus loads	Average annual orthoP concentrations

The ANFISP model was developed and tested in two steps. First the hydrological component, which used the SMAR model, was built and its performance tested in 11 catchments around the world, including the Brosna catchment in Ireland. Moreover, the efficiency of the SMAR model within the ANFISP model was compared with an alternative hydrological model, the simple linear reservoir (SLR) model (Nash and Foley, 1982). In the second step, the ANFISP model was extended further by incorporating the GOPC for use in modelling the diffuse phosphorus loads. The performance of the resulting model was tested in the Oona Water catchment in Northern Ireland. The soil water and assessment tool (SWAT) model (Arnold et al., 1998) was then applied to the same catchment and its results compared with those obtained from the ANFISP model.

To test the neuro-fuzzy national P model, data from 84 catchments in Ireland was used. These catchments had been previously used by Daly and Mills (2006) to test their national P model. The latter can be considered a special case of a neuro-fuzzy national P model when no clustering is used, that is the catchment is treated as a single unit. Hence, the results of this special case were compared with those from other two variants of the national P model where two and three clusters are applied respectively.

1.5 Organisation of the Report

This introductory section gives the background and objectives, and outlines the study methodology. The emphasis is on the importance of modelling the mobilisation and transportation of phosphorus pollution originating from diffuse sources since it represents a tool used in implementing the programme of measures of the WFD. It also introduces the new modelling technique which is based on the ANFIS model.

Section 2 describes in detail some of the important concepts related to the fuzzy modelling approach and also provides a thorough description of the structure of the ANFIS used in this study. It also presents a literature review of the application of fuzzy modelling in water quantity and quality studies.

The application of the ANFISP is outlined in Section 3, while Section 4 focuses on the application of the neuro-fuzzy national P model. The final section looks at the study's overall conclusions and details some recommendations for future work.

2 Fuzzy Logic Modelling Approach

2.1 Introduction

With the escalation of pressures on water resources because of the rapid increase in industrialisation and urbanisation, the implementation of river basin management plans, such as those that will be carried out as part of the WFD has become essential. Such management plans are normally developed and applied at a catchment level, and this requires the development of appropriate catchment models. In Ireland, it is envisaged that a key point in the application of catchment models is that they should be useful and relevant to management objectives, which themselves need to be well identified (Irvine et al., 2005).

The relationships between the catchment and the movement of pollutants and the response of the aquatic ecosystem to anthropogenic impacts are a fusion of very complex processes. As a result, the natural behaviour of the catchment is difficult to describe rigorously and this in turn has led to the advent of catchment models of various degrees of complexity. These models vary from simple black-box and empirical models (e.g. simple linear reservoir (SLR) model (Nash and Foley, 1982)), to medium complexity models (e.g. soil moisture and accounting routing (O'Connell et al., 1970)), to complex physically based models (e.g. Système Hydrologique Européen (SHE) model (Abbott et al., 1986a, b)).

None of these models performs consistently better in all cases. This is because of the effects of three sources of error (McIntyre and Wheater, 2004): (i) limitations of the calibration algorithm and uncertainty of the model parameters; (ii) error in the calibration data; and (iii) inadequacy of the model structure. Different measures to tackle each of these errors have been already investigated. For example, different methods for addressing uncertainties – such as the generalised likelihood uncertainty estimation (GLUE) procedure (Beven and Binley, 1992) – have been implemented as prediction tools of the data and parameter uncertainties. Likewise, Wagener and Wheater (2002) proposed a tool, based on an uncertainty analysis, to be used to suggest an appropriate structure for the model. Markov chain Monte Carlo (MCMC) methods, which incorporate sophisticated statistical inference techniques, have also been used widely to assess parameter uncertainty in various hydrological modelling applications (e.g. Fortin et al., 2004; Reis Jr and Stedinger, 2005).

Despite the progress that these measures have allowed, there is still difficulty in finding a single model that can be manipulated to work reasonably well at *all* parts of the catchment. The reason mainly stems from the catchment's heterogeneity and the dynamic process involved. One way to address this is to assign *an individual set of parameters* for each homogenous part of the catchment. Beven (1993) suggested that although distributed models have been developed to account for catchment heterogeneity and its requirements, they usually suffer from the symptom of over-parameterisation, which leads to the equifinality of parameter sets. This occurs when more than one set of parameters provides an adequate match of the model output to the calibration data. Therefore, hydrologic modellers resort to either black-box or conceptual models because of to the simplicity in calibrating their parameters. However, they lack a mechanism for considering catchment heterogeneity.

This current project proposes a new modelling approach. This attempts to improve the performance of black-box and conceptual models by using them within a framework of 'fuzzy analysis'. A neuro-fuzzy model is proposed because of its ability to combine a fuzzy inference system and a neural network optimisation algorithm in one model. Two different types of neuro-fuzzy model are developed here. As noted above, the first type can be used to model a diffuse phosphorus transport load on a daily basis (and is described in Section 3). The second performs the modelling on an annual basis and is outlined in Section 4. First, the background of fuzzy theory and how it is used for modelling purposes are explained.

2.2 Background on Fuzzy Set Theory

A crisp variable is the variable that takes on a precise value. Thus, on the basis of the Boolean set theory this variable is given a value of 1 to indicate its belonging to a certain set of objects and a value of 0 otherwise. Opposite to the crisp variable is the 'fuzzy variable', which consists of an interval of values between the minimum and maximum values the variable can take. This way, the fuzzy variable could have some degree of belonging to various sets of objects. The mathematics of the fuzzy variable is all based on the fuzzy set theory (Zadeh, 1965; Zimmermann, 1985). This theory has been introduced as a mathematical method to characterise and represent uncertainty and imprecision in data and functional relationships. Fuzzy sets are especially useful when the data is not sufficient to characterise uncertainty by means of standard statistical measures involving the estimation of probability distributions and their parameters (e.g. mean, standard deviation, etc.). The central concept of fuzzy set theory is the 'membership function'. This represents numerically the degree to which an element belongs to a set. Thus, a fuzzy set consists of a set of ordered pairs containing an element and its membership value. As Eq. 2.1 illustrates, mathematically a set is called fuzzy $\tilde{F}$ in a universe if it consists of ordered pairs such that:

$$\tilde{F} = \left\{ \left(\omega, \mu_{\tilde{F}}(\omega) \right) : \omega \in \Omega, u_{\tilde{F}}(\omega) \in [0,1] \right\}, \tag{2.1}$$

where Ω is the universal or reference space consisting of points ω_i ; $u_{\tilde{F}}(\omega)$ is the degree of membership of ω in the set $\tilde{F}$.

At every point in the interval a value (between 0 and 1) of the membership function indicates the degree of confidence one might have for that particular value of the fuzzy number (Ganoulis, 1994). To illustrate this concept, suppose flows in a river are classified into three subsets, based on flow (Q): (i) low flow, (ii) medium flow and (iii) high flow. Figure 2.1 shows three triangular membership functions for the low (u_L(Q)), medium (u_M(Q)) and high (u_H(Q)) flow subsets in a catchment. So, for example, when the value of Q is 45 m^3/sec the degrees of membership u_L(45), u_M(45), and u_H(45) are 0, 1/3, and 2/3 respectively. These values represent a measure of uncertainty when associating the flow value to each of the three subsets. The value of 0 for u_L(45) indicates that this flow value certainly does not belong

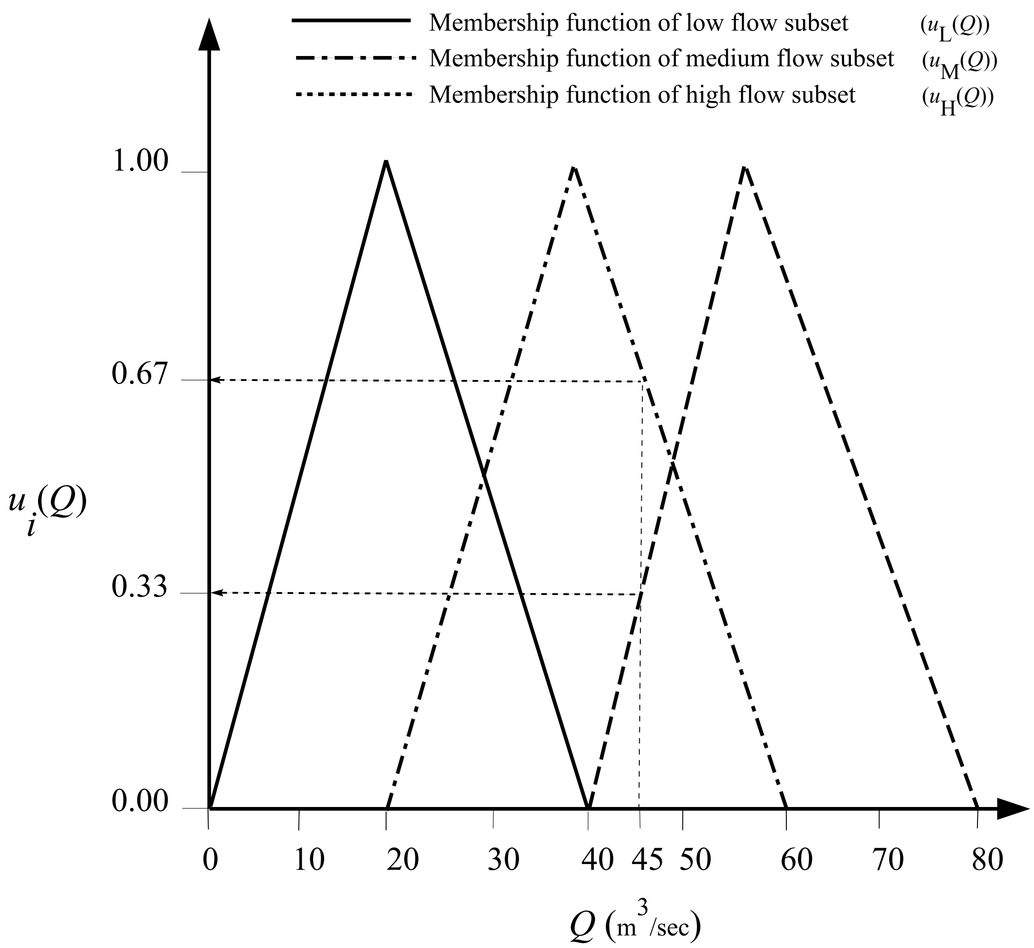

Figure 2.1. Membership functions of low, medium and high flow subsets.

to the low flow subset while the values of 1/3 and 2/3 for $u_M(45)$, and $u_H(45)$ respectively show that there is higher confidence that the flow value is in the high flow subset than the medium flow subset, although the possibility of associating it to both subsets still exists. The ability to evaluate a degree of membership of a variable to each fuzzy subset can facilitate determining a weight giving to the output of a model using this fuzzy subset as input.

Fuzzy numbers are analogous to random variables, with membership functions as crude forms of probability density functions. However, the basic rules of arithmetic of fuzzy sets are different from those of probability theory. Thorough descriptions of fuzzy arithmetic can be found in most text books about fuzzy theory and its applications (e.g. Ganoulis, 1994; Kaufmann and Gupta, 1991). However, in particular due to the 'extension principle' in fuzzy arithmetic, it is possible to calculate functions of fuzzy numbers that represent the foundation of fuzzy modelling described below.

2.3 Fuzzy Modelling

The growing interest in fuzzy modelling, commonly known as fuzzy inference systems (FIS), can be attributed to three advantages reported by Haberlandt et al. (2002): (i) the ability to work for highly non-linear processes; (ii) the transparency of the results (IF-THEN rules); and (iii) the ability of the system to include prescribed knowledge, as well as the chance of stepwise integration of more results if available. Nayak et al. (2004) attributed these advantages to the characteristic structure of fuzzy modelling that allows a non-linear mapping from input space to output space. This mapping is accomplished by a number of fuzzy IF-THEN rules, each of which describes the local behaviour of the mapping. Hence, these rules can be interpreted as a series of local models of the real system (Jacquin and Shamseldin, 2006).

The basic structure of fuzzy modelling is a rule-based or knowledge-based system consisting of three conceptual components: (i) fuzzy logic; (ii) fuzzy decision rules; and (iii) fuzzy reasoning (Jang, 1993). In contrast to the Boolean 1–0 logic, fuzzy logic permits intermediate values for any judgement statement, that is, it applies a continuous, multi-valued logic between 0 and 1 (Marce et al., 2004). Fuzzy decision rules are implemented by IF-THEN rules, each of which describes the local behaviour of the mapping. The parameters of the IF-THEN rules (referred to as 'antecedents' or 'premises' in fuzzy modelling) define a fuzzy region of the input space. The output parameters (referred to as 'consequents' in fuzzy modelling) specify the corresponding output. In the last step, fuzzy reasoning is used to derive conclusions from a set of fuzzy decision rules and it acts in this sense as an inference procedure.

The procedure for developing a fuzzy model, which has been described by different authors (e.g. Xiong et al., 2001; Haberlandt et al., 2002; Nayak et al., 2004), consists of three steps: (i) fuzzification; (ii) logic decision and (iii) defuzzification. Fuzzification involves the identification of the input variables and the control variables (i.e. outputs), the division of both the input and control variables into different domains, and the choosing of the membership functions. Logic decision involves the design of the IF-THEN inference rules, the calculation of the degree of applicability of each IF-THEN rule, and the determination of the output fuzzy set. Defuzzification involves converting the fuzzy outputs of the IF-THEN inference system into crisp output variables. Takagi and Sugeno (1985) suggested an approach where steps (ii) (logic decision) and (iii) (defuzzification) are amalgamated into one step and this approach represents an alternative to the widely used three-step Mamdani approach (Mamdani and Assilian, 1975).

2.4 Partitioning of the Input and Output Variables Space

The efficiency of any fuzzy model depends on the success in partitioning the input and output variables space correctly. Vernieuwe et al. (2005) proposed two different approaches to partitioning the rainfall and discharge space used in a rainfall–runoff fuzzy model. The first approach is 'grid partitioning' while the second is based on the fuzzy clustering algorithm.

The grid partitioning approach generally requires prior knowledge and experience to define the membership functions of all the variables. However, due to a lack of such knowledge for most of the practical applications, Vernieuwe et al. (2005) used an objective method to identify a suitable partitioning in which the variables were partitioned into a number of fuzzy sets, and the membership functions for the fuzzy sets were varied to investigate different shapes, including triangular, trapezoidal and generalised bell-shaped, and Gaussian.

Vernieuwe et al. (2005) varied the number of fuzzy sets of each variable between 2 and 5, and different combinations of these fuzzy sets were tested. For each combination, the fuzzy model was formulated in a manner similar to the adaptive neuro-fuzzy model so that the back propagation algorithm of the latter can be used to determine the parameters of the membership function. The performance of each combination was assessed on the basis of simulating discharge.

In the second approach, the idea of fuzzy clustering is used to divide the data space into fuzzy clusters, each representing one specific part of the system behaviour. After projecting the clusters onto the input space, the antecedent parts of the fuzzy rules can be found. In this way, one cluster corresponds to one rule of the fuzzy model. There are two possible ways for determining membership functions. In the first method, clusters are projected orthogonally onto the axes of the variables and the membership functions are fitted to these projections. The second method uses multidimensional variable membership functions, i.e. the fuzzy clusters are projected onto the input variables space. Using this method, the membership degree of a data point is computed directly in this projected cluster according to its distance from the projected cluster centre. Vernieuwe et al. (2005) described two fuzzy clustering methods: (i) subtractive clustering (Chiu, 1994) and (ii) the Gustafson–Kessel algorithm (Gustafson and Kessel, 1979). The former method is used in the ANFIS model developed in this study and it will be described along with the model in the next section.

2.5 Neuro-Fuzzy Model

One of the most recent advances in fuzzy modelling is the evolution of neuro-fuzzy models. These are a fusion of an artificial neural network (ANN) and fuzzy logic (FL) models. Both the ANN and FL are artificial intelligence models because they are intended to resemble the way the human brain system works. The prototype for both methods is transposed into a mathematical formulation to allow the modelling of many existing natural systems, including river basins. Generally, the FL component contains explicit information about the system that can be measured (e.g. visible properties of an object such as height, colour, etc.), while the ANN deals with implicit or derived information (e.g. the infiltration capacity of a soil) that is best determined by calibration. Thus, the knowledge in the ANN is stored in an opaque fashion whereas the FL provides a fuzzy rule base consisting of directly understandable statements in a natural language (Jantzen, 1998).

Nayak et al. (2004) describe neuro-fuzzy modelling as a way of applying various learning techniques developed in the ANN literature to FL modelling by integrating them both in a single framework. Abraham (2001) classified the degree of integration into three broad categories: (i) cooperative models, (ii) concurrent models and (iii) fully fused models.

2.5.1 Cooperative Model

In this model, the ANN learning mechanism is used to determine the FL membership functions and fuzzy rules from the training data. Thus, ANN works as a preprocessor to FL and its contribution ceases after determining the FL parameters. Membership functions of the FL are usually approximated by the training data, while each fuzzy rule is determined by a clustering approach (self-organising map) or clustering algorithm.

2.5.2 Concurrent Model

The ANN model assists FL in determining the parameters continuously. Furthermore, ANN is used to process the FL outputs if they are not directly applicable to the process.

2.5.3 Fused Model

The ANN structure and learning algorithms are used to build the FL model and determine its parameters respectively. The resulting model shares data structures and knowledge representation. The conventional learning algorithm of the ANN, the gradient descent method, cannot be applied in neuro-fuzzy modelling because of the possible non-differentiable nature of the objective functions. However, it is possible to tackle this problem by either using differentiable functions in the FL system or applying learning algorithms that do not require differentiable objective functions. A number of fused neuro-fuzzy types are available, including:

(a) Fuzzy adaptive learning control network;

(b) Adaptive neuro-fuzzy inference system (ANFIS);

(c) Generalised approximate reasoning-based intelligent control;

(d) Neuro-fuzzy control;

(e) Fuzzy inference and neural network in fuzzy inference software;

(f) Fuzzy net;

(g) Evolving fuzzy neural network;

(h) Self-constructing neural fuzzy inference network;

(i) Evolutionary design of neuro-fuzzy systems.

Among these neuro-fuzzy types, ANFIS has been used widely in hydrological applications (e.g. Chen et al., 2006; Nayak et al., 2004; Marce et al., 2004; Bazartseren et al., 2003) and hence it is employed for this study.

2.6 Adaptive Neuro-Fuzzy Inference System (ANFIS)

The ANFIS model implements the Takagi–Sugeno fuzzy approach to obtain a direct crisp value for the model output(s). The ANFIS model (Fig. 2.2) consists of five layers configured in a fashion similar to any multilayer feed-forward neural network. The first layer has a node for each of the fuzzy subsets of each input variable. Each node in this layer generates the membership grade of the fuzzy subset for the input variable. Different membership functions, such as Gaussian, generalised bell shaped, trapezoidal shaped and triangular shaped can be used. The second, third and fourth layers have equal nodes and each of these nodes corresponds to a specific IF-THEN rule. The function of each node in the second layer is to multiply the membership grades of all fuzzy subsets included in a specific IF-THEN rule to obtain the weight for this rule which will be normalised at the corresponding node in the third layer. The nodes in the fourth layer compute the contribution of each rule towards the model output(s). Each output variable is represented by a neuron in the fifth layer and this neuron computes the overall output of the ANFIS. Parameter calibration uses an optimisation method that combines least squares minimisation and a back propagation algorithm, as described by Nayak et al. (2004).

Chen et al. (2006) named the five layers of the ANFIS as (i) input nodes, (ii) rule nodes, (iii) average nodes, (iv) consequent nodes and (v) output nodes respectively. To illustrate the mathematical representation of the ANFIS, assume that there are two inputs (x and y) and one output (Z) as shown in Fig. 2.2. Moreover, assume that each input has two fuzzy subsets ($A1$ and $A2$ for x; $B1$ and $B2$ for y) and thus there are four possible combinations of fuzzy subsets, each of which is associated with an IF-THEN rule. Equations 2.5 and 2.6 can then summarise this ANFIS model.

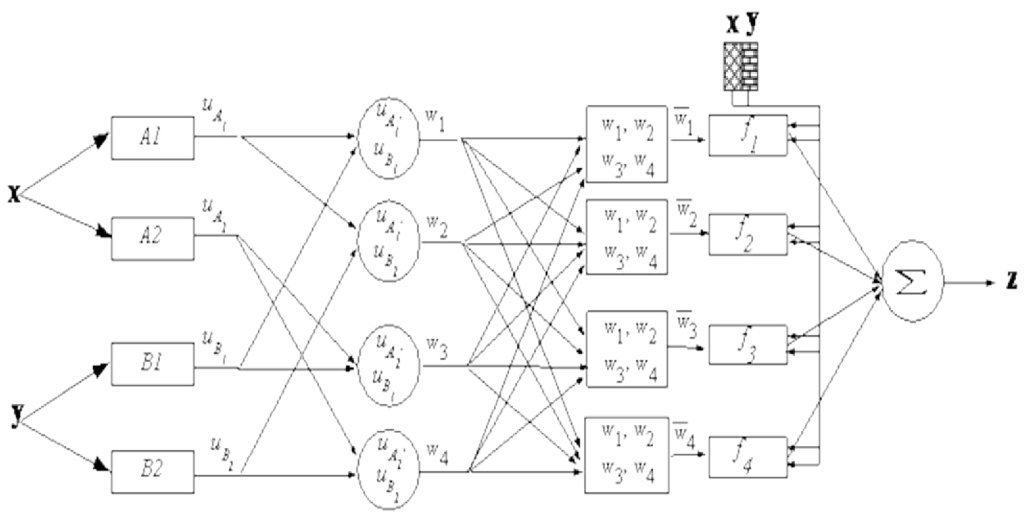

x and y: inputs; Z: output; $A1$ and $A2$: fuzzy sub-sets for *x; $B1$* and *$B2$*: fuzzy sub-sets for *y; u_{A1}* and *u_{A2}: membership functions for A1 and A2 respectively; u_{B1}* and *u_{B2}: membership functions for B1 and B2 respectively; w_m: firing strength or weight; $\overline{w}_m$: normalised weight;*
f_m: a first order Takagi–Sugeno fuzzy model; $\sum$: summation sign.

Figure 2.2. Architecture of ANFIS model.

As Eq. 2.2 shows, Layer 1 (input nodes): The outputs $O_{1,i}$ and $O_{1,i+2}$ from the nodes of this layer are:

$$\begin{aligned} O_{1,i} &= u_{Ai}(x) \\ O_{1,i+2} &= u_{Bi}(x) \end{aligned} \qquad i = 1,2\,, \tag{2.2}$$

where x and y are the crisp inputs to node i, and Ai and Bi are the linguistic labels characterised by fuzzy subsets with membership functions u_{A1} and u_{B1} respectively.

Layer 2 (rule nodes): The AND or the OR operator is applied to obtain one output that represents the result of the antecedent for that rule; i.e. firing strength or weight w_m. Hence, as Eq. 2.3 shows, the outputs of this layer $O_{2,m}$ are the product of the corresponding grades from layer 1 and this is represented as:

$$\begin{aligned} &O_{2,m} = w_m = u_{Aj}(x) \times u_{Bk}(y)\,, \\ &j,k = 1,2 \text{ and } m = 2(j-1)+k \end{aligned} \tag{2.3}$$

Layer 3 (average nodes): The normalised weights $\bar{w}_m$ are computed in this layer as the ratio of each ith rule's weight to the sum of all rules' weight. Hence, as Eq. 2.4 shows, the outputs $O_{3,m}$ of this layer are given by:

$$O_{3,m} = \bar{w}_m = \frac{w_m}{\sum_{m=1}^{4} w_m} \quad m = 1,\ldots,4 \tag{2.4}$$

Layer 4 (consequent nodes): The Takagi–Sugeno fuzzy model is used in this layer to compute the contribution of each ith rule toward the total output. Hence, as Eq. 2.5 shows, the outputs $O_{4,m}$ of this layer are:

$$O_{4m} = \bar{w}_m f_m = \bar{w}_m \left(a_{m0} + a_{m1}x + a_{m2}y\right), \; m = 1,\ldots,4 \tag{2.5}$$

where f_m is a first order Takagi–Sugeno fuzzy model and a_{m0}, a_{m1}, and a_{m2} are its coefficients.

Layer 5 (output nodes): The overall output $O_{5,1}$ is computed in this layer by summing up all the incoming signals and this represents the defuzzification process which produces a crisp output (Eq. 2.6):

$$O_{5,1} = \sum_{m=1}^{4} \bar{w}_m f_m = \frac{\sum_{m=1}^{4} w_m f_m}{\sum_{m=1}^{4} w_m} \tag{2.6}$$

2.7 Review of Previous Applications of Fuzzy Methods in Hydrologic-Related Studies

Previous applications of fuzzy methods in hydrologic-related studies can be classified into three categories. In the first category, fuzzy methods have been used in flood-prediction models of the rainfall–discharge relationship. The second category consists of fuzzy water-quality models. The third category relates to where fuzzy methods have been used to study issues related to parameter estimation, such as calibration, uncertainty analysis and sensitivity analysis. The following sections review previous studies in each of the three categories.

2.7.1 First Category: Fuzzy Modelling of Rainfall-Discharge Relationship

Jacquin and Shamseldin (2006) explored the application of Takagi–Sugeno fuzzy inference systems to rainfall–runoff modelling. Two different fuzzy models were developed to account for the non-linearity in the catchment response due to catchment wetness and seasonality. In their first model, the input to the antecedent and the consequent parts of the model consists solely of the most recently observed rainfall values. Their second type of model required only the day of the year as input to the antecedent part. To minimise the number of fuzzy rules required for the different combinations of the fuzzy subsets of the most recent rainfall values for the first type, a rainfall index with different fuzzy subsets was used as a sole input. This index was obtained from running the simple linear rainfall–runoff model of Nash and Foley (1982). For the two model types, five different consequent structures were investigated. These structures represent five different homogenous polynomial models differing in the choice of variables. The first model structure contained only a constant term while the second model structure contained only one term for the rainfall index. Jacquin and Shamseldin (2006) tested a third model structure which was a combination of the first and the second models. The variables of the fourth model structure are all terms calculated from the convolution of the observed rainfall values and the pulse response function of a conceptual gamma function (Nash) model (Nash, 1957) with a specified memory length. Finally, the fifth model structure adds a constant term to the structure of the fourth model. These models were examined using six catchments from different regions around the world. Jacquin and Shamseldin (2006) concluded that the fuzzy model Type 1 generally performed better than Type 2. Moreover, the performances of the two fuzzy models were compared with the performances of four different conventional rainfall–runoff models in the same six catchments. This comparison showed that no single best fuzzy model has emerged for all catchments.

Vernieuwe et al. (2005) investigated three different fuzzy rule-based models of the Takagi–Sugeno type relating rainfall to catchment discharge. The models differ in the methods used to partition the spaces of the input and output variables and hence the identification of the number of membership functions and their locations for each variable. The three methods include: (i) grid partitioning, (ii) subtractive fuzzy clustering and (iii) the Gustafson–Kessel clustering algorithm. Rainfall and discharge data of the River Zwalm catchment in Belgium for 1994 was used to calibrate the models while data for the period from 1995 to 1998 was used for validating the models. The three models have been compared on the basis of the results of Nash–Sutcliffe index (Nash and Sutcliffe, 1970) and the root mean square of errors. The values of the two criteria were comparable for the three models and the best values were obtained in the case of the Gustafson–Kessel clustering algorithm.

Chen et al (2006) built an adaptive neuro-fuzzy inference system (ANFIS) flood forecast model able to account for the rainfall–runoff patterns in the Choshui river in Central Taiwan. The appropriate inputs to the ANFIS were derived by analysing the available rainfall and flow data sets in the catchment. The analysis suggested that upstream flows at the study location, some of the antecedent flows for this location and the average rainfall over the catchment were the key inputs. The results were compared with a conventional back propagation neural network model and showed that the ANFIS can effectively and reliably construct an accurate flood forecasting model.

Alvisi et al. (2006) tested a neural network model and two fuzzy models, one based on the Mamdani approach (Mamdani and Assilian, 1975) and the other on the Takagi–Sugeno approach (Takagi and Sugeno, 1985), to forecast water levels in the Reno river at the Casalecchio di Reno catchment (Bologna, Italy). Two different types of rainfall information were tested: (i) spatial and time-aggregated rainfall, and (ii) distributed time and space rainfall. Both fuzzy models performed well in forecasting flows when the aggregated rainfall data and a limited number of fuzzy rules were used. In contrast, the neural network model performed better when the distributed rainfall data was used, that is, more input information is included.

Nayak et al. (2004) developed an ANFIS to model time series of flow in the Baitarani river in Orissa State, India. The inputs to the ANFIS were the flow values at different lag times. The number of lag-time steps was not decided from the beginning but rather different models with up to six lag-time steps were tested. Moreover, the premise, which is commonly adopted in statistical modelling, of using normally distributed data before finding the model parameters was investigated by Nayak et al. (2004) by comparing the models developed on transformed (into normal domain) and non-transformed input data. A cross-validation technique was followed to check the ability of each model. The calibration period was divided into four subsets and then the model was repeatedly re-estimated, leaving out one different subset each time. The average root mean square of errors on the four subsets that have been left out defined the cross-validation error, and the model structure that gave the minimum value for the error was considered to be the best fit. The results of the best ANFIS model were compared with an artificial neural network (ANN) model and auto-regressive moving average (ARMA) model, and this showed that the new modelling approach outperformed the other two older approaches in terms of computational speed, forecast errors, efficiency, peak flow estimation, and so on.

One of ANFIS's merits is its ability to handle situations with scarce data, e.g. in a short-term water level prediction. This aspect has been explored by Bazartseren et al. (2003) in a comparative study on a short-term water level prediction using ANN and ANFIS, as well as the linear statistical models, auto-regressive moving average (ARMA) and auto-regressive exogenous (ARX) input models. Their assumption was that the driving force to change water level at a given location is primarily a change in water level upstream, which represents a notion of a flood wave propagating downstream or flood routing. A multilayer perceptron ANN with one hidden layer was used, while the ANFIS was a fuzzy inference model of the Takagi–Sugeno type. A number of rules and a shape of membership functions were specified beforehand and, in this case, a triangular membership function was applied. Different lag times were investigated to determine the optimum travel time. The four models – ANN, ANFIS, ARMA and ARX – were tested in the Oder and Rhine rivers. The ANN and ANFIS were better for predicting over longer lead times than the ARMA and the ARX models. Moreover, the ANN was slightly more accurate than the ANFIS.

The concept of combining the outputs of flood forecasting models was extended by Xiong et al. (2001) using a first-order Takagi–Sugeno fuzzy system. Their method was compared with three methods: (i) the simple average method (SAM); (ii) the weighted average method (WAM) and (iii) the neural network method (NNM) developed by Shamseldin et al. (1997). The Takagi–Sugeno fuzzy system demonstrated its ability as a combination method with a similar degree of efficiency as both the WAM and NNM in 11 different catchments.

Ozelkan and Duckstein (2001) used fuzzy set theory to develop a fuzzy conceptual rainfall–runoff modelling framework to deal with parameter uncertainties of conceptual rainfall–runoff models that are related to data and/or model structure. The modelling framework comprises two steps. First, the conceptual rainfall–runoff system is fuzzified, and then different operational modes are formulated using fuzzy rules; second, the parameter identification aspect is examined using fuzzy regression techniques. The methodology was illustrated using: (i) a linear conceptual rainfall–runoff model, (ii) an experimental two-parameter model and (iii) a simplified version of the Sacramento soil moisture accounting (SAC-SMA) model with six parameters (Ozelkan and Duckstein, 2001). Calibration of the three models was carried out using fuzzy regression techniques. First, bi-objective fuzzy regression and tri-objective fuzzy regression techniques were applied to identify the parameters of the first model. Data from three different events from the sub-catchment 'Lucky-Hill' of the experimental catchment 'Walnut Gulch' in Arizona was used for calibration. The validation was obtained from running the model for two additional events. The calibration techniques contributed to obtaining a reliable rainfall–runoff model and to reducing possible model error in the case of uncertain data. For the other two models, a fuzzy least squares regression has been used and the parameters of the models were identified with unconstrained optimisation. These models were tested with synthetic data under controlled heterogeneous and homogeneous error scenarios and both fuzzy and conventional (crisp) least squares optimisation approaches were compared. Calibration of the fuzzy conceptual rainfall–runoff model using fuzzy least squares regression, with fuzziness introduced into both rainfall and runoff, usually gave more stable parameter estimates than those obtained assuming non-fuzziness (crisp) rainfall and runoff time series.

A new method where fuzzy arithmetic was used to enhance the counter-propagation neural network was investigated by Chang and Chen (2001). In this method, each neuron in the hidden layer of the neural network is assumed to represent a fuzzy rule derived from clustering the input data. With this feature included, the neural network is able to cluster, learn and construct rainfall–runoff relations to predict the 1-hour-ahead stream flow of the Da-Cha river in Taiwan. Supervised and unsupervised procedures were used to calibrate the weights of the network between the input and the hidden layers and between the hidden and the output layers respectively. While the unsupervised procedure was employed for clustering the input vectors to separate distinct sets of input data, the operation of the unsupervised procedure was controlled by the objective of minimising the errors between the neural network outputs and the actual outputs. The performance of the new neural network model was better and more reliable than a conventional auto-regressive moving average with exogenous input (ARMAX) model.

Despite its superiority to other models in many cases, fuzzy logic models come third to ANN and ARMA models respectively in forecasting water levels 6-hour-ahead in the River Ouse gauge at Skelton, above York, in Northern England (See and Abrahart, 2001). However, the neural model used in that study was a hybrid neural network model which uses a fuzzy logic model to combine two neural network types – a self-organising map and multilayered perceptron. The former was used to group the river levels into objective classes while the latter was used to develop a forecasting model for each class. The linking of the individual models for each class into a single forecasting system was achieved by a fuzzy logic model. A genetic algorithm method was used to calibrate the fuzzy logic model. Three types of input data were used in the forecasting: (i) rainfall data of four stations in the catchment; (ii) water levels at the study location and (iii) water levels at four other locations upstream.

2.7.2 Second Category: Fuzzy Modelling of Water-Quality Variables

Dixon (2004) coupled a neuro-fuzzy model with a GIS to predict groundwater vulnerability in a relatively large watershed in north-west Arkansas, USA. Primary input data, such as a digital elevation model (DEM), land use/land cover, soils, geology and water quality, were manipulated in the GIS to generate the secondary input data required by the neuro-fuzzy model. This included the soil hydrologic group, depth of the soil horizons, soil structure of the A horizon, as well as the original land use/land cover. They used the neuro-fuzzy classfier for the JAVA platform developed by Nauck and Kruse (1999). Their results were encouraging and showed the potentiality of the proposed methodology. Later Dixon (2005) carried out a sensitivity analysis of the neuro-fuzzy model and found it sensitive to the number of fuzzy subsets, the shape of the membership functions, the nature of the rule weights and the validation technique used during the learning processes.

The ANFIS model's validity and advantages over customary models for estimating fluvial nutrient loads in catchments subject to time-varying human impacts were tested by Marce et al. (2004). In their work, ANFIS was compared with two methods based on rating curves and ratio estimators in modelling time series of fluvial loads. Two catchments of different size and human impact history in Spain and the USA were used as case studies. The ANFIS results produced unbiased estimates of loads and were generally better than the other two methods. Most importantly, the ANFIS allows the implementation of a homogenous and model-free methodology (i.e. without the need to establish a formal physically based or conceptual model for the problem being resolved) over the entire time series of concentration, and hence a single model could be used to estimate the load series. Moreover, it works in real space without the need to logarithmically transform and re-transform data.

Haberlandt et al. (2002) successfully used fuzzy rules to dynamically regionalise the results of computer simulations from the process-based nitrate leaching model, soil and water integrated model (SWIM) (Krysanova et al., 1998), in the Saale river basin, a large tributary of the Elbe. Nine separate fuzzy rule systems, one for each soil type in the catchment, were used to model all possible conditions in the catchment. The input variables for the fuzzy model were chosen based on their impact on the nitrogen dynamics and their availability for future scenario analysis. Nine input variables representing climate, water fluxes, amount of fertiliser applied and crop uptake of nitrogen were included. The number of variables and the number of rules in each system were determined through a series of correlation analysis and trial and error procedures.

Differences between an evolution that keeps and an evolution that changes the identity of morphological characteristics of a catchment have been realised as a fuzzy process by Sriti et al. (2005). In their work, a fuzzy model of evolution was introduced and allowed for an approximation of changes and processes. State transitional variables were described as fuzzy numbers used in certain mathematical operations, providing a way to evaluate the changes in the catchment morphology. These variables represent continuous properties (e.g. slope, aspect, roughness) and morphological features (e.g. plane, channel, ridge, pass, peak, pit) which have been extracted and identified from several DEM snapshots derived from a physical experimental erosion model designed to study the influence of natural constraints (e.g. rain, lithology) in land-surface relief dynamics.

2.7.3 Third Category: Use of Fuzzy Method in Issues Related to Parameter Estimation

The uncertainty in two dependent variables – soil water pressure and maximum evapotranspiration rate – due to uncertainty in the independent variables in the analytical solution of the Darcy–Buckingham equation was measured using a method based on an extension of fuzzy arithmetic (Schulz and Huwe, 1997). First, a fuzzy subset with a certain membership function for each independent variable was described. The minimum and maximum values of this variable at various levels (between 0 and 1) cutting the membership function were then inserted individually in the analytical solution to obtain the corresponding values for the output variables. The results of this procedure provide a way to describe fuzzy membership functions for the output variables. The interval between the minimum and maximum values at various levels cutting these functions was used as a measure of uncertainty. The fuzzy method developed in Schulz and Huw's (1997) study has been compared with the classical stochastic approach to uncertainty analysis. This comparison showed that the differences between the fuzzy and the stochastic concepts and highlighted the advantages of the fuzzy method over the stochastic method. Moreover, the sensitivity of the fuzzy results to the shape of the membership functions of the input variables was also investigated and this demonstrated the strong impact of different shapes of membership functions.

The need for multi-objective functions in calibrating parameters of a rainfall–runoff model was addressed in a fuzzy method proposed by Yu and Yang (2000). They presented a fuzzy multi-objective function (FMOF) where two conventional objective functions, the root mean square of errors (RMSE) and the mean absolute per cent error (MPE), were included. Each objective function has a fuzzy membership function used to indicate its degree of acceptance. The value of the membership function varies from 0 to 1 and describes the degree of acceptability from 'bad' to 'good'. The performance of the FMOF in calibrating a modified version of the Hydrologiska Byråns Vattenbalansavdelning (HBV) model (Zhang and Lindstorm, 1997) was compared with the performances of the two conventional objective functions included in the FMOF. The comparison results showed that the model calibrated with either the RMSE and the MPE alone tends to match high and low flow periods respectively while the FMOF leads to improved simulation over the a wide range of flow stages.

2.8 Conclusions

Fuzzy theory was introduced to allow the accounting of imprecise or uncertain variables through the use of membership functions defining the degree by which a value belongs to a certain subset. In addition, fuzzy arithmetic techniques have evolved significantly and this contributed to the success of applying the fuzzy theory in various applications, including water resources. Recently, neuro-fuzzy models have been invented to produce a model that combines the capabilities of fuzzy modelling and artificial neural networks. The prominent type of neuro-fuzzy models that has been used widely in various hydrological applications is the ANFIS. A modified version of the original ANFIS has been proposed in this study for use in hydrologic and water-quality applications relevant to the implementation of the WFD. These applications are fully described in the next two sections.

3 Adapative Neuro-Fuzzy Inference System Phosphorus (ANFISP) Model

3.1 Introduction

The WFD has set a stringent target of bringing all fresh water bodies in Europe to ‘good status’ by 2015. Therefore, immediate action is required to alleviate the existing pollution pressures and eutrophication of rivers and lakes, for which phosphorus (P) pollution from diffuse sources is the main culprit (Mainstone and Parr, 2002). Meeting such environmental objectives of the WFD necessitates the adoption of a well-structured assessment of risk, coupled with an appropriate model that can be applied to explore management scenarios (Irvine et al., 2005). As a result, the use of a mathematical model is essential to predict the impacts of applying management measures at catchment level. Furthermore, this allows the possibility of integrating the results from all catchments that form a river basin to obtain the impacts at that level, thus achieving the aims of the WFD.

Referring to the drivers, pressures, state, impact and response (DSPIR) conceptual framework (Irvine et al., 2005), a diffuse P catchment model can be classified as a ‘pressure-state’ model. Such a model relates the state of P concentrations in surface water with the anthropogenic pressures in the land. Hence, diffuse P loss from land to water is a complex process influenced by all factors affecting the soil P cycle and the hydrological condition. Three hydrological variables (soil moisture, surface runoff volume and base flow volume) have a direct influence on some of the biochemical processes of the soil P cycle as well as the P transportation mechanisms. Therefore, a P model that simulates the temporal and spatial variations of the soil P cycle variables must always be accompanied by a hydrological model to provide values for these three hydrological variables. In addition, some sort of a hydrodynamic model is incorporated to account for the overland and the subsurface transport of P to the receiving water.

A wide range of P diffuse models are readily available, e.g. the soil and water assessment tool (SWAT) (Arnold et al., 1998), the hydrological simulation programme – FORTRAN (HSPF) (Bicknell et al., 1997), the large-scale catchment model (LASCAM) (Viney et al., 2000), the integrated catchment model – phosphorus (INCA-P) (Wade et al., 2002) and the GOPC (Nasr et al., 2005). Despite the successful application of these models to catchments of different climatic, hydrologic, and agrochemical conditions, none of them has exhibited a consistent performance for all conditions. For instance, the performance of a model could vary from one catchment to another although they both lie in the same region. However, generally simple conceptual lumped diffuse P models often perform adequately, particularly for behaviour within the range of the data used to calibrate its parameters (Beven, 2000). With this modelling approach a natural catchment can be modelled by assigning different sub-lumped-models to different spatial units within the catchment (e.g. Chen and Adams, 2006; Marechal and Holman, 2005; Ajami et al., 2004). Similarly, different sub-models could be used to represent the various patterns in the values of the temporal variables (e.g. Shamseldin and O’Connor, 1996; Ahsan and O’Connor, 1994; Kachroo and Natale, 1992). The success of this approach could be attributed primarily to its ability in capturing the non-linearity in the catchment behaviour because of the spatial heterogeneity and time-varying character. The choice of a suitable lumped model for use in each of the sub-catchments is critical to its success and practicality. It should have a small number of parameters to reduce the total number to be estimated for the combined model, thereby reducing the computational requirements. This is also likely to reduce potential problems caused by model over-parameterisation, such as ill-conditioning (Bruen and Dooge, 1992) or equifinality (Beven, 1993), in which a number of different combinations of parameter values give similar model fits and so a single optimal parameter set is difficult to determine.

As noted above, in this study, a new fuzzy modelling approach is proposed whereby a number of lumped diffuse P models, each of which represents a local model in a catchment, can be combined. The SMAR model (O’Connell et al., 1970) is employed for the hydrological component of the diffuse P model and the GOPC model (Nasr et al., 2005) used for the phosphorus component. The two models have been fitted within a framework of a special type of neuro-fuzzy model, called adaptive neuro-fuzzy inference system (ANFIS), to produce a combined lumped model. The resulting combined model – called the ANFISP diffuse (or simply ANFISP) model – is assumed to have a structure with sufficient complexity required for modelling the flow and P variables.

The ANFISP model has two operational modes: (i) hydrological modelling and (ii) P modelling. The reliability of the results from the model when used for P modelling depends on the results obtained from the hydrological modelling. Therefore, the performance of the SMAR hydrological model was investigated thoroughly by applying it to 11 different catchments from around the world. In addition, the model performance was also compared with the SLR model (Nash and Foley, 1982), which is always used as a base model to compare more substantive models. Finally, the complete ANFISP model was been applied to the Oona Water catchment (Co. Tyrone) to examine its performance in reproducing the discharges and the total P loads at the catchment outlet. The performance of the model in this case was then compared against the fully physical-based SWAT model (Arnold et al., 1998). The comparison was important to allow an evaluation of the performance of the new ANFISP model (which needs small amounts of spatial data and information) against the SWAT model (which requires relatively large amounts for the same quantities).

3.2 Conceptual Representation of the ANFISP Model

Following the multi-linear model approach pioneered by Bruen (1985), Becker and Kundzewicz (1987), Kachroo and Natal (1992), and Todini and Wallis (1977), the proposed sub-models approach was previously used to build different rainfall–runoff models. The work of Bruen (1985) is the most relevant to this approach. In his work, a quasi-linear model was constructed using a combination of linear sub-models. An illustration of the structure of this quasi-model, with a single threshold, is given in Fig. 3.1. Note: (i) The input series, *I*, is effectively divided into a number of separate series (e.g. I_1, I_2, etc.), each of the same length as the original. The division procedure is performed in two steps. First, the range of values in the input series is divided into a number of parts by threshold levels (partitions) of fixed values. Then the magnitude of each input value determines the division in which it lies, and the entire input in that division or band is then assigned to the corresponding time series.

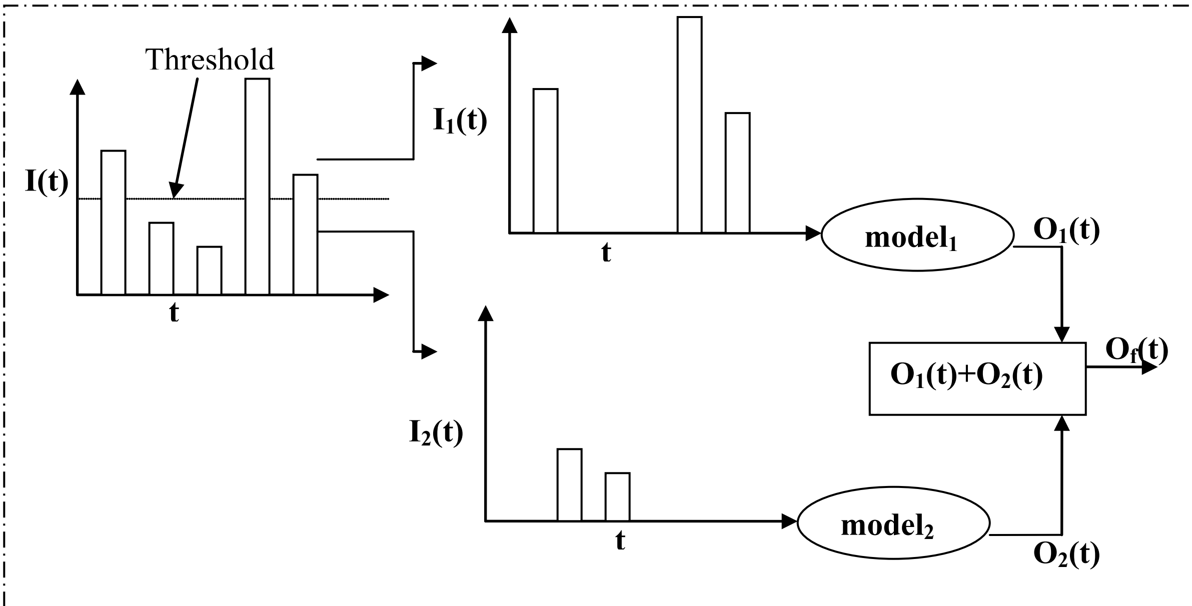

I: input time series; I_1, I_2: sub-series 1 and sub-series 2 of the input time series; t: time; model$_1$, model$_2$: models used to calculate outputs O_1 and O_2 using I_1 and I_2 as inputs respectively; O_1, O_2: output time series 1 and output time series 2 corresponding to I_1 and I_2 respectively; O_f: combined final output time series.

Figure 3.1. Structure of quasi-linear model proposed by Bruen (1985).

(ii) The output from each of the separated input series (e.g. O_1, O_2) is obtained from a number of separate models (e.g. $model_1$, $model_2$). (iii) The total output (e.g. O_f) is the sum of the outputs from each of the different models applied to the corresponding separated inputs. This allows the overall model to respond differently to low rainfall compared to high rainfall.

In essence, a number of sub-models are constructed to describe the relationship between the input and the output for different ranges of their values representing different hydrologic conditions. This requires that each input value should be assigned to a specific subset (e.g. low values, medium values, high values). Such an approach assumes the inputs can be assigned to the subsets with certainty but there are times where uncertainty might occur, such as when the magnitude of an input value is close to a partition threshold value. The method proposed here attempts to address this uncertainty using the principles of fuzzy logic theory whereby different levels of memberships of input to all subsets are estimated. These degrees of memberships can be taken as the weights given to the outputs from the models corresponding to the subsets.

To illustrate the proposed method, Fig. 3.1 has been extended in Fig. 3.2 which shows, still for the case of a single threshold, how the concept of the membership of fuzzy subsets is used to define weights given to the sub-models. Unlike Bruen's method (Bruen, 1985), the input series (e.g. I) is not separated here but alternatively it is assumed that for certain hydrologic conditions there is a sub-model (e.g. $model_1$, $model_2$) and a membership function (e.g. mf_1, mf_2) associated with it. The former produces the output (e.g. O_1, O_2) from the sub-model while the latter calculates membership values used to estimate the weight given to that output (e.g. w_1, w_2). The final output value (e.g. O_f) from the combination is the weighted average of the outputs from the models used for each subset. It is worth mentioning that the method described above is valid for the case of a lumped catchment. However, if the catchment is divided into sub-catchments, then the method can be applied separately to each sub-catchment and the final output can be estimated as the area-weighted average of the outputs of each of the sub-catchments (where routing to the catchment outlet is considered part of the sub-model).

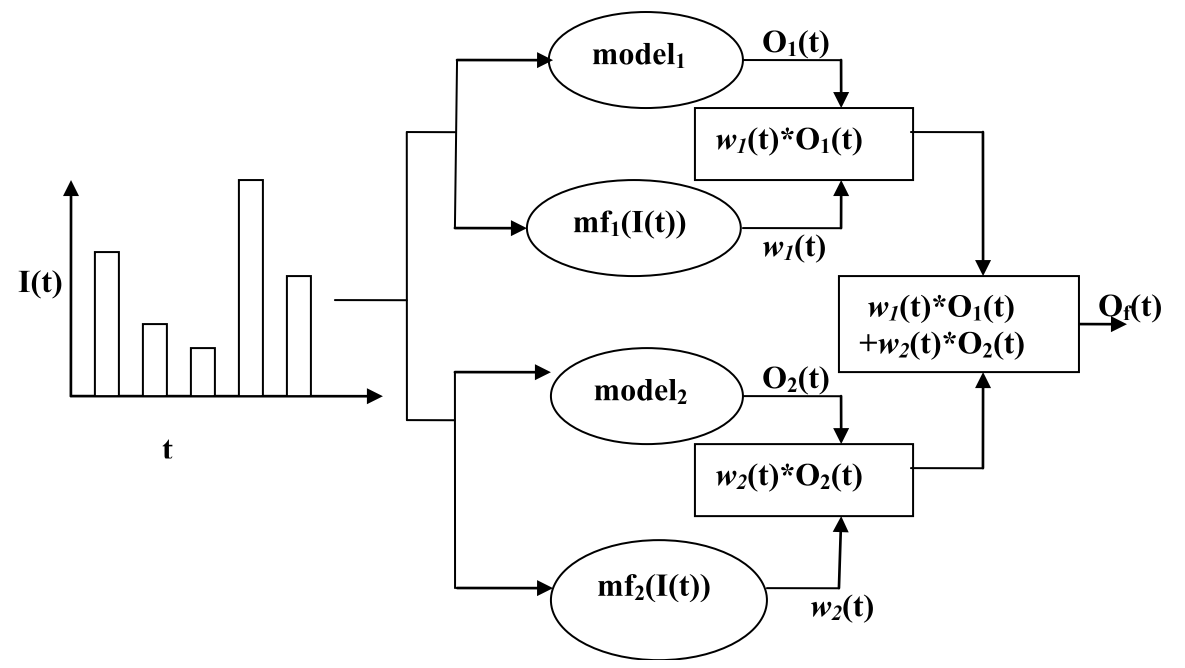

I: input time series; t: time; $model_1$, $model_2$: sub-models used to represent different hydrologic conditions; O_1, O_2: outputs calculated by $model_1$ and $model_2$; mf_1, mf_2: membership functions associated with the different hydrologic conditions; w_1, w_2: weights applied to the outputs of the models; O_f: combined final output time series.

Figure 3.2. Sub-models combination using fuzzy logic principle of membership function.

3.3 The ANFISP Model

Ozelkan and Duckstein (2001) described any catchment model as a system composed of sub-modules to represent the sub-elements of this modelled system coupled together in order to produce a synergic effect reflected at the output of the system. The representation of the catchment model in this modal structure is equivalent to the branching structure in an algorithm flow diagram resulting from IF-THEN fuzzy rules (Gupta and Sorooshian, 1983). In the present work, the aim is not to utilise the IF-THEN fuzzy rules as the model core but rather to improve the performance of deterministic catchment models by using a number of IF-THEN fuzzy rules to create specific localised versions of these models which are better able to respond to local variations in the pattern of temporal and spatial data. The ANFISP model generates continuous simulation of the output variable(s) using continuous data of the input variable(s). In this sense, it is similar to the fuzzy logic model that has been developed by Jaquin and Shamseldin (2006) to account separately for variation in catchment wetness and for catchment seasonality. The structure of the ANFISP model, which has been described in Section 2.7, represents an abstract of a rule-based or knowledge-based system consisting of three conceptual components: (i) fuzzy logic, (ii) fuzzy decision rules and (iii) fuzzy reasoning (Jang, 1993).

3.3.1 Fuzzy Logic

The function of the fuzzy logic component is to represent the uncertainty of assigning a membership for any value of the system input and output variables to certain fuzzy subsets of that variable. To achieve this, a continuous and multi-valued logic membership function between 0 and 1 is defined for each of the fuzzy subsets. The value obtained from this function provides a qualitative representation of the uncertainty in such a way that the range between 0 and 0.5 can be divided to encompass the various degrees of uncertainty, whereas the remaining range is made for the various degrees of certainty.

3.3.2 Fuzzy Decision

The fuzzy decision rules consist of a number of fuzzy IF-THEN rules. The antecedents or premises of the IF-THEN rules define a fuzzy region of the input space, while the output or the consequent parameters specify the corresponding output. Each IF-THEN rule describes the local behaviour of the mapping between the inputs and the outputs of the system, and, in this sense, it can be interpreted as a sub-model of the entire system. To perform the mapping, an appropriate mathematical model must be used. The discharge and total P (TP) load are the two targeted variables in the modelling here. To obtain simulations of these variables, two models in a series must be used. The first model, the SMAR model, generates the discharge as its output and, moreover, it produces all the hydrological variables required by the second model, the GOPC model, which simulates the TP load. This indeed makes the quality of the performance of the first model (SMAR) highly influential in the overall modelling process. Therefore, to ensure the suitability of the SMAR model as a hydrological model, its performance within the ANFIS model must be compared against the performance of a naive benchmark model and here the SLR model (Nash and Foley, 1982) has been selected for this purpose. Such a comparison can indicate the relative improvement in model performance obtained by using a conceptual model such as the SMAR model over that of a simple model such as the SLR model. In contrast, the complete ANFISP model is compared against the complex SWAT model. The purpose of the comparison in this case is to judge the performance of the new ANFISP model, based on the performance of a sophisticated model such as SWAT. Note that SWAT has been used as an independent model and has not been included in the fuzzy logic model as in the case of the SLR model.

3.3.3 Fuzzy Reasoning

In the fuzzy reasoning component, an inference procedure is implemented whereby outputs of all the IF-THEN rules are combined and then transformed into crisp values, if they were not already so, to obtain the final outputs from the fuzzy model. A weighted average combination of the individual outputs is applied in this case. The weight given to the output of a certain IF-THEN rule is determined by multiplying the values of the fuzzy membership functions of the input variables that constitute that rule.

3.4 The Soil Moisture Accounting and Routing Model

O'Connell et al. (1970) developed a quasi-physical rainfall–runoff model known initially as the layers model, but later renamed the soil moisture accounting and routing (SMAR) model. In this model, a water balance component is connected with a flow routing component to create an adequate conceptualisation of the hydrological processes involved in flow generation. Using a number of empirical and physically plausible relationships, the non-linear water balance component distributes the available moisture between evaporation, soil storage and overland runoff. The routing component of the model simulates the flow of water across the land and inside the stream channels until it reaches a controlling point where the discharge is measured. The simulation accounts for attenuation and wave diffusion of the runoff and base flow volumes separately, with different conservative linear time-invariant elements.

A number of modifications to the original structure of the model have been introduced (Khan, 1986; Liang, 1992) and the latest version by Tan and O'Connor (1996) is used here (Fig. 3.3). It has eight parameters in the water balance component and three parameters in the routing component. In addition, the initial condition of the groundwater storage is considered as a parameter bringing the total to 12.

The way by which SMAR transforms the rainfall into discharge is summarised in Fig. 3.3. The model assumes that any catchment is composed of a set of horizontal soil layers, each of which may contain water up to a maximum depth called *CAP* which represents a parameter in the model. The last (i.e. bottom) layer may have a maximum depth less than *CAP*. The total combined water storage depth of these layers is a parameter of the model, which is usually denoted *ST*. The evaporation input (E_p) to the SMAR model is either the actual (pan) evaporation depth or the potential evaporation calculated by Penman's equation. Moreover, E_p, is multiplied by a parameter t_{cv}, less than unity, in order to estimate the potential evaporation depth over the catchment. In the model, it is assumed that evaporation occurs from the layers only when there is no rainfall or when the rainfall is not sufficient to satisfy the potential evaporation demand ($t_{cv} \times E$). Any evaporation from the first layer occurs at a certain rate denoted by the parameter *C*. On the depletion of the water depth of the first layer, any subsequent evaporation from the second layer occurs at a rate of C^2, and so on. Hence, if all layers were full and there was no subsequent rainfall, then a constant potential evaporation applied to the catchment would reduce the soil moisture storage in approximately an exponential manner. Such evaporation would continue until either the storage of all the layers was depleted or the potential evaporation demand was satisfied fully.

On the other hand, when the rainfall exceeds the potential evaporation ($t_{cv} \times E$), depth runoff takes place. A fraction (H_{drcx}) of the excess rainfall (i.e. the rainfall less the potential evaporation) contributes to the generated runoff by producing the direct generated runoff component (r_1). The fraction H_{drx} is considered to be directly proportional to the ratio of the available water depth to the maximum depth in the top five layers, or in the total set of layers if the number of layers is less than five. The constant of proportionality (*NOP*) is a parameter of the model, with H_{drx} having a value between zero and *NOP*. Any remaining excess rainfall after subtraction of r_1 which exceeds a parameter, represents the maximum infiltration capacity Y_{cap} (mm/day) and also contributes to the generated runoff as r_2. This represents the component of runoff in excess of the infiltration capacity. After subtraction of both the direct runoff (r_1) and the runoff in excess of the infiltration capacity (r_2), the remaining excess rainfall replenishes each soil layer in turn, beginning from the first (i.e. the top) layer downwards until either the rainfall excess is exhausted or all layers are full. Any surplus remaining is further divided, depending on a weight parameter G_x, into two portions, the first portion being envisaged as a groundwater runoff component (r_g) while the second is considered as a subsurface runoff component (r_3). The latter is added to the direct runoff (r_1) and to that in excess of the infiltration capacity (r_2) in order to produce the total generated surface runoff (r_s).

The total generated surface runoff (r_s) is routed through the gamma function model which has two parameters, namely the shape parameter *NH* and the lag parameter *KH*. The groundwater runoff (r_g) is multiplied by a fraction *GF* to determine the actual amount available for routing through a single linear reservoir with a storage coefficient parameter (k_g). The remaining fraction of the groundwater runoff $(1 - GF)r_g$ is assumed to go into the inactive groundwater storage and this will not appear again in the system. The value of the fraction *GF* should be between 0 and 1 and it is a parameter of the model. In addition, the initial groundwater storage (*GS)* is also considered as a parameter.

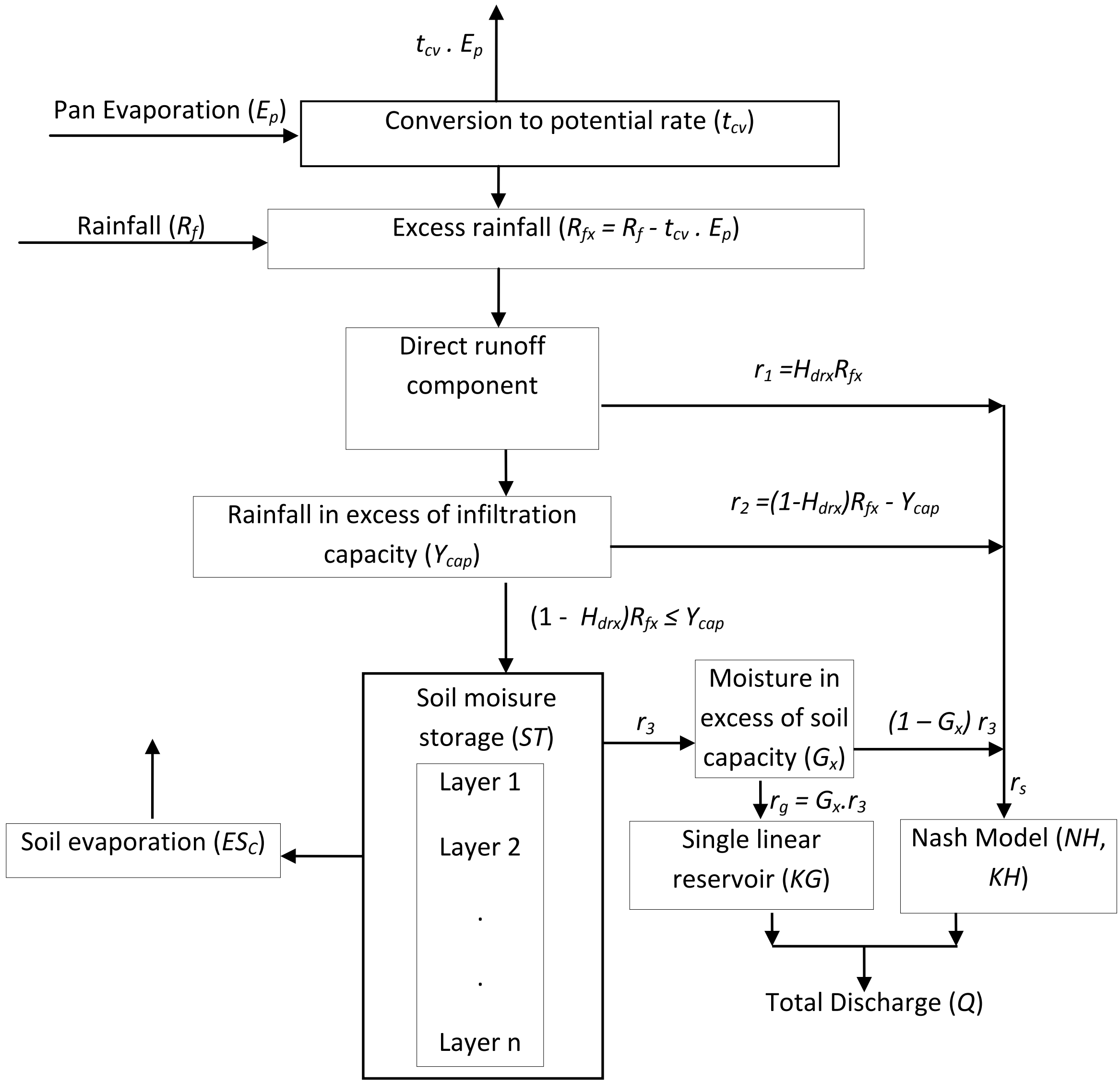

E_p: evaporation input; t_{cv}: conversion factor of evaporation; E_{sc}: soil evaporation; R_f: rainfall input; R_f: excess rainfall; H_{dr}: direct runoff component; H_{drx}: A fraction of the excess rainfall that contributes to direct runoff; Y_{cap}: maximum infiltration capacity; ST: soil moisture storage; G_x: rainfall input; r_1: direct runoff; r_2: runoff in excess of infiltration capacity; r_3: subsurface runoff component; r_g: groundwater runoff component; r_s: total generated runoff; NH: shape parameter of the Nash model; KH: lag parameter of the Nash model; KG: storage coefficient parameter of the single linear reservoir model.

Figure 3.3. Structure of the SMAR model.

The sum of the outputs of the two routing components, r_g and r_s, is the SMAR model estimated discharge. In total, the SMAR model has 12 parameters: nine of them (ST, CAP, t_{cv}, C, NOP, Y_{cap}, G_x, GF, GS) are used in the water balance component while the remaining three parameters (NH, KH, K_g) are used in the routing component. Some of these parameters can be fixed at appropriately chosen values while the rest, if not all, are usually estimated by optimisation.

3.5 The Simple Linear Reservoir Model

The simple linear reservoir (SLR) model assumes a linear time invariant relationship between rainfall and discharge, expressed by a convolution summation relation. Here, an additional term has been added in order to include evaporation values in the modelling, giving Eq. 3.1:

$$Q_i = G\sum_{j=1}^{m} R_{i-j+1}h_j + \alpha E_i + \varepsilon_i \ , \qquad (3.1)$$

where Q_i, R_i, and E_i are the discharge, rainfall and evaporation respectively at the ith time step, h_j is the jth ordinate of the discrete pulse response function, m is the memory length of the system, G is the gain factor, α is a coefficient of the evaporation term (this can be set to zero if evaporation is to be ignored), and ε_i is the error term. Usually, the sum of the h_j terms is unity.

This is a multiple linear regression of the observed discharge on the previous observed rainfall values and the current evaporation value. For the pulse response terms, h_j, either a parametric or non-parametric form can be used, and the two-parameter Nash cascade model (Nash, 1957) is used here. The discrete h_j terms are calculated from its impulse response function $h(t)$ which has the following form (Eq. 3.2):

$$h(t) = \frac{1}{kr \times \Gamma(nr)} \times \left(\frac{t}{kr}\right)^{nr-1} \times e^{-t/kr} \ , \qquad (3.2)$$

where $\Gamma(n)$ is the gamma function.

Thus, the SLR model, with the pulse response function in parametric form, has four parameters, G, nr, kr and α.

3.6 The Grid Oriented Phosphorus Component Model

The GOPC model (Nasr et al., 2005) is a generic phosphorus module developed to simulate the processes in the soil P cycle and the transportation of different phosphorus components over the land and through the subsurface (Fig. 3.4). The soil phosphorus state variables in the GOPC consist of the soil soluble phosphorus (SSP), the fresh organic phosphorus (FROP), the fixed organic phosphorus (FXOP), the easily soluble inorganic phosphorus (ESIP), and the fixed or insoluble inorganic P (FIP). The FROP represents the organic matter that is easily mineralised and this consists of the manures and the decayed plant and microbial biomass. On the other hand, the FXOP contains the humus material which mineralises slowly. The inorganic phosphorus in the soil is divided into two types: the ESIP and the FIP. With respect to the phosphorus export in the GOPC model, the overland flow transports two forms of phosphorus, dissolved phosphorus (DP) and particulate phosphorus (PP), whereas the DP is the only form delivered by base flow. The dynamic changes in the soil storage of each state variable is described by a mass balance equation which relates the input fluxes, the output fluxes, and the rate of change of the storage. At each time step, all mass balance equations are solved simultaneously using a method described by Nasr (2004) to obtain the mass of each state variable in the model. All the input and the output fluxes in the GOPC model are shown in Fig 3.4 and their description can be found in Nasr et al. (2005).

The original GOPC model has been simplified in this study by lumping the SSP, ESIP, and FIP into a variable called mineral P (MP) while the FROP and FXOP are lumped into a variable called organic P (OP). Mass balance equations of this simplified version are as shown in Eqns 3.3 to 3.9.

Mineral P:

$$\frac{MP_i - MP_{i-1}}{\Delta t} = fm_i - QP_i - GWP_i - IBMP_i + ZMP_i \ , \qquad (3.3)$$

where MP is the mass of mineral P storage (mass/area), fm is the input to the mineral P storage (mass/area/time), QP is dissolved P transported by surface runoff (mass/area/time), GWP is dissolved P transported by base flow (mass/area/time), $IBMP$ is the immobilisation of mineral P (mass/area/time), ZMP is the mineralisation of organic P (mass/area/time), Δt is the time step of the simulation (time) and i is the index for the time.

Organic P:

$$\frac{OP_i - OP_{i-1}}{\Delta t} = fo_i - SRP_i + IBMP_i - ZMP_i \ , \qquad (3.4)$$

where OP is the mass of organic P storage (mass/area), fo is the input to the organic P storage (mass/area/time) and SRP is the attached P transported by surface runoff (mass/area/time).

At each time step mineralisation of organic P and immobilisation of mineral P are obtained by the following two equations respectively:

$$ZMP_i = OP_i \times kgopc_4 \ , \qquad (3.5)$$

$$IBMP_i = MP_i \times kgopc_5 \ , \qquad (3.6)$$

where $kgopc_4$ and $kgopc_5$ are coefficients to determine the rate of the mineralisation and immobilisation processes respectively.

Transport of dissolved P via surface runoff ($qpgopc$) is estimated according to the following equation:

$$qpgopc_i = MP_i \times rs_i \times kgopc_1 \ , \qquad (3.7)$$

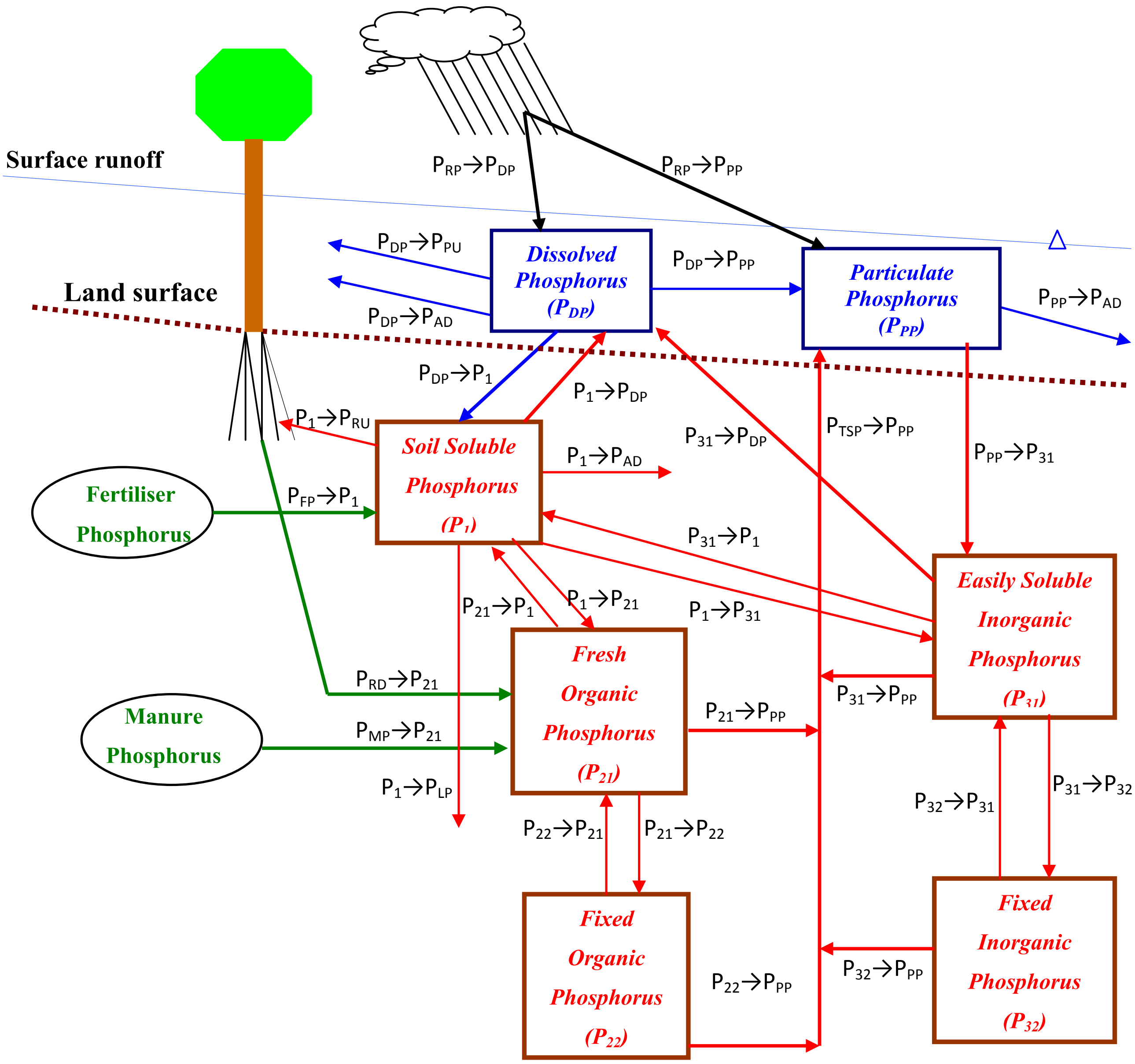

P_{DP}: dissolved phosphorus; P_{PP}: particulate phosphorus; P_1: soil soluble phosphorus; P_{21}: fresh organic phosphorus; P_{22}: fixed organic phosphorus;

P_{31}: easily soluble inorganic phosphorus; P_{32}: fixed soluble inorganic phosphorus; P_{RP}: rainfall phosphorus load; P_{FP}: fertiliser phosphorus load; P_{MP}: maure phosphorus load.

P_{PU}: phosphorus transported by advection process; P_{PU}: plant uptake of phosphorus; P_{RU}: root uptake of phosphorus; P_{RD}: phosphorus in root decay material; P_{LP}: labile phosphorus; P_{TSP}: total soluble phosphorus.

Figure 3.4. Structure of the GOPC model.

where *rs* is the surface runoff obtained from the hydrological model (SMAR in this case) (depth/time) and $kgopc_1$ is a coefficient.

The contribution of dissolved P by base flow (*gpgopc*) is modelled in similar fashion to the surface runoff. The only difference here is that the soil moisture content of the soil has been included in the equation to account for the amount of dissolved P which is available for transport by base flow. The equation has the following form:

$$gpopc_i = MP_i \times \theta_i \times rg_i \times kgopc_2 \tag{3.8}$$

where *rg* is the base flow obtained from the hydrological model (SMAR in this case) (depth/time), θ is the soil moisture content obtained from the hydrological model (SMAR in this case) (depth/depth) and $kgopc_2$ is a coefficient.

It is assumed that only fine sediment organic material enriched with P is susceptible to transport by surface runoff during the occurrence of storm event. The amount (*sdpgopc*) transported by this mechanism is hence a function of surface runoff (*rs*) and it can be estimated by the following equation:

$$sdpgopc_i = OP_i \times rs_i \times kgopc_3 \, , \tag{3.9}$$

where $kgopc_3$ is a coefficient.

In total, the GOPC model has 21 parameters which have to be determined by calibration.

3.7 The SWAT Model

The soil and water assessment tool (SWAT) model is a continuous model working at the basin scale that is used to look at the long-term impacts of management and also the timing of agricultural practices within a year (Neitsch et al., 2001). The model was obtained by merging the simulator for water resources in rural basins (SWRRB) (Williams et al., 1985) and the routing outputs to the outlet (ROTO) models (Arnold et al., 1995). The goal of developing the SWRRB model is mainly the prediction of the effect of management decisions on water and sediment yields with reasonable accuracy for ungauged rural basins throughout the US (Arnold and Williams, 1987). Nasr and Bruen (2006) described in detail the hydrological and the phosphorus components of the SWAT model. In addition, they explained the set-up of the model for three Irish catchments (including the Oona Water catchment used in this study).

The hydrological phase in SWAT provides the required parameters for the phosphorous calculations. The most important parameter is the runoff volume computed by the modified soil conservation service (SCS) curve number method. In this method, the curve number varies non-linearly with the moisture content of the soil, exhibiting a drop as the soil approaches the wilting point, while there is an increase to near 100 as the soil approaches saturation. Another significant flow parameter to the phosphorous modelling is the lateral subsurface flow or interflow which represents a stream flow contribution originating below the soil surface but above the zone where rocks are saturated with water. The model applies the kinematic storage method to estimate this stream flow component. The last stream flow component, which has a valuable use in the model prediction of both the sediment and P, is the water contributed by the shallow aquifer or the base flow. The model solves the water mass balance equation in the aquifer to estimate the base flow contribution. Finally, the P associated with the sediment requires the calculation of the amount of sediment removed from the land surface, and for this purpose the model uses the modified universal soil loss equation (MUSLE).

The soil profile is allowed in SWAT to be divided into several layers with variable hydraulic and chemical properties. For each layer the soil P pool is assumed to be comprised of fresh organic P, active and stable organic P, soluble P, and active and stable inorganic P. The soil P processes which the model accounts for are decay of plant residue, decomposition of the fresh organic matter, mineralisation and immobilisation, adsorption, desorption and plant uptake. The amount of soluble P removed in runoff is predicted using solution P at the top 10 mm of soil, the runoff volume and a partition factor. Phosphorus transported with sediments is calculated by a loading function which estimates the daily organic P runoff loss, based on the concentration of organic and active inorganic P in the top layer, the sediment yield, and enrichment factor. This factor represents the ratio of the P concentration on the detached sediment material to that in the parent soil.

3.8 Application of the ANFISP Model

As noted above, the development of the ANFISP model is a two-step process. First, the hydrological component of the ANFISP is developed and tested. At this stage the ANFISP model is equipped with the SMAR hydrological model. To ensure the suitability of SMAR as a hydrological model, its performance within the ANFISP model was compared against the performance of the SLR model (Nash and Foley, 1982). The complete ANFISP model is obtained in the second step by adding the GOPC model, which allows the modelling of phosphorus loads, to the hydrological model obtained from the first step.

3.9 Hydrological Component of the ANFISP Model

Testing the ANFISP hydrological component is based on assessing the performance of two separate scenarios formulated to account for the temporal variations (ANFISP_T) and the spatial variations (ANFISP_S) respectively. The model structure for both scenarios is similar to the one illustrated in Fig. 2.2. All ANFISPs used in this study employ the Gaussian function to represent the membership function of all temporal input variables to the models. This function has the following analytical expression (Eq. 3.10):

$$f(x) = \exp\left(\frac{-(x-\mu)^2}{2\sigma^2}\right), \tag{3.10}$$

where $f(x)$ is membership value of a variable x to certain fuzzy subset, and parameters μ and σ specify the location and spread of the function and require calibration.

As outlined previously, the two models, SLR and SMAR, are used in the consequent part of the ANFISP in both modelling scenarios. It is worthwhile stressing at this point that the resulting consequent part of the ANFISP for each scenario can be visualised as a collection of either SLR or SMAR sub- or local models determined according to the IF-THEN rules acting in parallel. Indeed, it is the generation of such a configuration, as an alternative method of involving the temporal and spatial pattern variations of the variables in modelling the rainfall–runoff relationship that is sought in this study.

3.9.1 ANFISP_T Modelling Scenario

In the ANFISP_T scenario there are two inputs – rainfall and evaporation – and the output, discharge is calculated using one or other of the catchment models. To distinguish between the ANFISP_T variant which uses the SLR model and the other which uses SMAR in the consequent part, they are called ANFISP_T_SLR and ANFISP_T_SMAR respectively. For each model a total of ten possible rainfall and evaporation fuzzy subset combinations are formulated as indicated in Table 3.1. The performances of all ten cases are evaluated separately for 11 catchments from different parts in the world. Details of these 11 catchments are given in Table 3.2.

Table 3.1. The ANFISP_T scenario cases used to test the hydrological component.

Model	Case	No. of fuzzy subsets	
		Rainfall	Evaporation
ANFISP_T_SLR ANFISP_T_SMAR	1	1	1
	2	1	2
	3	2	1
	4	2	2
	5	3	1
	6	3	2
	7	3	3
	8	4	4
	9	5	5
	10	6	6

The total number of parameters (*npar*) requiring calibration is determined from:

1. The number of fuzzy subsets for the rainfall (nr_{fsub}) and the evaporation (ne_{fsub});
2. The number of the IF-THEN rules (this is equal to $nr_{fsub} \times ne_{fsub}$); and
3. The number of the model parameters (P) (4 for SLR and 12 for SMAR).

The relation used to calculate *npar* is given here in Eq. 3.11:

$$npar = 2(nr_{fsub} + ne_{fsub}) + (nr_{fsub} + ne_{fsub})P \ . \tag{3.11}$$

The first term in the above equation gives the total number of the Gaussian function parameters (Eq. 3.10)

Table 3.2. Details of the test catchments.

Catchment name	Country	Area (km²)	Starting date of data	No. of data points	Memory length (day)
Bird Creek	USA	2344	1-Jan.-1955	2922	15
Blue Nile	Sudan	175125	1-Jan.-1992	1461	15
Brosna	Ireland	1207	1-Jan.-1969	3652	30
Chu	Vietnam	2370	1-Jan.-1965	3652	15
Halda	Bangladesh	779	1-Jan.-1980	2556	15
Kelantan	Malaysia	12867	1-Jan.-1975	2922	20
Nan	Thailand	4609	1-Jan.-1978	3287	20
Sg. Bernam	Malaysia	1090	1-Jan.-1977	2556	25
Shiquan-3	China	3092	1-Jan.-1973	2922	15
Sunkosi-1	Nepal	18000	1-Jan.-1975	2922	30
Wolombi Brook	Australia	1580	1-Jan.-1963	1826	15

for all fuzzy subsets while the second term gives the total number of the SLR or SMAR model parameters. Thus, there are two sets of parameters that need to be determined by the calibration process. The first set is the parameters of the Gaussian membership functions of the rainfall and evaporation. The second is the parameters of the models (SLR and SMAR) which are used to relate the rainfall and evaporation (input variables) with the discharge (output variable). The overall optimisation problem is non-linear and it has been found that if the two sets of parameters are to be determined altogether the calibration will be very poor and hence the calibration is performed in a sequential iterative procedure:

1 Initial values are given to the parameters of the SLR and SMAR models in the ANFISP_T_SLR and ANFISP_T_SMAR respectively.

2 By holding the SLR and SMAR parameters to the initial values, the Gaussian function parameters of the rainfall and evaporation subsets are determined by using the genetic algorithm (Holland, 1975), which represents a global heuristic search method. The operation of the genetic algorithm (GA) is broadly based on the Darwinian theory of 'survival of the fittest', as potential solutions to a given optimisation problem contend and 'mate' with each other to evolve improved solutions. The GA codes the parameter values as genes in a chromosome and uses probabilistic rules to advance the search process. The starting point for the operation of the GA is the random generation of an initial population of parameter sets. From this initial population, pairs of parameters sets are randomly chosen, depending on their fitness evaluated on the basis of the value of the selected objective function. The chosen pairs are subsequently used to generate a new population of parameters sets (i.e. the next generation), using the genetic operators of 'crossover' and 'mutation' to generate 'offspring'. The newly generated population is anticipated to be better than the older one. The process of generating new populations continues until a pre-specified 'stopping-criterion' is fulfilled (e.g. when the specified number of function evaluations is reached).

3 The Gaussian function parameters are then held constant and the parameters of the SLR and SMAR models are recalibrated in a second optimisation step. The least squares method is used for the linear optimisation problem resulting in the ANFISP_T_SLR, whereas the GA is used for the non-linear one in the ANFISP_T_SMAR.

4 If the resulting objective function is less than a specified tolerance the calibration stops; otherwise, steps 2 to 3 are repeated. Note that the initial values of the parameters of the SLR and SMAR models in this case are the ones obtained from the calibration in step 3.

A split-sampling approach was used for model testing, in which the available data for each catchment was split into two parts. The first part (67%) was used in the model calibration while the second (33%) was used in verifying the calibrated models. Two criteria are used in calibration and validation:

1 The Nash–Sutcliffe index (NSR^2) (Nash and Sutcliffe, 1970) (Eq. 3.12):

$$NSR^2 = 1 - \frac{\sum_{i=1}^{n}\left(x_i - \hat{x}_j\right)^2}{\sum_{i=1}^{n}\left(x_i - \bar{x}\right)^2}, \quad (3.12)$$

where x_i is the observed value, $\hat{x}_j$ is the value estimated by the model, $\bar{x}$ is the mean of the observed values, $\bar{\bar{x}}$ is the mean of the estimated values and N is the number of data values. The NSR^2 index describes the ability of the model to explain the variability in the data. A good model is one that has a value of NSR^2 close to 1.

2 The average relative error (ARE) of the estimated discharge peaks over a threshold is given by Eq. 3.13:

$$ARE = \left(\sum_{i=1}^{Np}\frac{\left|\ddot{A}Q_{pi}\right|}{Q_{pi}}\right)\times 100 = \left(\sum_{i=1}^{Np}\frac{\left|\hat{Q}_{p} - Q_{pi}\right|}{Q_{pi}}\right)\times 100, \quad (3.13)$$

where Np is the number of the selected peaks over the chosen discharge threshold, and $\hat{Q}_{pi}$ and Q_{pi} are the ith model estimated and observed discharge peaks over the threshold respectively. In general, the lower the relative error, the better is the performance of the model. A value of ARE of zero indicates a perfect matching of the annual flood peak, while large values of ARE would be an indication of the failure of the model to reproduce the annual peak. The calculation of the ARE requires the a priori specification of the discharge threshold. In the present study, the discharge threshold value to be used in conjunction with the ARE conservatively is set here as the mean discharge. The use of such a discharge threshold value enables the evaluation of the efficacy of the model in producing the high-peak discharges.

In addition to these numerical criteria, the observed and the simulated hydrographs for some catchments for each calendar year have been plotted to illustrate the fit of the hydrograph shapes.

3.9.2 ANFISP_S Modelling Scenario

Here the performance of the ANFISP_S model with the SLR and the SMAR sub-models is assessed. The first case is called ANFISP_S_SLR while the latter is called ANFISP_S_SMAR. However, unlike the ANFISP_T scenario, the modelled catchment in the ANFISP_S scenario is divided spatially into a number of homogenous hydrologic characteristics units (HHCUs). Although, analogous to hydrologic response units (HRUs) (e.g. Quiroga et al., 1996), HHCUs are defined and determined in a somewhat different way. The inputs to each HHCU are the catchment averages of rainfall and evaporation.

If the rainfall and evaporation for each HHCU are used as fuzzy variables then their fuzzy subsets can be used to determine the number of IF-THEN rules in the consequent part of each sub-ANFISP_S model for each HHCU. However, as only one fuzzy subset is used for rainfall and likewise only one for evaporation, the resulting combined sub-ANFISP_S model is essentially a model describing different homogenous spatial units, i.e. each IF-THEN rule represents a sub-model describing the rainfall–runoff relationship for a given HHCU, and the final estimated runoff value is the weighted sum of the contribution from all the HHCUs. This is a type of semi-distributed modelling that can be easily implemented either within or in conjunction with a GIS by overlaying three map layers: (i) the catchment boundary; (ii) the land-use map and (iii) the soil map. The number of HHCUs obtained with this GIS procedure is based only on elevation, land use and soil type, and here they are determined with an innovative approach based on the subtractive clustering algorithm (SCA) (Vernieuwe et al., 2005).

3.9.2.1 Determination of the HHCUs for the Brosna Catchment

Each HHCU is expected to have a unique rainfall–runoff relation used to estimate its contribution to the catchment outflow. A large number of spatially related parameters such as elevation, soil permeability, soil roughness, bedrock transmissivity, etc. could influence the rainfall–runoff response and could be used to characterise the HHCU. However, for this study, the number of such variables is limited to the DEM, the land-use map (CORINE, 1990) and the soil map (Gardiner and Radford, 1980), and these were used to test only the NFM_S for the Brosna catchment, a sub-catchment in the Shannon river basin. From these three basic maps (Figs 3.5 to 3.7), four spatial variables are calculated by the GIS: (i) elevation, (ii) slope, (iv) land use and (iv) soil type.

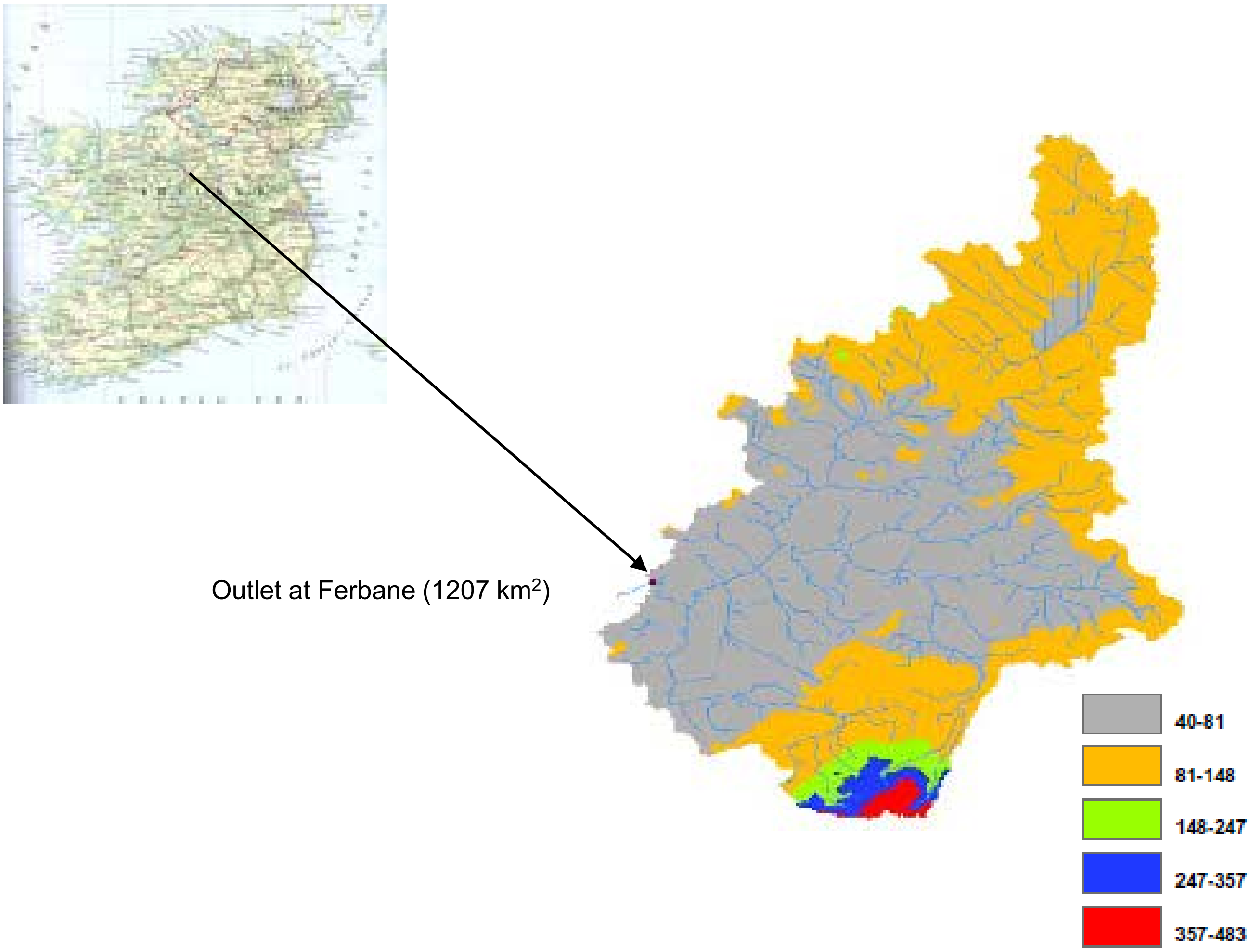

Figure 3.5. Brosna catchment – location, digital elevation model (DEM) and streams network.

The original categories of soil types and elevation bands are used without any changes since they are the primary governing parameters in characterising the response to the rainfall. Despite the original land-use map having 19 different categories, here land use has been aggregated into four main types: (i) agriculture, (ii) urban, (iii) forest and (iv) wetland (Fig. 3.8). Similarly, the slopes obtained directly from the DEM have been assigned to one of three groups: (i) for slopes between 0% and 8%, a slope index is taken as 4%; (ii) for slopes between 8% and 15%, a slope index is taken as 12% and (iv) for slopes greater than 15%, a slope index is taken as 20%. The Brosna river flows in a south-westerly direction to an outlet point at Ferbane which drains 1207 km^2 of catchment area. The plotting of the rainfall, evaporation and discharge data is given for this catchment in Fig. 3.9.

Table 3.3. Combination alternatives of the four spatial variables used in the subtractive clustering algorithm (SCA).

ID	No. of variables	Variables
2A	2	Elevation + Land use
2B	2	Elevation + Soil
2C	2	Slope index + Land use
2D	2	Slope index + Soil
2E	2	Land use + Soil
3A	3	Elevation + Land use + Soil
3B	3	Slope index + Land use + Soil
4	4	Elevation + Slope index + Land use + Soil

For each of the various combination alternatives, which are summarised in Table 3.3, the four input spatial variables are passed on to the SCA in order to obtain

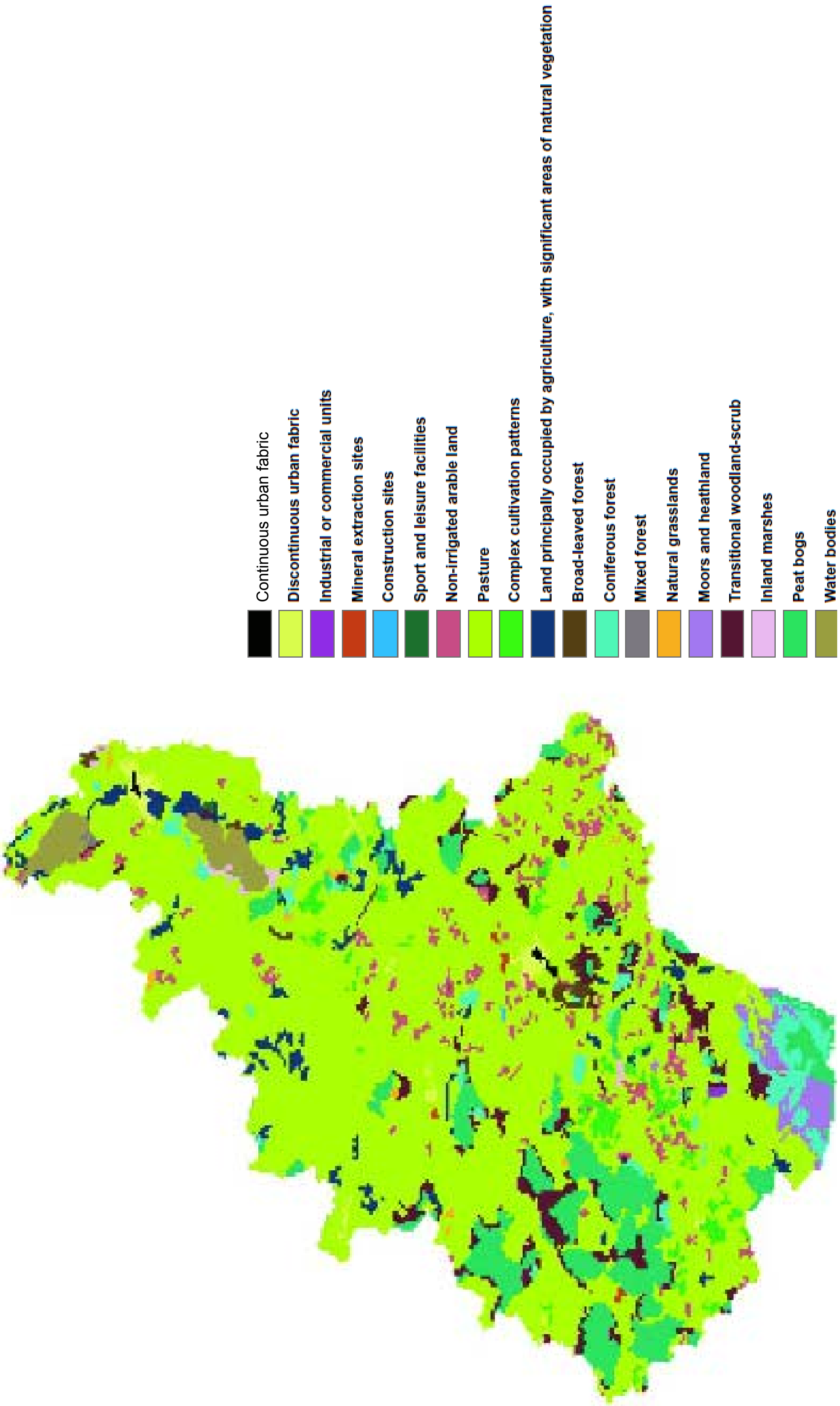

Figure 3.6. Brosna catchment – CORINE land-use classes.

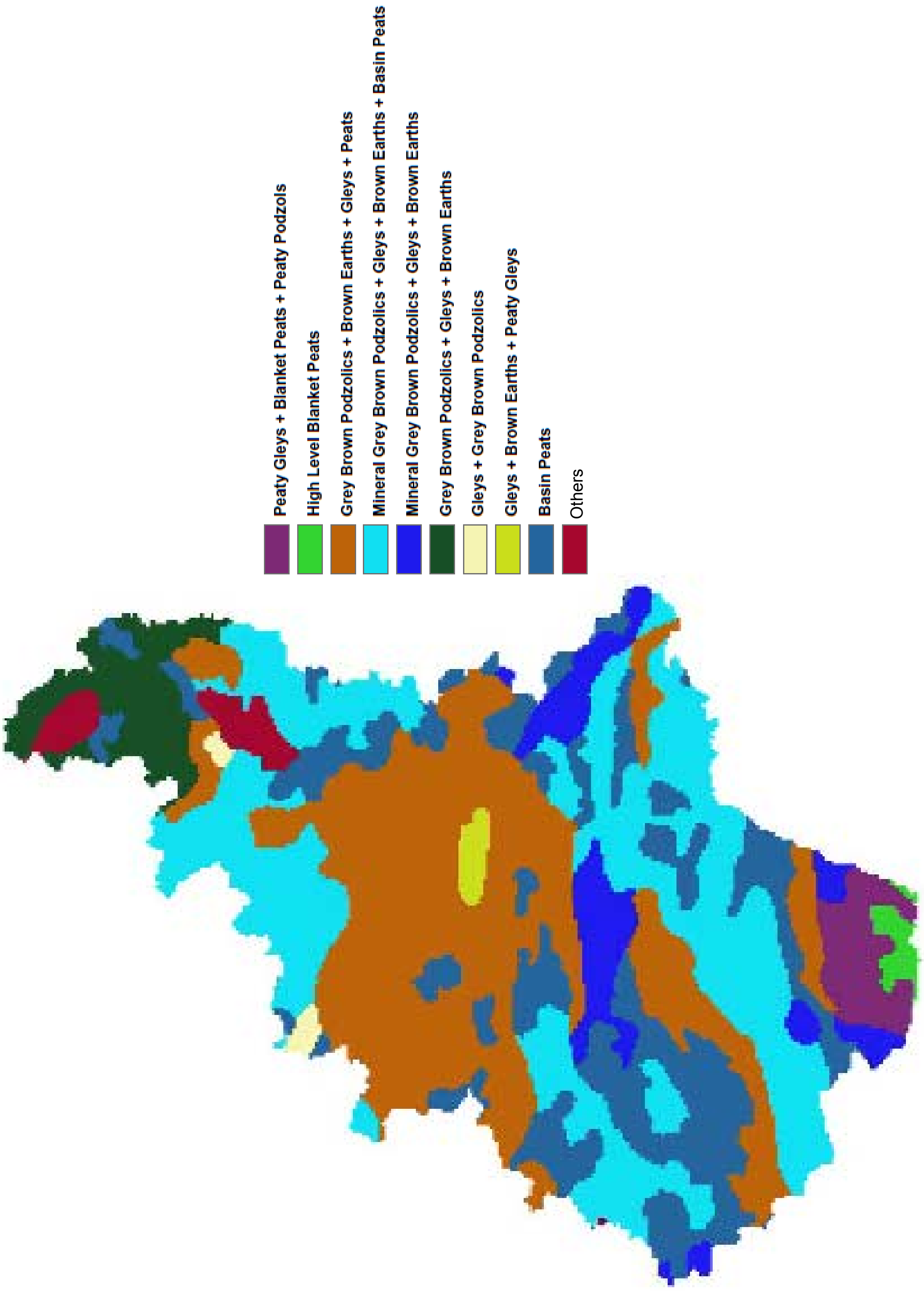

Figure 3.7. Brosna catchment – soil types.

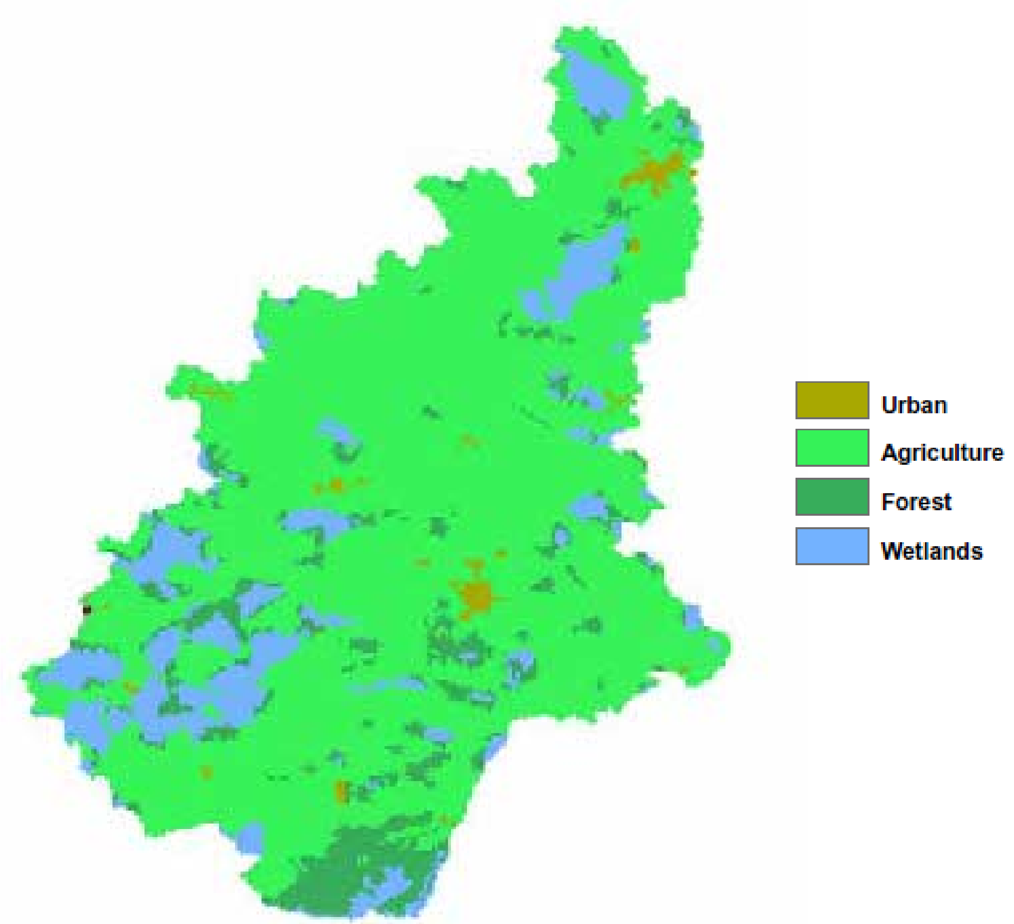

Figure 3.8. Brosna catchment – general land-use classes.

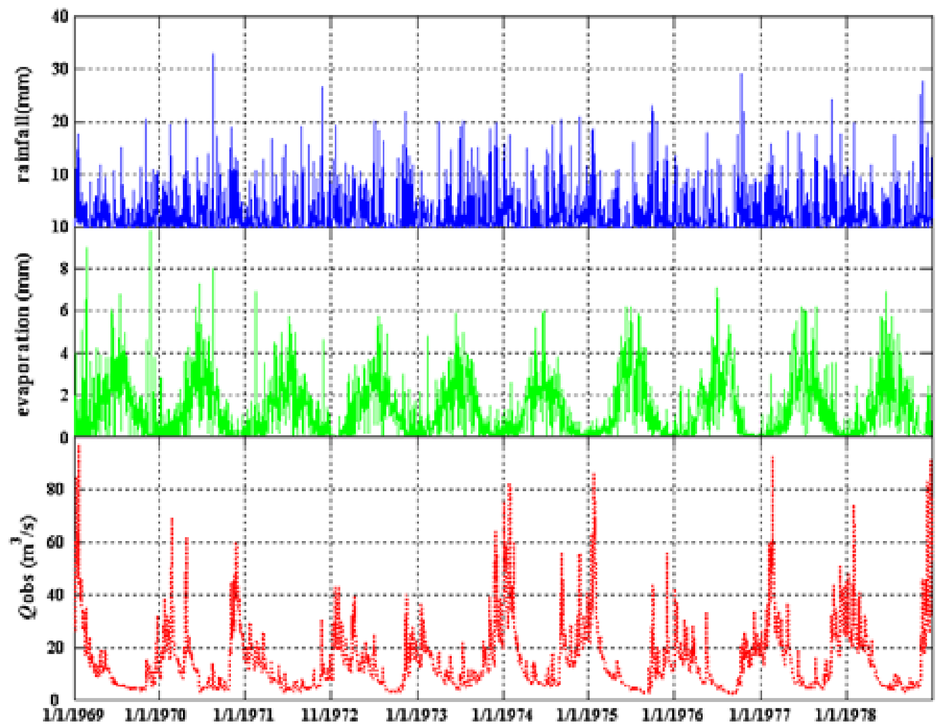

Figure 3.9. Rainfall, evaporation and discharge (*Q*) time series – Brosna catchment.

a different number of HHCUs. The resolution of the resulting clusters in each combination alternative can be adjusted by changing the parameters in the SCA (cf. Vernieuwe et al., 2005). To illustrate the SCA, suppose that there are a number of data points z (e.g. cells in a grid defining a catchment) of two spatial variables x and y. Then each data point $Z_j = (x_j, y_j)$ is assigned a potential $POET_j$ according to its location with respect to all other data points as set out in Eq. 3.14:

$$POET = \sum_{k=1}^{N} \exp\left(-\left(\frac{4}{r_a^2}\right) \times \|z_j - z_k\|^2\right), \qquad (3.14)$$

where N is the number of data points, $\|.\|$ is the Euclidean distance and r_a is a positive constant called the cluster radius.

From Eq. 3.14 it can be seen that the potential of a data point to be taken as a cluster is higher when more data points are closer. Thus, the data point with the highest potential, denoted by $POET_1^*$, is considered as the first cluster centre $c_1 = (x_{c1}, y_{c1})$. The potential is then recalculated for all other points, excluding the influence of the first cluster centre, according to Eq. 3.15:

$$POET_j^{new} = POET_j^{old} - P_1^* \exp\left(-\left(\frac{4}{r_b^2}\right)\right) \times \|z_j - c_1\|^2, \qquad (3.15)$$

where $r_b = \eta r_a$ is the radius defining the neighbourhood that will have measurable reductions in potential, and η is a positive constant called the 'quash factor'.

Again, after potential recalculation with the above equation, the data point with the highest potential $POET_2^*$ is considered to be the next cluster $c_2 = (x_{c2}, y_{c2})$ if

$$POET_2^* \succ \bar{\varepsilon} POET_2^*, \qquad (3.16)$$

with $\bar{\varepsilon}$ the accept ratio. If this is not the case but the condition in Eq. 3.17 holds, the data point is still accepted as the next cluster centre c_2:

$$\frac{d_{\min}}{r_a} + \frac{POET_2^*}{POET_1^*} \geq 1, \qquad (3.17)$$

where $d_{\min}$ is the minimal distance between c_2 and all previously founded cluster centres (Eq. 3.17).

Further iterations can then be performed to obtain new clusters c_l. If a possible cluster centre does not fulfil the above described conditions, it is rejected as a cluster centre and its potential is set to 0. The data point with the next highest potential $POET_k^*$ is selected as the new cluster centre and retested. The clustering ends if the following condition is fulfilled:

$$POET_k^* \succ \underline{\varepsilon} POET_1^*, \qquad (3.18)$$

where $\underline{\varepsilon}$ is the reject ratio (RR) (Eq. 3.18).

The reject ratio (RR) was found to have the most influence on the cluster resolution. The RR is used

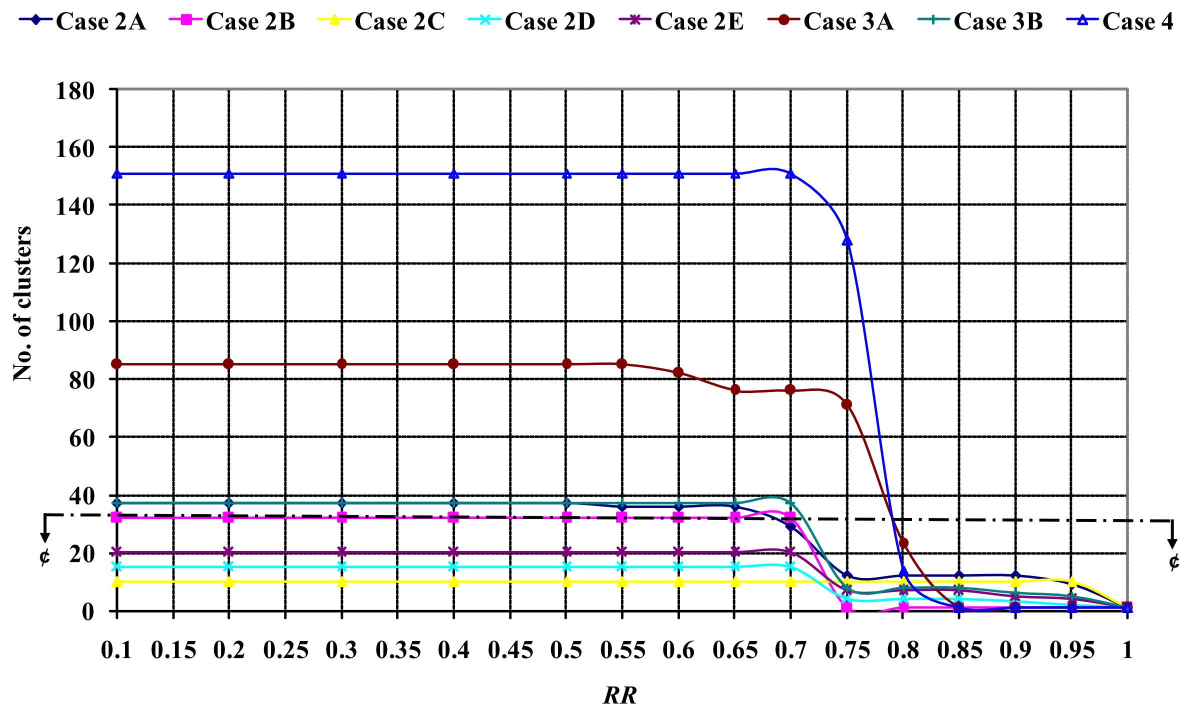

Figure 3.10. Number of clusters vs *RR* for all combination alternatives used in the ANFISP_S_SLR and ANFISP_S_SMAR modelling cases.

by the SCA as a stopping criterion to halt any further attempts to determine new clusters. For each combination alternative the *RR* was varied from 0.1 to 0.5 in increments of 0.1, and from 0.5 to 1 in increments of 0.05. The calculated numbers of clusters are plotted against the reject ratio in Fig. 3.10. It is clear that for all combination alternatives, changing the *RR* value between 0.1 and 0.65 did not change the number of the resulting clusters. Then there is a gradual drop in the number of clusters corresponding to an increase in *RR* up to 0.8, which is followed again by a constant number of clusters until *RR* reaches the value of 0.95. The *RR* value of 1 corresponds to one cluster and this is consistent with a lumped catchment. Note that for the combination alternatives 3A and 4 the number of clusters corresponding to *RR* values less than and equal to 0.75, which is significantly higher than the corresponding values for the other cases.

For each combination of spatial variables an upper limit of 40 clusters (shown by section ¢–¢ in Fig. 3.10) is applied to select cases to be considered in the ANFISPs tested here. The choice of 40 is somewhat arbitrary but the aim is to avoid an excessive number of parameters in the ANFISPs. As the number of clusters remains constant for a range of *RR* values, the number of cases tested for the ANFISP_S_SLR and ANFISP_S_SMAR models in the Brosna catchment varies from one combination alternative to another (Table 3.4).

Generally, when more than one subset is used for the rainfall and evaporation, then the number of parameters to be calibrated for each case in the ANFISP_S scenario is obtained by multiplying the number of parameters for the ANFISP_T scenario (given by Eq. 3.11) by the number of clusters or HHCUs involved. However, as one fuzzy subset is used for both rainfall and evaporation in the ANFISP_S scenario then only the parameters of the models (SLR and SMAR) must be calibrated. Therefore, there is no need for the sequential iterative procedure used in the ANFISP_T scenario and instead only the least squares method is used for the linear optimisation problem in the ANFISP_T_SLR, whereas the GA is used for the non-linear one in the ANFISP_T_SMAR. The NSR^2, *ARE* criteria and hydrograph plotting are also used to assess the performance of the models in this scenario.

Table 3.4. The ANFISP_S scenario cases used to test the hydrological component.

Model	Case	No. of HHCUs
ANFIS_P_S_SLR_2A_, ANFIS_P_S_SMAR_2A_	1	1
	2	9
	3	12
	4	29
	5	36
	6	37
ANFIS_P_S_SLR_2B_, ANFIS_P_S_SMAR_2B_	1	1
	2	32
ANFIS_P_S_SLR_2C_, ANFIS_P_S_SMAR_2C_	1	1
	2	10
ANFIS_P_S_SLR_2D_, ANFIS_P_S_SMAR_2D_	1	1
	2	2
	3	3
	4	4
	5	15
ANFIS_P_S_SLR_2E_, ANFIS_P_S_SMAR_2E_	1	1
	2	4
	3	5
	4	7
	5	20
ANFIS_P_S_SLR_3A_, ANFIS_P_S_SMAR_3A_	1	1
	2	23
ANFIS_P_S_SLR_3B_, ANFIS_P_S_SMAR_3B_	1	1
	2	5
	3	6
	4	8
	5	37
ANFIS_P_S_SLR_4_, ANFIS_P_S_SMAR_4_	1	1
	2	14

3.9.3 Results of the ANFISP_T and the ANFISP_S Scenarios

The key issue is to determine whether the introduction of combined sub-models to account for temporal or spatial pattern variations improves the simulation compared to that of a single lumped catchment model. First, the results corresponding to the lumped case (Case 1 in Table 3.1 for ANFISP_T and Cases 1 of all combination alternatives in Table 3.4 for ANFISP_S) are calculated. These provide a baseline to be used in assessing the second set of results corresponding

Table 3.5. NSR2 and ARE results for the ANFIS_P_T scenario in the 11 catchments.

Model	Catchment	Best case	*NSR*² (%)				*ARE* (%)			
			Lumped case		Best combined case		Lumped case		Best combined case	
			Calib.	Valid.	Calib.	Valid.	Calib.	Valid.	Calib.	Valid.
ANFISP_T_ SLR	Bird Creek	9	15.86	23.34	24.37	42.54	71.99	81.57	72.99	79.31
	Blue Nile	10	71.69	71.38	87.44	77.82	28.94	22.45	25.43	24.08
	Brosna	8	49.36	32.36	60.24	40.53	29.92	34.37	28.35	33.27
	Chu	9	15.23	29.13	39.27	56.95	57.64	55.73	55.01	52.72
	Halda	8	53.43	69.84	67.63	67.78	38.95	49.57	38.60	52.75
	Kelantan	10	28.88	22.78	52.39	34.78	33.16	29.25	26.79	30.45
	Nan	10	65.29	68.94	69.57	69.54	39.05	33.69	39.98	44.46
	Sg. Bernam	8	60.35	52.14	62.73	47.90	24.88	26.77	27.00	31.47
	Shiquan-3	8	13.45	6.32	28.33	24.40	54.16	49.95	51.76	49.80
	Sunkosi-1	9	77.80	78.78	80.73	82.10	27.86	25.95	27.35	23.55
	Wolombi Brook	9	10.27	-17.03	30.03	17.31	80.33	71.88	71.60	92.62
ANFISP_T_ SMAR	Bird Creek	7	85.85	66.58	89.72	75.27	67.70	60.50	67.45	63.73
	Blue Nile	4	93.26	83.00	94.57	86.53	17.37	29.65	16.22	24.28
	Brosna	4	87.93	83.86	89.81	86.18	15.66	19.17	15.37	18.01
	Chu	10	35.30	43.20	81.46	64.72	69.68	70.52	59.56	65.51
	Halda	10	62.42	69.56	83.76	68.82	34.45	43.35	33.26	54.25
	Kelantan	5	84.67	47.70	87.26	46.81	20.06	27.70	19.70	27.63
	Nan	7	76.36	80.48	83.88	80.70	34.71	26.29	33.29	27.30
	Sg. Bernam	4	73.51	21.49	76.40	5.93	23.38	43.05	23.22	46.19
	Shiquan-3	5	19.69	17.96	23.32	17.24	78.37	83.93	75.46	79.82
	Sunkosi-1	5	80.49	79.90	82.78	80.28	26.57	24.93	25.64	25.56
	Wolombi Brook	10	34.74	-33.82	89.15	58.39	70.41	108.54	59.11	112.46

to the best combined case. In each scenario, the best combined case can be described as the one with the highest NSR^2 during the calibration period compared to the others in the same group. The best combined case is an improvement over the lumped case if it scores a higher value for the NSR^2 criterion and a smaller value of the *ARE* criterion. In addition to these two numerical criteria, a graphical comparison of the simulated and observed hydrographs allowed a visual assessment of model fit.

In addition, the suitability of using a linear model, such as the SLR model, or a non-linear model, such as the SMAR model, in the fuzzy model is also addressed in the discussion.

3.9.3.1 ANFISP_T scenario – Lumped Case vs the Best Combined Case

For the ANFISP_T_SLR and ANFISP_T_SMAR models, the NSR^2 and *ARE* values for the calibration and validation periods are summarised for the 11 test catchments in Table 3.5. There is an improvement in the NSR^2 values during calibration for the best combined case over the lumped case. However, the best combined case improved the NSR^2 values for validation in nine catchments, the exceptions being Halda and Sg. Bernam for the ANFISP_T_SLR, and in seven catchments, the exceptions being Halda, Kelantan, Sg. Bernam and Shiquan-3 for the ANFISP_T_SMAR model. In one of these catchments, Sg. Bernam, the NSR^2 values during validation of the best combined case were markedly lower than the corresponding values for the lumped case in both the ANFISP_T_SLR and ANFISP_T_SMAR models, the differences being insignificant in the rest of the catchments.

In terms of the *ARE* criterion during calibration, the best combined case was better than the lumped case for the ANFISP_T_SLR in all but three catchments (Bird Creek, Kelantan and Sg. Bernam). During validation the combined models of the ANFISP_T_SLR gave better *ARE* values than the lumped case in five catchments but worse in six catchments (Blue Nile, Halda, Kelantan, Nan, Sg. Bernam and Wolombi Brook). The values of the *ARE* for calibration of the ANFISP_T_SMAR model exhibited a consistent improvement of the best combined case over the lumped case, whereas the values of the corresponding validation were worse in six catchments (Bird Creek, Halda, Nan, Sg. Bernam, Sunkosi-1 and Wolombi Brook).

The best combined case was not consistent for the ANFISP_T_SLR and ANFISP_T_SMAR models. For the former model each of Cases 8 and 9 was the best in four catchments, while Case 10 was the best in three catchments. Different trends were obtained in the latter model as each of Cases 4, 5 and 10 was the best in three catchments and Case 7 was the best in two catchments.

3.9.3.2 ANFISP_T_SLR vs ANFISP_T_SMAR

The values of the NSR^2 and *ARE* criteria are shown in Table 3.5 for the 11 catchments and for both the lumped case and the best combined case. There was no single best model in all cases. For the lumped case, the NSR^2 values for the ANFISP_T_SMAR model were better than the values of the ANFISP_T_SLR in all catchments for calibration and in all but two catchments (Sg. Bernam and Wolombi Brook) in validation. The ANFISP_T_SMAR was better than the ANFISP_T_SLR in all but one catchment (Shiquan-3) in calibration and in all but three catchments (Sg. Bernam, Shiquan-3 and Sunkosi-1) in validation.

The ARE values showed even more mixed results as ANFISP_T_SMAR did not outperform ANFISP_T_SLR in terms of *ARE* for the lumped case at two catchments (Chu and Shiquan-3) during calibration and at five catchments (Blue Nile, Chu, Sg. Bernam, Shiquan-3 and Wolombi Brook) during validation. Similar results hold for the best combined case in calibration. It holds also in validation but with the addition of two more catchments (Halda and Sunkosi-1).

3.9.3.3 Hydrographs Matching in the ANFISP_T Scenario

The observed and simulated hydrographs of the best combined cases of ANFISP_T_SLR and ANFISP_T_SMAR for four catchments, Blue Nile, Brosna, Chu and Wolombi Brook are plotted in Figs 3.11 to 3.14. Each of the four catchments exhibits different hydrological behaviour and this is reflected in the shape of its hydrograph. In addition, the period of each hydrograph is chosen to be within the validation period for two reasons: (i) to verify the model parameters and (ii) to ensure that there is no influence for any initial conditions on the models' performances.

The four graphs demonstrate the ability of the ANFISP_T_SMAR to capture most of the hydrograph features. This model showed an outstanding performance in reproducing the observed hydrograph in the Chu catchment (Fig. 3.13), and to some extent the one in the Blue Nile catchment (Fig. 3.11). In the other two catchments, Brosna and Wolombi Brook (Figs 3.12 and 3.14 respectively), features such as rising limb, recession and base flow were better generated by this model than the individual peaks.

The ANFISP_T_SLR was able to match the non-linearity in the two flashy catchments, Chu and Wolombi Brook (Figs 3.13 and 3.14 respectively). In contrast, this model, with its linear component, was particularly bad for the Brosna, which has a large base flow component, and for the Blue Nile, which has a strong seasonal pattern.

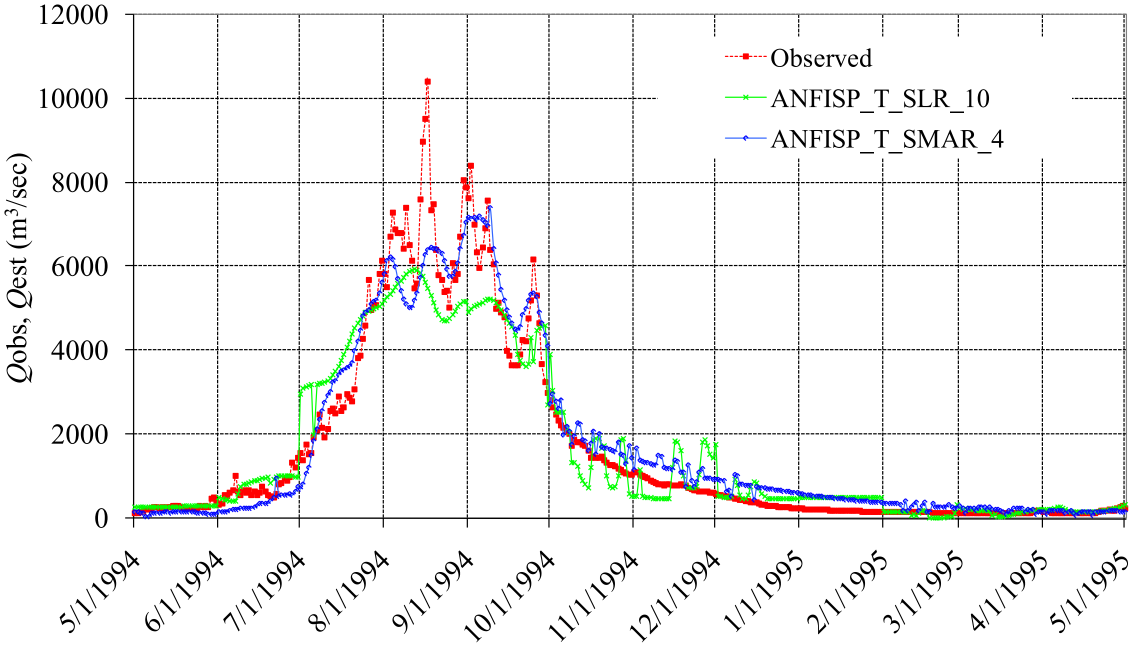

Figure 3.11. Simulated and observed hydrographs of the Blue Nile catchment.

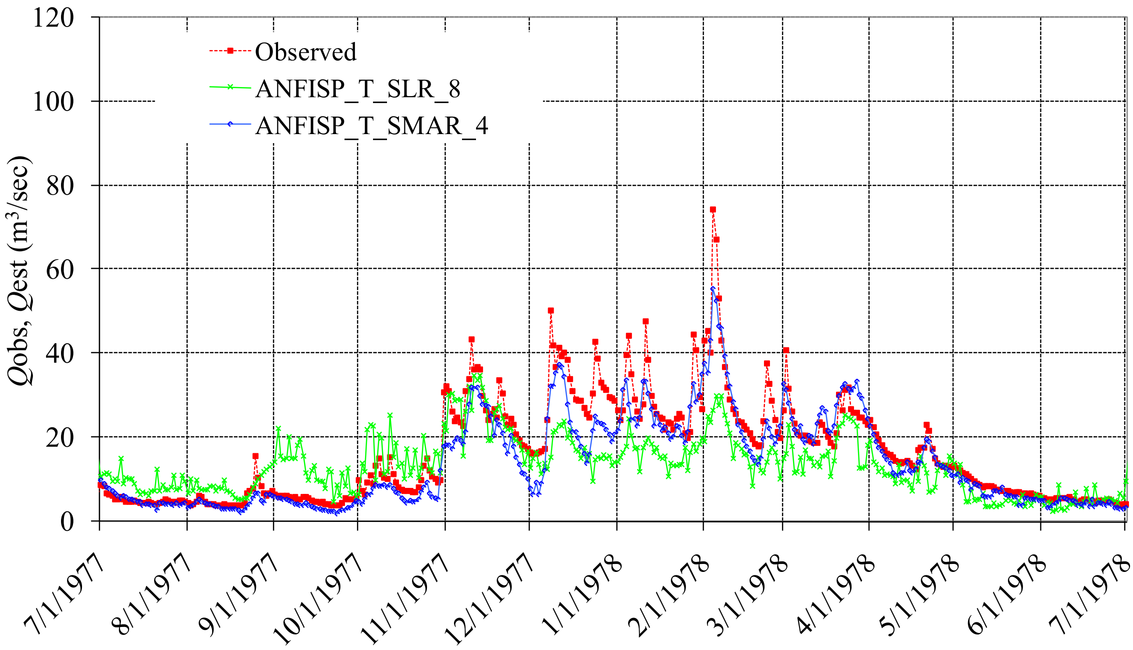

Figure 3.12. Simulated and observed hydrographs of the Brosna catchment.

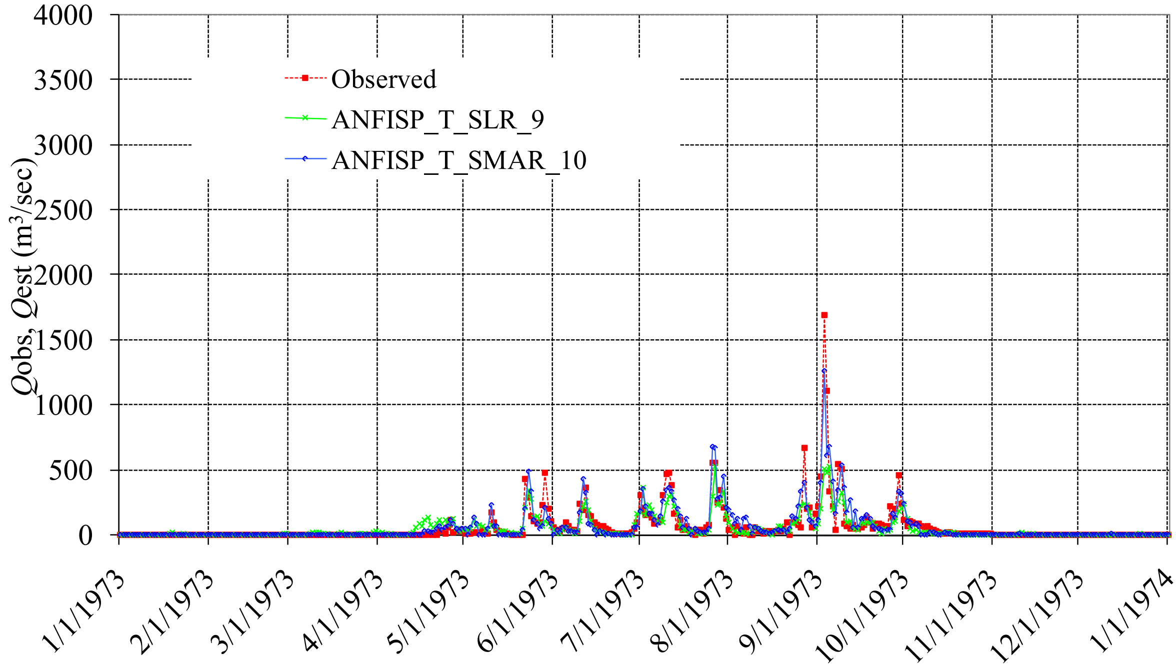

Figure 3.13. Simulated and observed hydrographs of the Chu catchment.

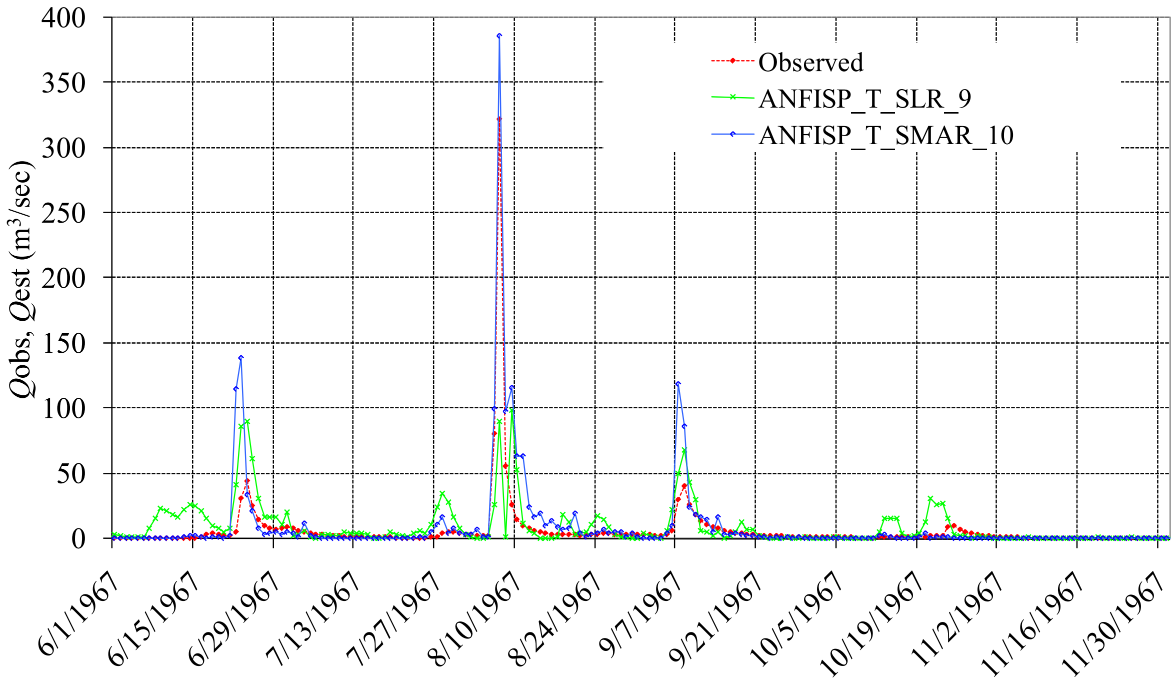

Figure 3.14. Simulated and observed hydrographs of the Wolombi Brook catchment.

Table 3.6. *NSR*² and *ARE* results for the ANFISP_S scenario – Brosna catchment.

Model	id.	case	No. of HHCUs	*NSR*² (%)		*ARE* (%)	
				Calib.	Valid.	Calib.	Valid.
ANFISP_S_SLR	2A,2B,…,4	1	1 (lumped model)	49.36	32.36	29.92	34.37
	2A	2	9	50.18	32.68	29.47	33.98
	2B	2	32	48.87	31.04	30.26	34.71
	2C	2	10	50.07	32.65	29.54	33.99
	2D	3	3	50.44	32.93	29.15	33.76
	2E	3	5	50.42	32.92	29.29	33.90
	3A	2	23	49.26	31.75	30.29	34.75
	3B	2	5	50.22	32.95	29.34	33.90
	4	2	14	49.94	32.35	29.81	34.32
ANFIS_S_SMAR	2A,2B,…,4	1	1 (lumped model)	87.96	84.18	15.44	18.60
	2A	6	37	91.17	87.91	13.68	16.38
	2B	2	32	90.25	86.50	14.08	16.67
	2C	2	10	90.31	82.90	14.19	19.64
	2D	4	4	91.28	85.82	13.63	17.86
	2E	4	7	91.16	84.53	13.86	19.23
	3A	2	23	90.67	85.68	14.44	18.03
	3B	3	6	91.23	85.59	13.99	17.98
	4	2	14	91.42	86.00	13.47	17.57

3.9.3.4 ANFISP_S Scenario – Lumped Case vs the Best Combined Case

Table 3.6 shows the values of the *NSR*² and *ARE* model efficiency criteria for the ANFISP_S_SLR and ANFISP_S_SMAR models for both calibration and validation, and for the lumped case and the best case for all spatial combination alternatives in the Brosna catchment. The results for the lumped case (treating the catchment as a single unit) of each of the ANFISP_S_SLR and the ANFISP_S_SMAR models were identical for all combination alternatives since this involved one HHCU and one fuzzy subset for rainfall and evaporation.

The *NSR*² results for calibration and validation for the ANFISP_S_SLR do not differ significantly from each other. In contrast, for the ANFISP_S_SMAR the *NSR*² values for calibration for the best cases were significantly higher than for the lumped case. In validation, a significant improvement in *NSR*² was obtained by the best case of the combination alternatives 2A, 2B and 4, for which the *ARE* values were amongst the lowest. There were no significant differences among the *ARE* values for the ANFISP_S_SLR, and likewise among those of the ANFISP_S_SMAR model. However, the *ARE* values of the ANFIS_P_S_SLR were all much greater than those of the ANFISP_S_SMAR. The results in Table 3.6 suggest that, while the 2A combination alternative performs significantly better than the lumped case, the improvement is not as impressive as that obtained for the ANFISP_T scenario.

3.9.3.5 ANFISP_S_SLR vs ANFISP_S_SMAR

The superiority of SMAR over SLR can be seen easily from the *NSR*[2] and the *ARE* values. The introduction of non-linearity in the SLR model through the combination of its sub-models did not produce any significant improvement. This is not surprising because the use of HHCUs in this context has no effect on the SLR model itself but rather it assigns weights to similar sub-models with the same characteristics as the lumped model. In contrast, in the SMAR model each sub-model adds to the non-linearity of the combined model and this in turn provides the greater flexibility required in modelling the rainfall–runoff relationship.

For both ANFISP_S_SLR and ANFISP_S_SMAR models, using large number of HHCUs, i.e. sub-models, did not improve the results significantly and this means there is an upper limit for the number of HHCUs above which no significant improvement can be expected. Thus, using an excessive number of HHCUs might result in including some redundant HHCUs which have no effect. Again, this behaviour is not surprising because the spatial parameters of the HHCUs have no influence on the models. Different responses would be obtained if some inputs to the sub-models depended on the characteristics of HHCUs.

3.9.3.6 ANFISP_T vs ANFISP_S

The important question arising out of the results for the two combination scenarios is which combination ANFISP scenario performs best. To answer this requires a comparison between the best models of the two scenarios. For illustration only, this is done here for the Brosna catchment as the ANFISP_S was applied for that catchment only. From Tables 3.5 and 3.6 it is possible to identify the ANFISP_T_SMAR_4 (Case 4) and ANFISP_S_SMAR_4_14 (combination alternative 4 and HHCUs = 14) as the best models for the two scenarios respectively in the Brosna catchment.

The *NSR*[2] and *ARE* results for these two models are not substantially different from each other. The fit between the observed hydrograph and the simulated hydrographs for each model are shown in Fig. 3.15 and

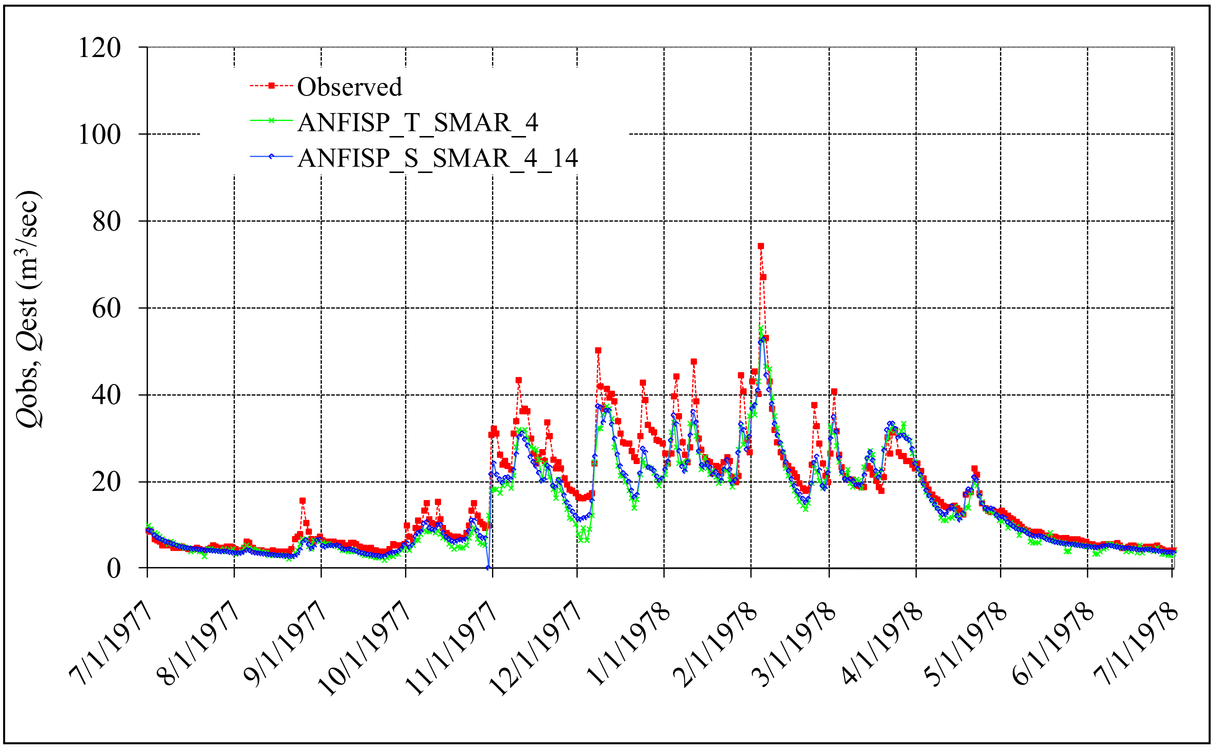

Figure 3.15. Comparison between ANFISP_T and ANFISP_S best models in the Brosna catchment.

they represent the same period used in Fig. 3.12. The visual comparison between the observed hydrograph and the two models does not show any major differences between models to the extent that one can be declared consistently superior to the other. Thus, the use of the ANFISP_S scenario, which is more data demanding compared to the ANFISP_T scenario, is not justified if the intention of the modelling is to produce outputs only for the outlet of a catchment. Therefore, only the ANFISP_T_SMAR model is used to generate the hydrological variables required by the GOPC model for the P modelling. Nevertheless, the use of the ANFISP_S scenario for the same purpose is worth investigating but this is left for future work.

3.10 Phosphorus Component of the ANFISP Model

The way in which the GOPC model has been formulated allows its use in conjunction with any potential hydrological model that produces the required variables. Nasr and Bruen (2006) used the Système Hydrologique Européen TRAnsport (SHETRAN) model (Ewen et al., 2000) as a hydrological model for the GOPC and applied them to simulate the TP load in three catchments in Ireland. In this study, the model was used in a fully distributed mode as each catchment had been divided into square cells of 100 m sides. In contrast, the GOPC in this present study was used in conjunction with the SMAR model in the ANFISP_T scenario. The resulting hydrological and P models were ANFISP_T_SMAR and ANFISP_T_GOPC respectively.

As mentioned earlier, the modelled catchment in the ANFISP_T scenario is considered as a single lumped unit; however, with the aid of IF-THEN fuzzy logic rules this lumped catchment configuration is transformed into a combination of sub-models. Each sub-model has a separate set of parameters representing different P transport behaviours that corresponds to different patterns of the two driving variables, rainfall and evaporation. Therefore, the total number of parameters ($npar_{\text{total}}$) which require identification can be determined as in Eq. 3.19:

$$npar_{\text{total}} = \left(npar_{SMAR} + npar_{\text{GOPC}}\right) * nrl + npar_{\text{MF}}\,, \qquad (3.19)$$

where $npar_{SMAR}$ is the number of parameters in the SMAR model, $npar_{GOPC}$ is the number of parameters in the GOPC model, nrl is the number of the fuzzy rules and $npar_{\text{MF}}$ is the total number of parameters of all membership functions of the fuzzy subsets of the input variables.

There are 21 parameters in the GOPC model used to model the TP load, whereas 12 parameters are used by SMAR to calculate the required hydrological variables. Table 3.7 shows the number of fuzzy rules in each modelling case of the ANFISP_T scenario tested in this study. The table also shows the number of fuzzy subsets used for rainfall and evaporation. A two-parameter Gaussian function was used for each membership function of the fuzzy subsets of the input variables and, as a result, the total number of parameters is twice the number of fuzzy subsets. The problem of calibrating all the above parameters is a non-linear one and was done with the GA. For each modelling case two groups of data were required. The first group, which includes rainfall, evaporation and discharge, was used to run and calibrate the ANFISP_T_SMAR model in a similar fashion to that described in Section 3.8.1. The second group, which includes the estimated amount of inorganic and organic fertiliser applications and the TP load at the catchment outlet, was used for the ANFISP_T_GOPC model. Here, the calibration is a one-step procedure since each of the input variables (inorganic and organic fertiliser applications) has only one fuzzy subset, then only the parameters of the GOPC model must be calibrated.

Table 3.7. The ANFISP_T scenario cases used to test the phosphorus component.

Model	Case	No. of fuzzy subsets		Number of rules
		Rainfall	Evaporation	
ANFISP_T_SMAR_, ANFISP_T_GOPC_	1	1	1	1
	2	1	2	2
	3	1	3	3
	4	1	4	4
	5	2	1	2
	6	2	2	4
	7	2	3	6
	8	2	4	8
	9	3	1	3
	10	3	2	6
	11	3	3	9
	12	3	4	12
	13	4	1	4
	14	4	2	8
	15	4	3	12
	16	4	4	16

All cases of the models shown in Table 3.7 were tested by applying them to the Oona Water catchment in Co. Tyrone. The catchment is part of an international river basin district managed collaboratively by the Republic of Ireland and Northern Ireland. The catchment area draining through the outlet at Shanmoy is 96 km^2 (Fig. 3.16). The CORINE map of this catchment (Fig. 3.17) shows that the dominant land use is grassland which ranges in quality from unimproved pasture to improved pasture and intensively used silage meadows. Significant areas of natural vegetation also exist. Carboniferous series sandstone and limestone characterise the catchment geology while the soil (Fig. 3.18) is part of an extensive drumlin belt and is clay rich and highly gleyed with low infiltration rates.

The available rainfall, evaporation and TP data covers the period from 1/10/2001 up to 31/1/2003 (Fig. 3.19). For the inorganic and organic fertiliser data, the amounts estimated by Nasr and Bruen (2006) were also used here. The first 67% of the data was used in the model calibration while the remaining 33% was used to verify the calibrated models. The NSR^2 criterion was applied to compare the results of all the modelling cases. Using the same data set, the SWAT model has been applied to the Oona Water catchment in a manner similar to that described in Nasr and Bruen (2006). All model parameters that had been used in the flow and P simulation were obtained through a manual calibration procedure. The simulated discharges by the model were compared with the results of the ANFISP_T_SMAR model, whereas the TP loads were compared with the ANFISP_T_GOPC results.

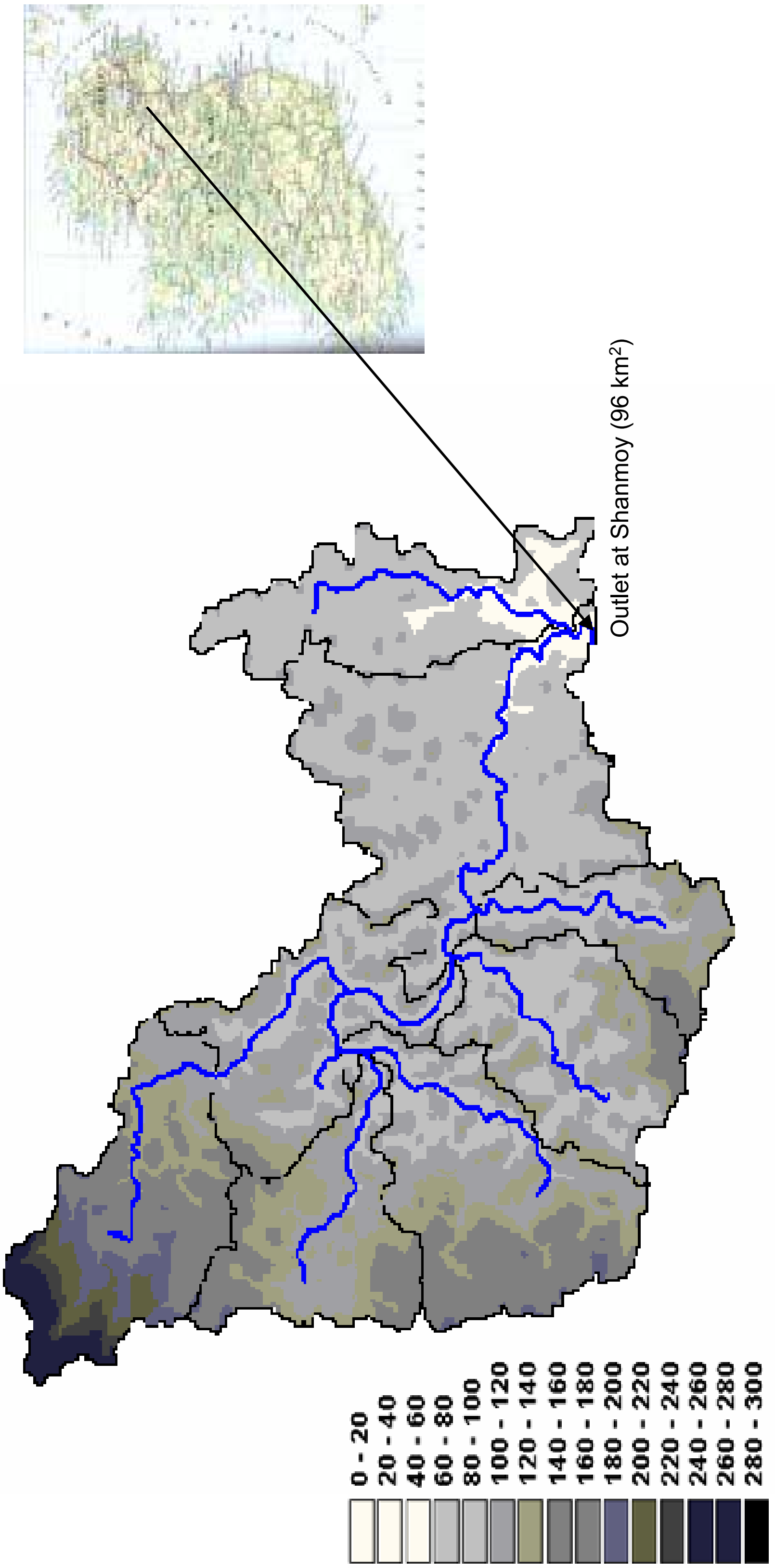

Figure 3.16. Oona Water catchment – location, DEM and streams network.

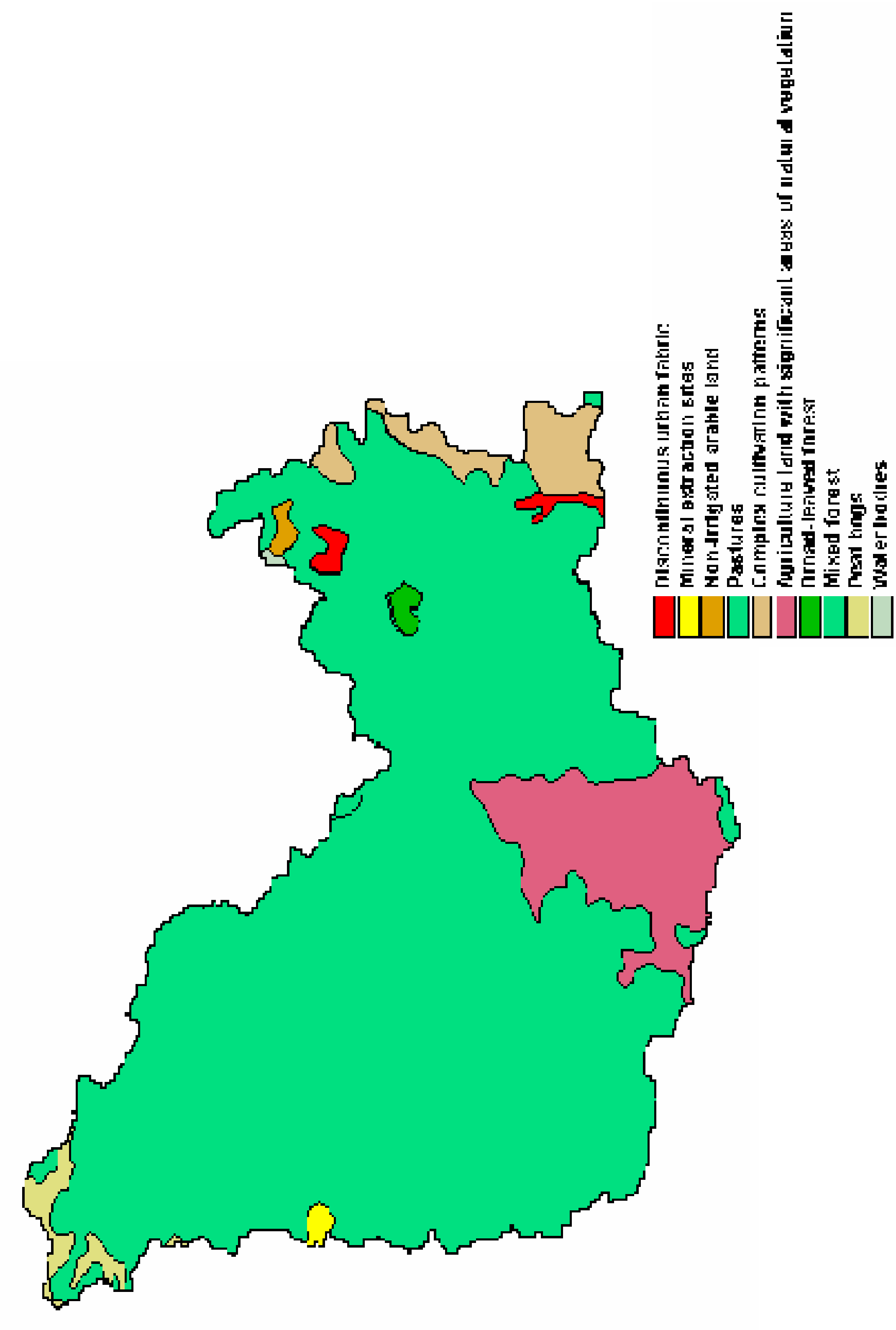

Figure 3.17. Oona Water catchment – CORINE land-use classes.

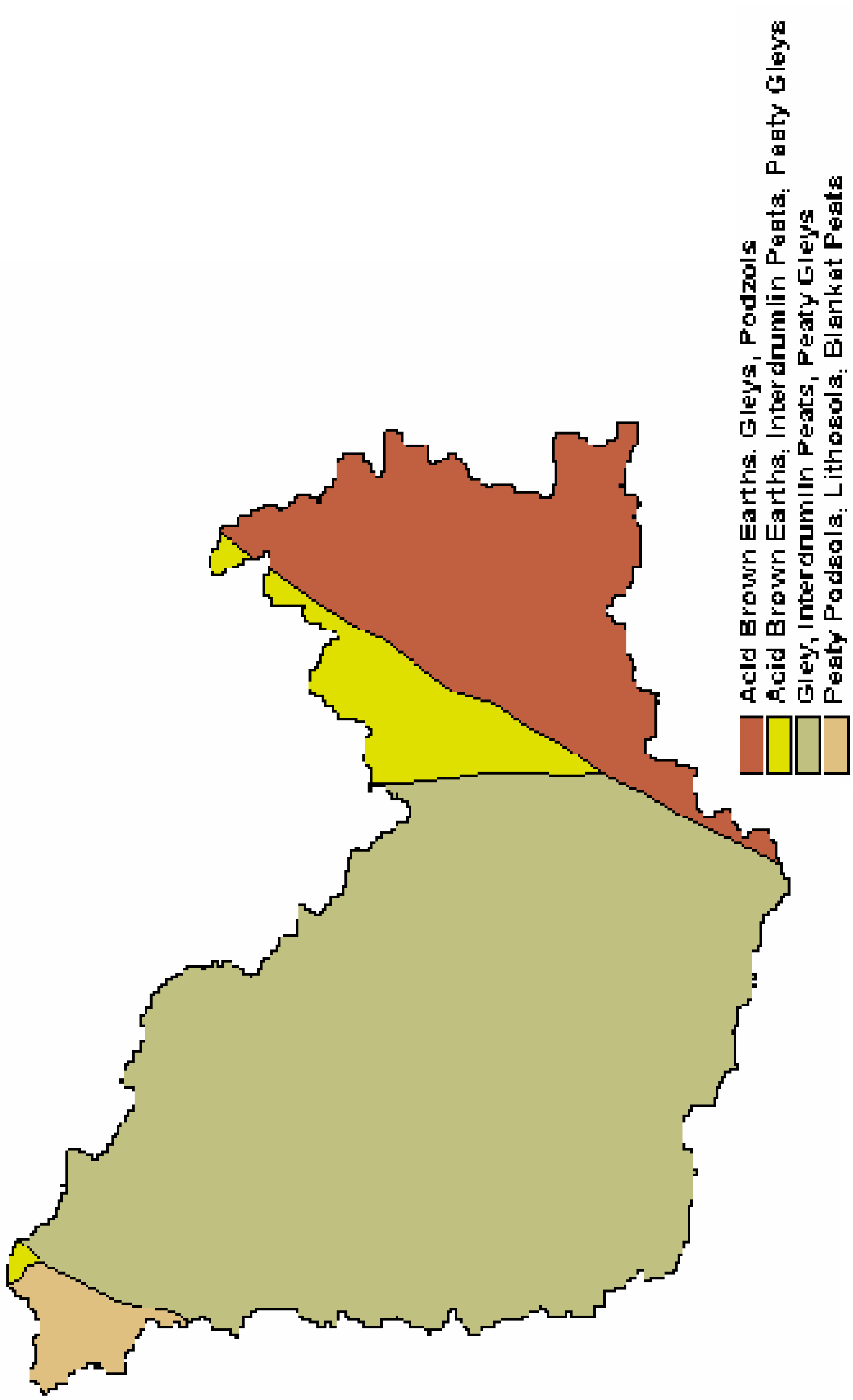

Figure 3.18. Oona Water catchment – soil types.

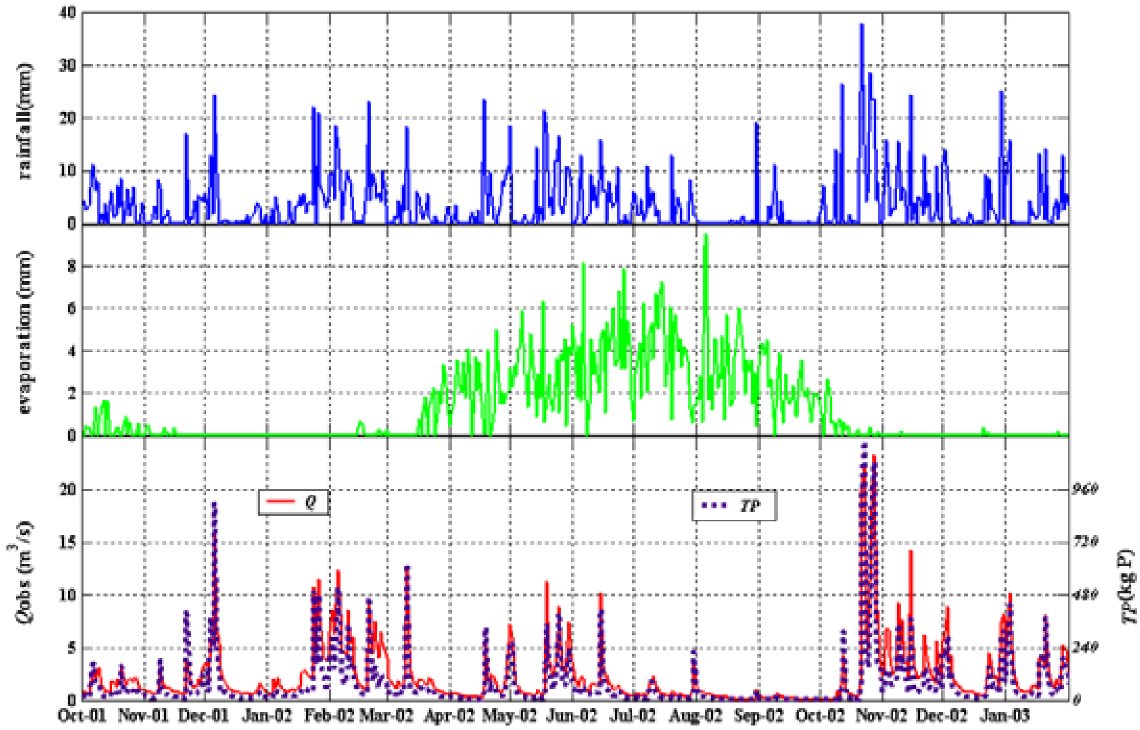

Figure 3.19. Rainfall, evaporation and discharge (*Q*) time series – Oona Water catchment.

Table 3.8. *NSR*^{2} (%) values of discharge (*Q*) and total phosphorus (TP) simulations by ANFISP_T_SMAR and ANFISP_T_GOPC – Oona Water catchment.*

Case	Q/ANFISP_T_SMAR			TP/ANFISP_T_GOPC		
	Calib.	Valid.	Rank	Calib.	Valid.	Rank
1	80.49	**73.21**	2	67.20	42.62	5
2	80.12	66.24	10	68.48	41.31	6
3	81.01	64.91	13	66.18	4.86	15
4	80.96	62.25	15	67.48	29.92	11
5	81.47	**73.11**	1	68.54	36.77	9
6	82.00	72.85	3	69.99	-22.25	16
7	**82.87**	65.35	12	**72.01**	13.21	13
8	81.28	66.44	9	69.38	37.38	8
9	81.68	65.64	11	69.55	34.67	10
10	81.92	70.01	4	69.96	53.75	2
11	81.11	69.88	5	69.59	38.17	7
12	81.63	67.06	8	71.80	6.84	14
13	74.82	62.12	16	49.98	48.15	4
14	81.93	67.10	7	69.46	17.44	12
15	81.94	63.89	14	71.55	**54.05**	1
16	82.64	68.87	6	69.40	48.79	3

*The underlined and bold figures are the best results among all cases during calibration and validation of the discharge (Q) and total phosphorus (TP) models.

3.10.1 Results

In Table 3.8, the NSR^2 values for the ANFISP_T_SMAR and ANFISP_T_GOPC models during calibration and verification in each case of the fuzzy rules are given. The ANFISP_T_SMAR results indicate the performance of simulating the discharge values at the catchment outlet, whereas the ANFISP_T_GOPC values assess the TP load simulation. The performances of all cases have been ranked according to their verification results since model validation is always crucial in determining the applicability of the model. If two or more cases score similar NSR^2 values in validation, then their rank is determined by their NSR^2 values in calibration. Two columns showing the ranking results for the two models are added in Table 3.8.

3.10.2 ANFISP_T_SMAR Flow Results

Cases 5 and 1 have NSR^2 values in validation of almost the same magnitude; however, the NSR^2 value for Case 5 in calibration outperforms the one for Case 1. Therefore, Case 5 has been ranked the top of the list. The best NSR^2 in calibration was obtained by Case 7 but its NSR^2 in validation was considerably poor and relegates it to 12th position in the ranking list. The worst NSR^2 values in calibration and validation are from Case 13 and both values are significantly lower than those for the best case.

For the best case (Case 5) two fuzzy subsets were used for the rainfall while a single one was used for the evaporation, and this resulted in two sub-models. On the other hand, the worst case (Case 7) used two fuzzy subsets for the rainfall and three for the evaporation.

3.10.3 ANFISP_T_GOPC TP Results

In calibration, the NSR^2 value of Case 7 for TP is the best and this case was also the best for the flow. This is not a surprising result because the flow simulation has a direct influence on the TP simulation: as a result, in calibration the best results for both variables are obtained from the same case. For Case 7, Fig. 3.20 shows plots of the observed and estimated values of the discharge and the TP during the validation period. The graphs illustrate the good performance of ANFISP_T_SMAR and ANFISP_T_GOPC in reproducing the low values while there are some deficiencies in their capturing some of the peaks.

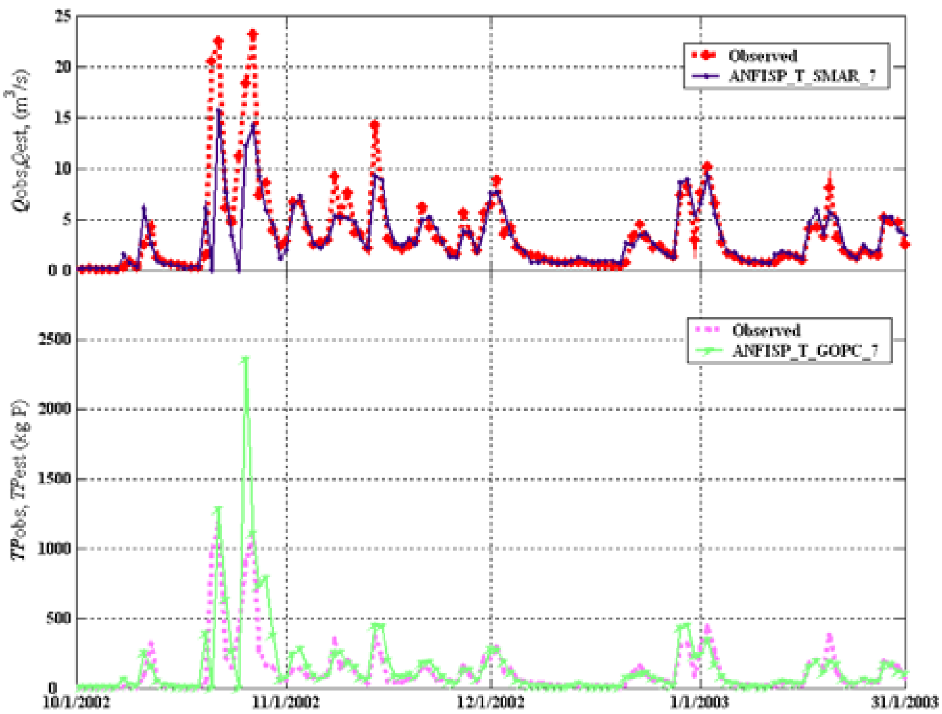

Figure 3.20. Plots of discharge (*Q*) and total phosphorus (TP) during validation for the ANFISP_T model (Case 7) in the Oona Water catchment.

The ranking list for TP results in validation is different from the flow one. At the top of this list is Case 15 which used four and three fuzzy subsets for the rainfall and evaporation respectively. In contrast, Case 6 with two rainfall fuzzy subsets and two evaporation fuzzy subsets is at the bottom. It is obvious that as many as 12 sub-models are required to adequately capture the variations in the processes involved in the TP simulation by Case 15. The discharge and TP plots of Case 15 are presented in Fig. 3.21. The hydrograph shapes do not differ much from those in Fig. 3.20 for Case 7. Likewise, the TP graphs for Cases 7 and 15 have similar shapes except for the largest two peaks, which have been underestimated by the latter and overestimated by the former. The differences in simulation of the largest peaks explain the better NSR^2 value for Case 15 than that for Case 7. Therefore, based on its superiority in terms of NSR^2 during validation and its comparable performance during calibration, Case 15 can be considered as the best model to simulate both the discharge and TP loads in the Oona Water catchment.

3.10.4 ANFISP vs SWAT

As mentioned previously, Case 15 was considered the best ANFISP model for both the discharge and the TP load simulation. Therefore, its results during the calibration and validation were compared against the SWAT results. For the calibration period, ANFIS_T_SMAR was best for discharge simulation, with an NSR^2 of 82%, but ANFISP_T_GOPC was best for simulating TP load, with an NSR^2 of 72%. These values considerably outperformed the corresponding ones of 73% and 60% for the discharge and the TP respectively from a manually calibrated SWAT model covering the same period. However, the validation test gave the opposite result with SWAT achieving a NSR^2 of 86% for both discharge and TP while ANFISP_T_SMAR had 72% for discharge and ANFISP_T_GOPC had 54% for TP. To explain the drop in NSR^2 values during the validation period for the ANFISP model, both the hydrograph and TP graphs are plotted in Fig. 3.22. It is obvious that peak values in the hydrograph and the TP graph were not well represented by the ANFISP model

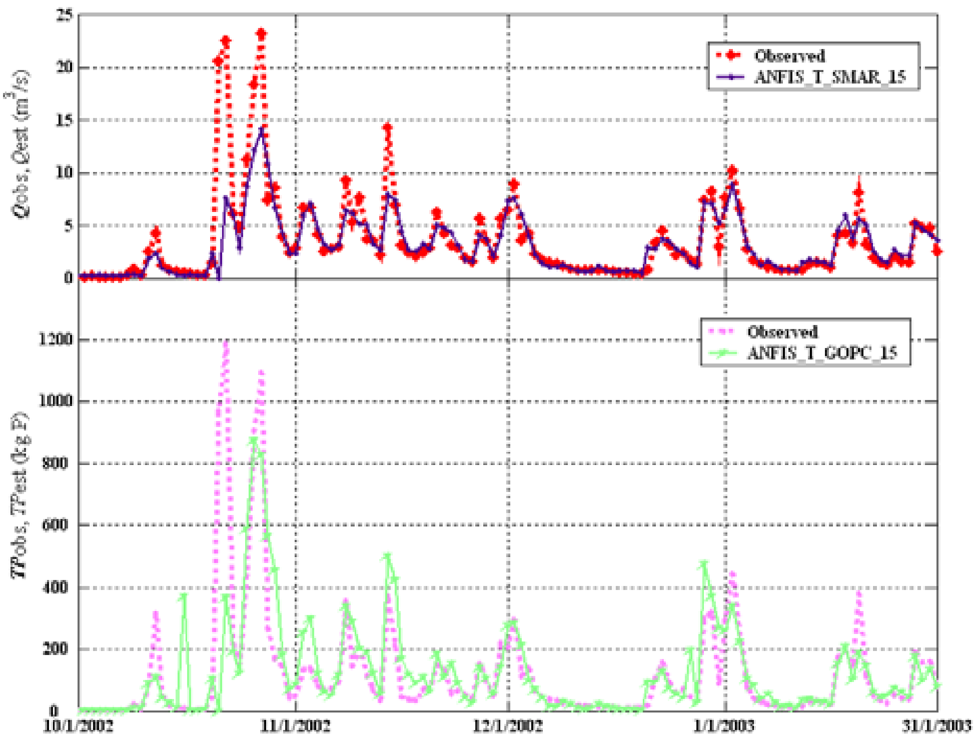

Figure 3.21. Plots of discharge (*Q*) and total phosphorus (TP) during validation for the ANFISP_T model (Case 15) in the Oona catchment.

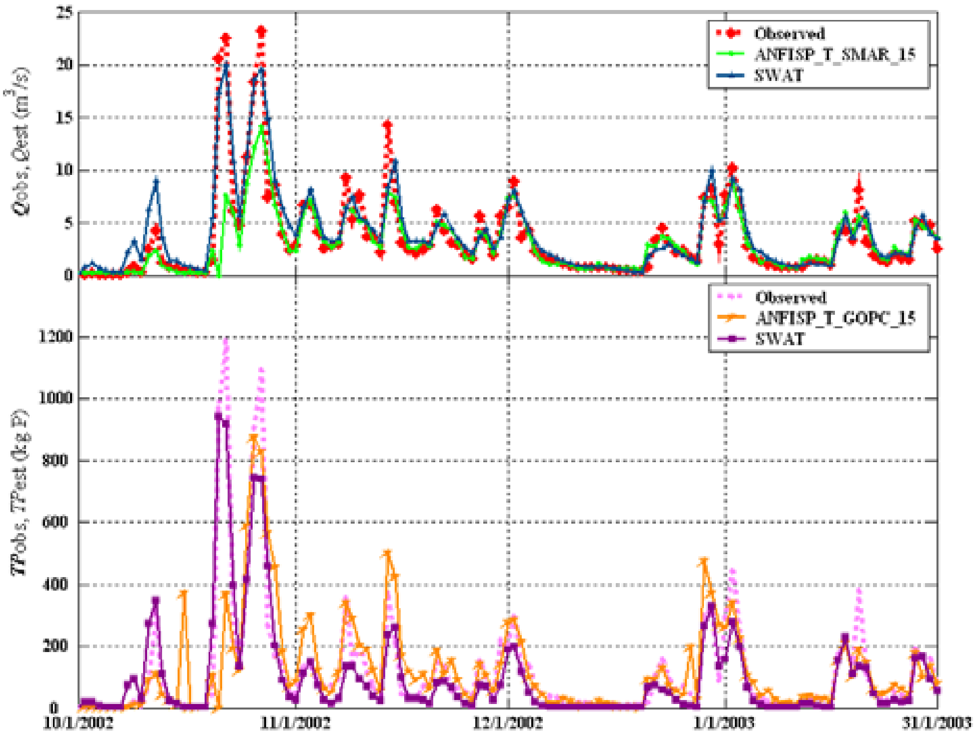

Figure 3.22. Plots of discharge (*Q*) and total phosphorus (TP) during validation for the ANFISP_T model (Case 15) and the SWAT model.

and this is the main cause for the drop in NSR^2 values. Therefore, for a good TP modelling it is important to have a good flow simulation, a feature that has been emphasised a number of times elsewhere in this section. The ANFISP model results are acceptable, although not better than the more complex SWAT, and its performance could be improved if more data become available for achieving better tuning to the parameters. Nevertheless, the model can still be useful for the cases where the time series modelling is the goal, because the efforts required to build the ANFISP model are far less than those needed for a fully distributed physically based model such as SWAT.

3.11 Conclusion

In this study, the state-of-the-art neuro-fuzzy modelling approach has been used to develop a new ANFISP model for simulating the hydrological and water-quality processes involved in diffuse P loss. The model provides continuous simulation for the discharges and the TP loads at the outlet of a catchment and, once calibrated, the model can be used to predict the values for the same variables under different initial and boundary conditions than those used in calibration. This feature of the model makes it suitable for use as a management tool which can be used in the implementation of the WFD.

The hydrological component of the ANFISP model has been constructed in a way that accounts for the spatial and temporal variations in modelling the rainfall–runoff relationship. The consequent part of the ANFISP model, which transforms the inputs (rainfall and evaporation) into output (discharge), comprises a number of lumped SMAR sub-models. In addition, the performance of the ANFISP with SMAR as its output (consequent) component was compared with the one that used the SLR model as its output component. For each model, two scenarios, ANFISP_T and ANFISP_S, were used to formulate sub-models to address the temporal and spatial pattern variations of the variables respectively.

In the ANFISP_T scenario, the two models ANFISP_T_SLR and ANFISP_T_SMAR, were applied to 11 catchments from around the world. A split-sample technique was used and in most cases the neuro-fuzzy combined sub-models were better than the lumped model. The ANFISP_T_SMAR model was, in general, better than the ANFISP_T_SLR.

To address spatial variation in response, an SCA was used in the ANFISP_S scenario to derive a number of HHCUs exhibiting homogenous hydrologic responses. Three spatial layers representing DEM, land-use and soil maps of the Brosna catchment in Ireland were processed by GIS software to prepare data for four variables (elevation, slope index, generalised land-use type and soil type) used in the clustering algorithm. For all possible combination alternatives between the four variables, the relation between the *RR* parameter of the SCA and the resulting number of HHCUs was investigated. A remarkable improvement was achieved by the best case of the sub-models of ANFISP_S_SMAR compared to the lumped model. The ANFISP_S_SMAR model outperformed the ANFISP_S_SLR significantly, and this is probably due to its inclusion of non-linearity. Only a small number of HHCUs were required to obtain improved results, and using a larger number of HHCUs had a diminishing effect on enhancing the results of the ANFISP_S_SMAR model.

Comparison between the best results of the ANFISP_T_SMAR and ANFISP_S_SMAR models revealed that they are not significantly different. Due to the simplicity in applying the ANFISP_T_SMAR model, this model has been extended by adding the GOPC model for use in simulating the TP loads. The complete ANFISP_T model has been used to reproduce the discharges and TP loads at the outlet of the Oona Water catchment in Northern Ireland. The rainfall and evaporation inputs have been represented in a fuzzy way while the estimated amount of the inorganic and organic fertiliser loads inputs have been used directly. Different numbers of fuzzy subsets for the rainfall and evaporation have been used in 16 different combinations, and for each combination different fuzzy logic rules have been formulated. The combination of the results of all rules in each case has been interpreted as a use of different sub-models representing various catchment behaviours in transporting P to water. The results showed that the best simulation for the discharge was achieved when using two fuzzy subsets for the rainfall and a single subset for the evaporation. For the TP, the use of four rainfall subsets along with three evaporation subsets was the best combination.

The best results for the ANFISP_T model in the Oona Water catchment has been compared with those obtained from the SWAT model. During calibration the former outperformed the latter while in validation the opposite was true. Despite this inconsistency in the ANFISP_T performance, the results are generally encouraging. They prove that using the model is worthwhile when a good prediction of TP export is needed and a fully distributed physically based model, and the spatial database it requires, are unavailable.

4 Neuro-Fuzzy National Phosphorus Model

4.1 Introduction

Nowadays there is huge demand for food to satisfy the increasing population of the world. Like most countries Ireland has continually improved its agricultural output in order to meet the local demand for food as well as for exports. Using the land in any intensive agricultural activity will inevitably cause adverse impacts on the environment. The two most recent reviews of the water-quality status in Ireland revealed that the diffuse transport of phosphorus by surface and subsurface flows from the soil to the receiving waters is one of the major environmental problems (Lucey, 2009; Clabby et al., 2008). To address this problem, there is a need for a catchment- based management strategy which encapsulates all elements contributing to the loss of phosphorus. The Water Framework Directive (WFD) was introduced by the European Parliament in 2000 to provide the legal grounds required in developing and enforcing the implementation of such a management strategy. It mandates a thorough investigation to predict the impacts which will be produced by each possible management alternative.

The Three Rivers project (MCOS, 2002) was one of the early and detailed studies conducted in Ireland with the aim of developing catchment-based monitoring and management systems for the Boyne, Liffey and Suir catchments. A related project was the Lough Derg/ Lough Ree Project (KMMP, 2001) which addressed the same objectives in the Lough Derg/Lough Ree catchment. In addition to the valuable management plans developed by these two projects, an important database required for modelling diffuse phosphorus loads has been generated. Daly and Mills (2006) used some of this database to develop an empirical model which is able to estimate the annual orthoP concentrations of phosphorus from diffuse sources at the outlet of a catchment. In their model, the catchment characteristics have been used solely to derive the input explanatory variables. Because of its simplicity and parsimony, this type of empirical approach to predicting diffuse phosphorus loads has been used widely in a number of applications, reported below. Usually models of this type do not incorporate in their structure any representation of the actual physical processes involved in the mobilisation and transport of phosphorus but instead they seek to establish a causal link between the phosphorus load and the catchment characteristics which influence it.

The current study attempts to strengthen the empirical modelling approach by applying the concept of fuzzy logic modelling in developing a new empirical model. As noted above, the model is expected to be used as a predictive tool at a catchment level across all the river basin districts in Ireland; an analogous approach can be used in other countries. For comparison with previous models, the same data as used by Daly and Mills (2006) was utilised here in the application of the new model.

4.2 Literature Review

The relationships between catchment characteristics and mean nitrate and orthoP concentrations in UK rivers have been examined by Davies and Neal (2007). In addition to land-use types, two additional indices were used as parameters to characterise the catchments. These were a base flow index (BFI) and effective rainfall (ER). A GIS layer for the former was readily available, whereas the latter was calculated as the difference between the standard annual average rainfall (SAAR) and the actual evaporation (AE). In the analysis, data from 161 sites were separated into two groups. The first group comprised 51 sites and was used to derive, by multiple regressions, the relationships between the catchment characteristics and the mean nitrate and orthoP. The remaining sites in the second group were used as an independent test of the validity of the analysis. The results indicated that the prediction of orthoP concentrations from catchment concentrations is less certain than that for nitrate, probably due to the unaccounted effects of discharges from sewage treatment works and the in-stream losses.

Meynendonckx et al. (2006) used data of 173 watersheds within two sub-catchments of the River Scheldt Basin (Flanders, Belgium) to study the influence of catchment characteristics on nitrate and phosphate concentrations. The catchment characteristics included rainfall, discharge loading of point sources, morphological characteristics (area, average slope, drainage density, elongation), land use and soil properties (soil texture and drainage). In addition, the relative influence of the riparian zone versus the whole catchment characteristics was also investigated. The best linear models, which related the catchment characteristics with the nitrate and the phosphate, were derived following an analysis to examine correlations within the data with two techniques: (i) a non-parametric Spearman rank correlation and (ii) partial regression analysis. The former was applied to determine the direction and magnitude of the interaction between individual catchment characteristics and nitrate and phosphate concentrations. The latter provided a way of examining the relative importance of the catchment characteristics grouped per environmental theme (precipitation, point sources, morphological characteristics, land use, soil properties). The results indicated that soil drainage variables had the strongest influence on nutrient concentrations. In comparison, land use and point source loading had a weaker influence. Regarding the influence of riparian zones, it has been found that land use close to the river was not a better predictor of the nutrient concentrations than land use away from the river. This suggests that the mediating impact of riparian zones is rather explained by the hydrologic pathways within the buffer strip (Meynendonckx et al., 2006).

To study the influences of discharges and different catchment characteristics on stream N concentration during base flow periods, Su et al. (2006) used data from 12 small sub-areas in a largely forested catchment in Japan. The catchment characteristics used in the study include slope, land-use type, soil type and normalised difference vegetation cover index (NDVI). A time series NDVI data set was used to represent the seasonal vegetation cover variations of different months. This data set was made from a time series of 11 Landsat thematic mapper (TM) images after atmospheric correction for the months from January to December (except September) during 1998 and 1999. It has been assumed that there were no significant variations of vegetation cover in the study area between the same months of different years and that the vegetation cover variations in different months of a year were caused only by seasonal variation.

To evaluate the influence of the catchment characteristics, bivariate and a multiple regression analyses were made between the catchment characteristics and various species of N concentration, including total N, nitrate, nitrite and ammonium. The results showed that the vegetation cover was strongly correlated to total N, nitrate, and nitrite concentrations. In addition, the significance of the catchment characteristics to N concentrations were ranked as vegetation cover, soil, topography and land use. The discharges of the base flow period showed no significant correlation with any species of the N concentrations and this is the opposite of the behaviour in high-flow periods. Further, no significant relationship was found between the ammonium and the catchment characteristics.

Using a number of spatial variables derived from land use, soil type, stocking densities, fertiliser phosphorus use and soil phosphorus levels, Daly and Mills (2006) carried out a series of regression analyses between different combinations of these variables and the average annual orthoP concentration. The objective was to identify the best empirical model that can describe the relationship between the catchment characteristics and the annual average orthoP concentrations. Data sets from 84 different catchments in Ireland were used in the analysis. These catchments were selected such that (i) nested catchments were avoided and (ii) diffuse pollution represented the main contributor to the stream in the catchment. Starting with all variables and using a backward stepwise regression procedure, it was possible to eliminate the variables which have no significant effect on the linear model. In the final model, only two variables were retained and hence deemed significant. These two variables were the Runoff Risk Index (RRI) and the Phosphorus Desorption Index (PDI). To determine the two indices the gley soil types were initially divided into categories based on the percentage of the gley soil in each soil association (i.e. mapping unit in Ireland). These categories were weighted according to potential risk and then summed over each catchment to give an area-weighted index.

Daly et al. (2000) developed a national empirical model to describe river P levels using available information on land use, land management, soil type and water quality for 35 Irish river sub-catchments. The statistical analysis used to develop and test the model indicated that predicted and observed river P concentrations were clustered according to catchment hydrology. Two clusters were identified: Cluster A where soil is predominantly wet and poorly drained and Cluster B where soil is predominantly well drained. River P levels in Cluster A were found to be significantly higher than those in the dry catchments of Cluster B.

Using an export coefficient allows an indication of the potential for phosphorus removal from the land surface under the assumption that the land use is a major control on phosphorus export. In a study to estimate diffuse phosphorus loads from the Boyne, Liffey and Suir catchments in Ireland, export coefficients for different land-use types were determined and then assigned to each land-use type identified in the Co-ordination of Information on the Environment (CORINE) land-use data set (MCOS, 2002). The assigned coefficients have been re-evaluated using auto-sampled total phosphorus concentrations and flow data obtained after three years of extensive monitoring in a pilot study area located in each of the three catchments. The export coefficients of phosphorus from grassland, arable and urban land use were found to be 0.32, 2.27 and 1.29 kg/ha/yr respectively. In another study, McGuckin et al. (1999) derived export coefficients of P from a number of CORINE land cover classes, using data for 30 sub-catchments of two major rivers in Northern Ireland. Multiple regression methods were applied, with soluble reactive phosphorus, soluble organic phosphorus and particulate phosphorus loads as dependent variables.

Lek et al. (1999) used an artificial neural network to produce an empirical relation for estimating the inorganic and total N concentrations. The artificial neural network model was developed and tested using 972 diffuse-source catchments across the USA. The resulting network had eight independent input variables related to catchment parameters (five on land-use features, mean annual precipitation, animal unit density and mean stream flow) and two dependent output variables (total and inorganic N concentrations in the stream). The trained artificial neural network was capable of learning the relationships between drainage area characteristics and N levels in streams, and it also was able to predict N export in an independent validation data set.

Mizagalewics (1996) developed an approach which has been used to derive regional catchment scale water-quality estimates in the Midwest rivers in the USA. Elementary catchments were obtained from the delineation of digital elevation data and then combined into stream gauge zones for which the only stream flows into and out of a zone are those measured at the zone boundary by stream gauges. The monthly stream flows were estimated using runoff coefficients to convert the rainfall values into flows. The mean annual concentration of the contaminant was estimated as a function of catchment characteristics, chemical fertiliser application rate and climatic characteristics. Monthly estimates were derived from this by applying a ratio of expected monthly to annual concentration.

Several other models of loss of diffuse-source nutrients have also been based on catchment characteristics (e.g. Berankova and Ungerman, 1996; Norton and Fisher, 2000; Behrendt, 1996; Pekarova and Pekar, 1996).

4.3 Estimation of Nutrients Loads using Catchment Characteristics

The above literature review showed that the level of nutrients, including phosphorus (P) and nitrogen (N), is usually an indicator of the situation in the upland catchment. Therefore, in situations where diffuse pollution is significant it is always possible to obtain an estimate, of whatever accuracy, from empirical models which relate them with the catchment characteristics. The catchment characteristics that result on a robust model may not be known in advance and hence a trial and error procedure is usually followed to determine those catchment characteristics. The relationship between the nutrients loads and the catchment characteristics is always described by a first order linear model (Eq. 4.1):

$$L = a_0 + \sum_{i=1}^{Ncat} a_i Z_i \ , \qquad (4.1)$$

where L it the nutrient load, the Z value defines a catchment characteristic, N is the total number of the catchment characteristics, a_0 is a constant term and a_i are the coefficients of the linear model.

The total number of terms in the linear model is equal to the total number of catchment characteristics that have been included in the model plus one. The constant term and the coefficients, which can all be called the ‘model parameters’, are estimated by using the least squares method. To obtain reliable estimates for the parameters, it is always recommended that data from as many sites as possible are used. However, it is also recommended to select sites from a homogenous region where similar catchment characteristics prevail so that the resulting model would be a better representation, but only of that region. Hence, it is not feasible to use such a model in regions other than the one used in estimating its parameters.

In the current research, a new approach was developed to produce a class of model that can be more readily applied in a number of different regions. This approach is based on fuzzy inference systems that integrate the outputs from a number of sub-models to estimate an overall output. Each sub-model can be considered as a representation to a specific region where the catchment behaviour is assumed homogeneous. The data used in developing the model are for the same 84 catchments used by Daly and Mills (2006) to develop their national phosphorus model. Such a national model is a tool of extreme importance in managing diffuse phosphorus pollution at a catchment level in each river basin district in Ireland. The newly developed model is aimed at providing an improved, but more complex, alternative national phosphorus model. The model is tested by using part of the data set to calibrate the model parameters and the remaining part to validate the performance of the resulting model.

4.4 Newly Developed Neuro-Fuzzy National Phosphorus Model

Using a single general equation to estimate diffuse P loads from the catchment characteristics may work well for a single homogeneous region but may not give good predictions outside this region. This is because of the wide variability in the behaviour of the catchments used to derive the equation. If among those catchments there is a dominant cluster of catchments with a homogenous condition, then this cluster would influence the parameter estimation process strongly. The estimated parameters would fit well for catchments in this cluster while its performance for other catchments may not be as good. It is possible to improve the model's performance if a separate model is defined for each cluster of homogenous catchments. However, when grouping the catchments into a number of clusters there will always be overlaps between these clusters because some catchments may have features from a variety of different clusters and may be difficult to assign to a single cluster. Here a catchment does not have to be a member of only one cluster, but is assigned a membership weighting relating to all clusters. The higher the weighting, the stronger the association between the catchment and that cluster. The current research's hypothesis is that if a separate phosphorus export model is calibrated for each cluster then a better diffuse phosphorus load prediction in a catchment can be obtained if, for a particular catchment, the outputs of all the cluster models were combined with weights related to the catchment's membership weighting for the cluster. This means that the models developed for each cluster contribute to the diffuse phosphorus load prediction in a catchment, depending on the degree by which this catchment belongs to the cluster. The structure of this newly developed neuro-fuzzy national P model is illustrated in Fig. 4.1. The mathematical form of this model, which here describes the relationship between the average annual concentrations of orthoP (resulted from diffuse phosphorus loads) and physical characteristics for catchment i, is as follows (Eq. 4.2):

$$orthoP_i = \left(\frac{\sum_{j=1}^{nc} w_j O_j}{\sum_{j=1}^{nc} w_j} \right)_i = \left(\frac{\sum_{j=1}^{nc} w_j \left(a_j + \sum_{k=1}^{nvar} b_{kj} x_k \right)}{\sum_{j}^{nc} w_j} \right)_i , \qquad (4.2)$$

where *orthoP* is the average annual P concentration at the outlet of catchment i, nc is the total number of catchment clusters, w_j is the weight given to the sub-model of the jth cluster, O_j is the output of the sub-model of the jth cluster, $nvar$ is the total number of independent variables defining the catchment characteristics used in the sub-model of each cluster, x_{kj} is the value of the independent variable (i.e. physical characteristic) and a and b are parameters of the linear sub-model for each cluster.

The model is a weighted average of a number of first-order polynomial sub-models. The number of sub-models is equal to the number of clusters (nc) deemed sufficient for producing a homogeneous grouping of the catchments, i.e. each cluster is composed of a number of catchments with similar characteristics. In addition, each cluster is represented by a centre point with properties that are assumed to be representative of all the catchments in the cluster. The k-means clustering algorithm (Hartigan and Wong, 1979) is used to assign the catchments into nc clusters and also to calculate a centre vector of the spatial variables for each cluster. In addition, a standard deviation vector for each cluster can be calculated using the resulting centre vector and

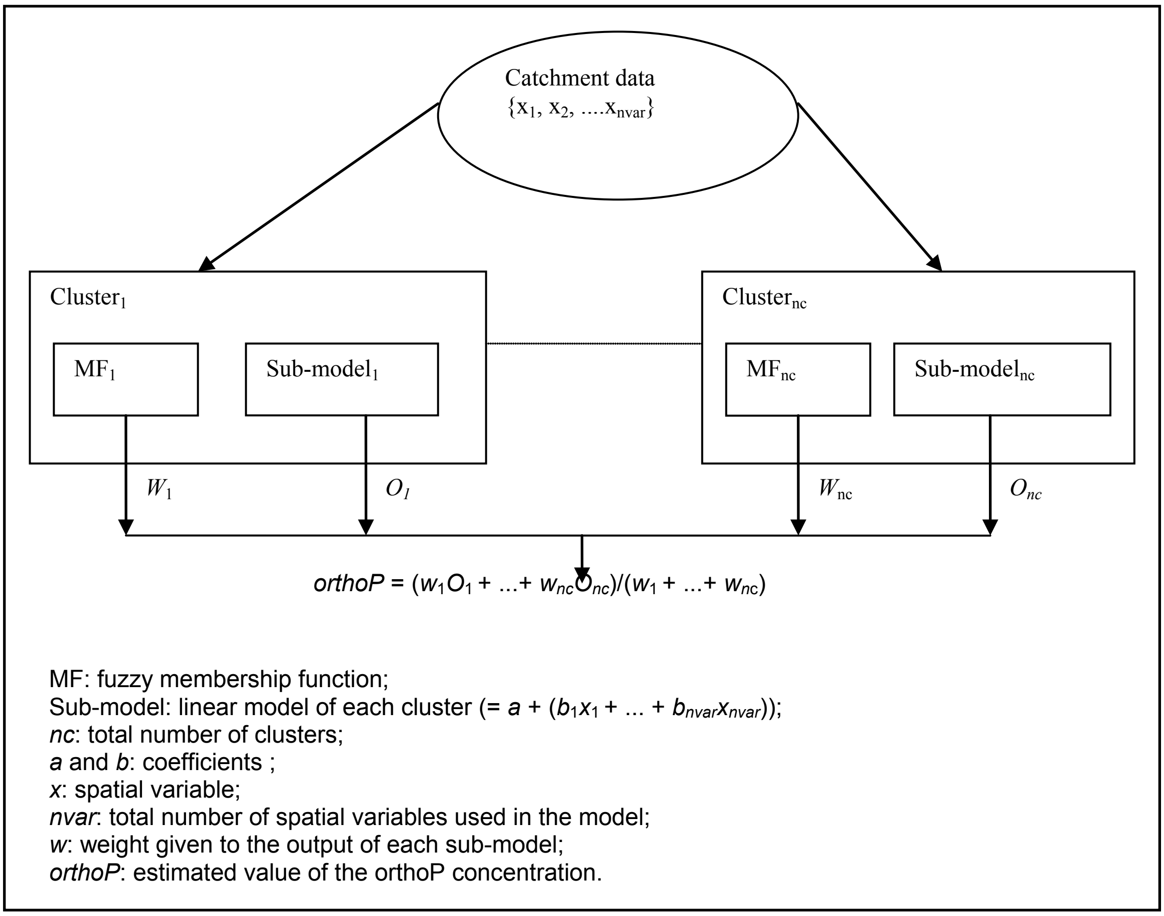

Figure 4.1. Neuro-fuzzy national phosphorus model.

the vectors of the spatial data for all catchments in the cluster.

By assuming that each cluster is a fuzzy set, it is possible to estimate the degree by which a catchment belongs to a cluster with a membership function. Here the Gaussian function was used for this purpose. This has two parameters: the location (c) and the scale (σ), while the spatial data vector (x) is the input variable. Equation 4.3 shows that the form of the Gaussian function is:

$$w = f(x) = \exp\left(-\left\|\frac{(x-c)^2}{\sigma^2}\right\|\right). \tag{4.3}$$

This function gives the weights (w) for Eqn. 4.2 which determine the contribution of a sub-model to the overall estimation of the orthoP concentration. After obtaining the weight (w) for each cluster, Eqn. 4.2 becomes a linear model relating the spatial variables with the orthoP concentration. The parameters of the linear model (a,b) for all clusters can then be found using the least squares method.

4.5 *k*-Means Clustering Algorithm

Clustering is the partitioning of a data set into subsets (clusters), so that the data in each subset (ideally) share some common trait. Some defined distance measure such as the Euclidean distance is often used to determine the proximity of the data in a cluster. The *k*-means clustering algorithm (Hartigan and Wong, 1979) is one of the simplest unsupervised learning algorithms for this partitioning when the number of clusters (k) is a priori. It consists of the following steps:

1 The main idea is to start with some initial choice of positions for the k centroids, one for each cluster. These initial centroids should be chosen carefully because different locations generate different results. They should be as far away from each other as possible, given the data set.

2 The next step is to take each point belonging to a given data set and associate it with the nearest centroid.

3 At this point k, new centroids are calculated as the points that represent the centres of gravity of the new clusters resulting from the previous step.

4 Steps 2 and 3 are repeated until the change in the k centroids is insignificant.

In essence, the algorithm aims at minimising an objective function, in this case a squared error function in the following form (Eq. 4.4):

$$J = \sum_{j=1}^{k} \sum_{i=1}^{n} \left\| x_i^{(j)} - c_j \right\|^2 , \tag{4.4}$$

where $\left\| x_i^{(j)} - c_j \right\|^2$ is a distance measure between a data point $x_i^{(j)}$ and the cluster centre c_j, and n is the total number of data points.

4.6 Application of the Neuro-Fuzzy National Phosphorus Model

As noted above, to apply the neuro-fuzzy national phosphorus model, data from 84 catchments from four different hydrological areas in Ireland (Fig. 4.2 and Table 4.1) were used. These were split into two sets, the first of which was used for model calibration and the second for validation. For a pre-specified number of clusters, the centre vectors, the standard deviation vectors and the linear models parameters were calculated in the calibration phase using the first data set. Then, for the validation, the second data set was used to verify the performance of the neuro-fuzzy national phosphorus model. The strategy of splitting the data set (84 catchments) into two parts for

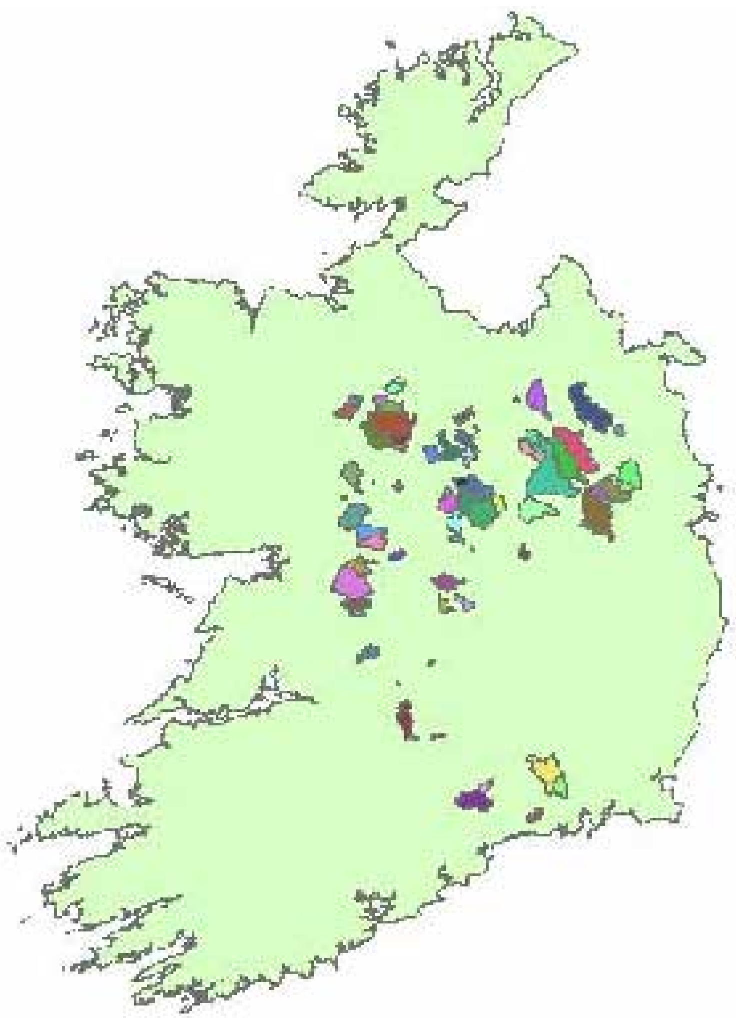

Figure 4.2. Location of 84 catchments used in the neuro-fuzzy national phosphorus model.

calibration and validation is important for the credibility of the resulting model. Therefore, the aim is always to select a representative sample from the available data set to be used in model calibration so that the resulting parameters could be versatile, i.e. valid for data sets other than those used during calibration.

Table 4.1. Number of catchments in four hydrological areas (7, 16, 25, and 26) used in the neuro-fuzzy national phosphorus model.

Hydrological area	No. of catchments
7	12
16	8
25	20
26	44
Total	84

To check the validity of the current model the calibration and validation process was repeated six times, each time with different data sets obtained as follows. First, the catchments in each of the four hydrological areas were ordered in sequence according to the code given to each catchment. Second, the catchments in each hydrological area were divided equally into two groups, A and B (Table 4.2). Third, the catchments in each group were further divided into two equal groups in the same fashion as obtaining Groups A and B. As a result of that, Group A was divided into AA and AB while Group B was divided into BA and BB (Table 4.2). Finally, six different scenarios, each representing a different strategy for splitting the data set, were formulated to be used in the calibration and the validation as in Table 4.3. Note that the same number of catchments is used in calibration and in validation for Scenarios 1 and 2. For the remaining scenarios, the number of catchments used in calibration was twice the number used in validation, i.e. 2/3 of the 84 catchments was used for calibration while the remaining 1/3 were used for validation.

Table 4.2. Grouping of catchments in each of the four hydrological areas.

Hydrological area	Number of catchments in each of the specified groups			
	Group A	Group B	Groups AA and AB	Groups BA and BB
7	6	6	3	3
16	4	4	2	2
25	10	10	5	5
26	22	22	11	11
Total	42	42	21	21

Table 4.3. Six different splitting scenarios used in calibration and validation of the neuro-fuzzy national phosphorus model.

Scenario	Clustering and calibration		Validation	
	Group(s)	No. of catchments	Group	No. of catchments
1	A	42	B	42
2	B	42	A	42
3	A + B + BA	63	BB	21
4	A + B + BB	63	BA	21
5	B + A + AA	63	AB	21
6	B + A + AB	63	AA	21

4.7 Variables of the Neuro-Fuzzy National Phosphorus Model

In the neuro-fuzzy national phosphorus model the dependent variable, the annual average orthoP concentration for a particular catchment, is estimated from values of the indices representing phosphorus desorption (PDI), runoff (RRI), geology (GEO), groundwater (GW), land use (LU) and soil (SO). The PDI and RRI were introduced by Daly and Mills (2006) in their national phosphorus model to quantify the potential risk of phosphorus loss from soil by the desorption process and transport of phosphorus by surface runoff respectively. Each index was obtained by calculating an area weighted average of risk categories defined subjectively for each soil type in a catchment. Daly and Mills (2006) found a strong correlation between both indices and orthoP concentrations and hence they have been included here in the neuro-fuzzy national phosphorus model. The maps of the other spatial variables in each catchment show different categories for each variable distributed over the catchment area. Any category which occupies more than 10% of the area in any of the 84 catchments has been eliminated from the model. Table 4.4 summarises the categories of the spatial variables included in the model.

For the 84 catchments, Table 4.5 presents some statistics of the measured orthoP concentrations which vary from a low of 0.004 mgP/l to a peak of 0.12 mgP/l; i.e. the range is 0.116 mgP/l. Their frequency distribution is shown in Fig. 4.3. Most of the catchments have an orthoP concentration between 0.016 mgP/l and 0.07mg/l.

Table 4.4. Spatial variables used in the neuro-fuzzy national phosphorus model.

Variable	No. of categories	Details of categories
P desorption index (PDI)	1	Continuous value
Runoff index (RRI)	1	Continuous value
Geology (GEO)	4	Sand and gravels,
		Carboniferous limestone,
		Ordovician,
		Rhyolite
Groundwater bodies (GW)	4	Gravel
		Karstic
		Poorly productive bedrock
		Productive fissured bedrock
Land use (LU)	4	Artificial surfaces
		Agricultural areas
		Forest and semi-natural areas
		Wetlands
Soil (SO)	6	Deep, well-drained mineral
		Shallow, well-drained mineral
		Deep, poorly drained mineral
		Poorly drained mineral soils with peaty topsoil
		Peats
		Miscellaneous

Table 4.5. Statistics of the orthoP concentrations in the 84 catchments used in the neuro-fuzzy national phosphorus model.

Statistic	Value (mgP/l)
Minimum	0.004
Maximum	0.12
Average	0.034
Standard deviation	0.024

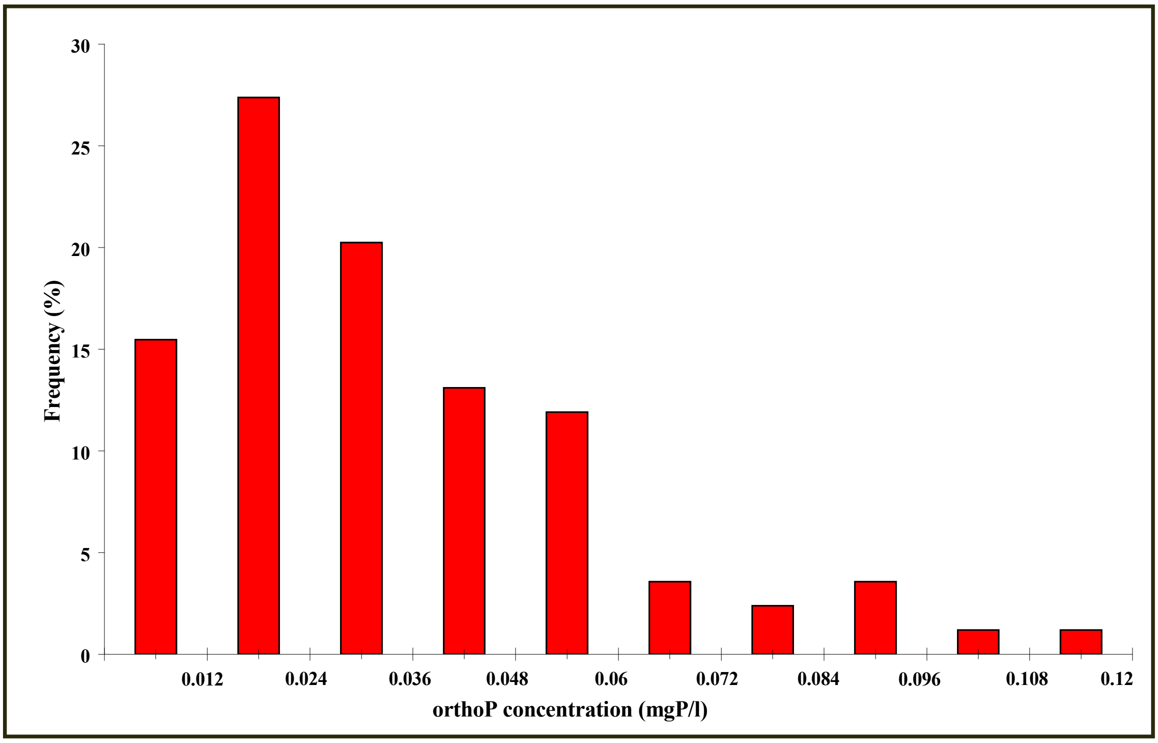

Figure 4.3. Frequency distribution of the orthoP concentrations in the 84 catchments used in the neuro-fuzzy national P model.

4.8 Formulation of Different Neuro-Fuzzy National Phosphorus Models

Because of the limited number of catchments with sufficient data available to calibrate the linear model parameters of all cluster sub-models in the neuro-fuzzy national P model described above, only modelling cases for two and three clusters have been investigated to date. For the six calibration–validation scenarios described in Table 4.3, the number of catchments in each cluster when divided into two clusters to the *k*-means clustering algorithm is given in Table 4.6. The corresponding numbers when all the catchments are divided into three clusters are given in Table 4.7.

Table 4.6. Number of catchments in each cluster – case of two clusters and for each of the six calibration–validation scenarios.

Scenario	No. of catchments	
	Cluster 1	Cluster 2
1	33	9
2	14	28
3	52	11
4	49	14
5	20	43
6	20	43

Table 4.7. Number of catchments in each cluster – case of three clusters and for each of the six calibration–validation scenarios.

Scenario	No. of catchments		
	Cluster 1	Cluster 2	Cluster 3
1	24	5	13
2	12	19	11
3	33	11	19
4	35	10	18
5	20	31	12
6	19	31	13

In cases where data are scarce, the amount of data places an upper limit on the number of parameters that can be calibrated. This in turn places an upper limit on the number of catchment characteristics and the number of clusters that can be used. Using many catchment characteristics, each with a number of categories, is not practicable if the resulting total number of parameters of the sub-models (for the case of two and three clusters) is larger than the number of data points in each of the six calibration–validation scenarios (Table 4.3). To satisfy this for each case, only a limited number of neuro-fuzzy national phosphorus models (Table 4.8), each with a different combination of catchment characteristics,

Table 4.8. Composition of different neuro-fuzzy national phosphorus models tested.

Model code	Catchment characteristics in model	No. of parameters for each sub-model	Total no. of parameters – case of two clusters	Total no. of parameters – case of three clusters
1	PDI + RRI	3	6	9
2	PDI + RRI + GEO	7	14	21
3	PDI + RRI + GW	7	14	21
4	PDI + RRI + LU	7	14	21
5	PDI + RRI + SO	9	18	27
6	PDI + RRI + GEO + GW	11	22	33
7	PDI + RRI + GEO + LU	11	22	33
8	PDI + RRI + GEO + SO	13	26	39
9	PDI + RRI + GW + LU	11	22	33
10	PDI + RRI + GW + SO	13	26	39
11	PDI + RRI + LU + SO	13	26	39

were formulated and their performance in estimating the annual orthoP concentrations were investigated here. When sufficient information from more than the 84 catchments used here becomes available, a wider range of model structures can be tested.

4.9 Results

For each of the six calibration–validation scenarios, the 11 neuro-fuzzy national phosphorus models listed above were assessed for the two-clusters and three-clusters cases on the basis of the coefficient of correlation (R^2) between modelled and measured annual average orthoP concentrations for both calibration and validation data sets. Two plots summarising the R^2 results for calibration and validation are shown here and discussed for each scenario. The discussion compares the performances of the 11 models for the case of two clusters and three clusters. The simplest model, model_1, where only PDI and RRI were used as independent variables, is considered a base model with which the performance of the other more complex models is compared. Thus, the differences in performances achieved by adding additional explanatory variables and/or model complexity can be determined.

4.9.1 Split-Sample Scenario 1

Fig. 4.4 **(Calibration)**: The R^2 values are all ranging from above 0.6 to above 0.9. Note that the use of three clusters or sub-models generated R^2 values better than the case of two clusters for all models. Compared to model_1 the performance of all other models showed an improvement in both the two- and three-clusters cases. The R^2 value for model_8 with three clusters is the best among all. Although in many cases it might be expected that the more complex model should do better than the simpler model in calibration, for the type of model considered here, the more complex model does not necessarily contain the simpler model as a special case, because the clustering may be different, and so it is possible for the simpler model to do better in calibration than a more complex one.

Fig. 4.5 **(Validation)**: The validation results are quite different from the calibration results for this scenario. The magnitudes are generally less than 0.4, indicating a poor performance. In general, the results for the two clusters outperformed their counterparts in the three-clusters case except for model_4 and model_11 where the opposite is true. For the three-clusters case some models including model_2, model_7, model_8 and model_10 produced negative R^2 values, an indication of very poor performance. This was similar for model_11 for the two-cluster case. When the results of model_1 were compared with the other models in the case of two clusters, it was found that the R^2 value for this model was marginally exceeded by few models, including model_2, model_3, model_6 and model_9. For the case of three clusters, the R^2 value of model_1 was exceeded only by the value of model_4, which is also the best among all models in both the two- and three-clusters cases.

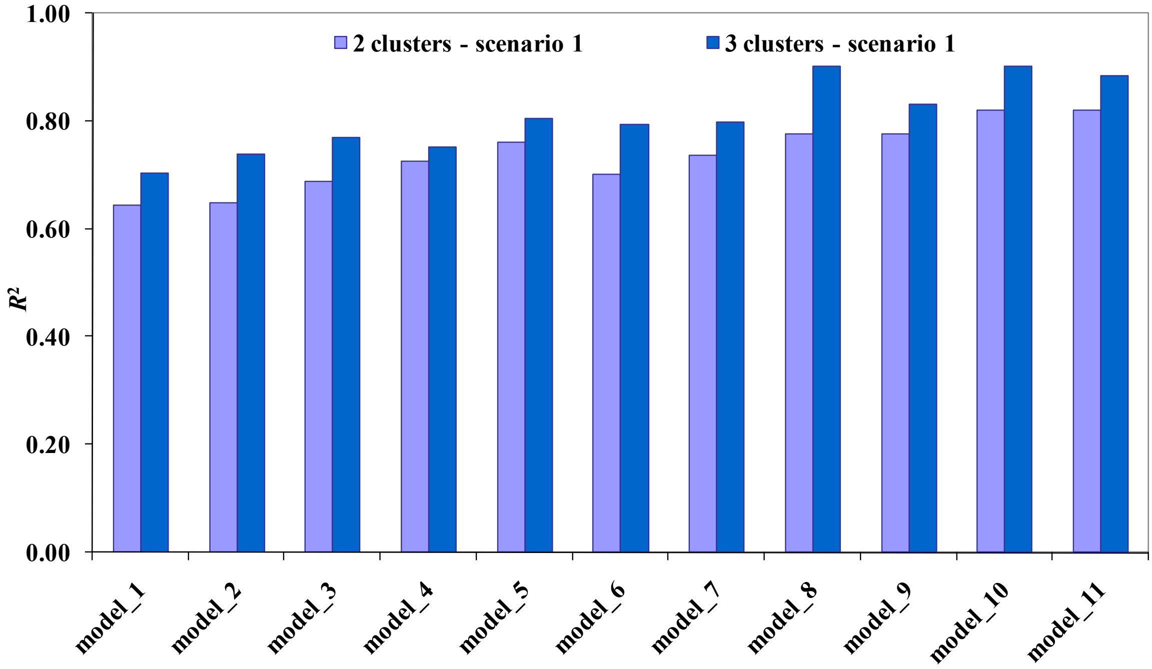

Figure 4.4. ***R*²** **results during calibration – Scenario 1.**

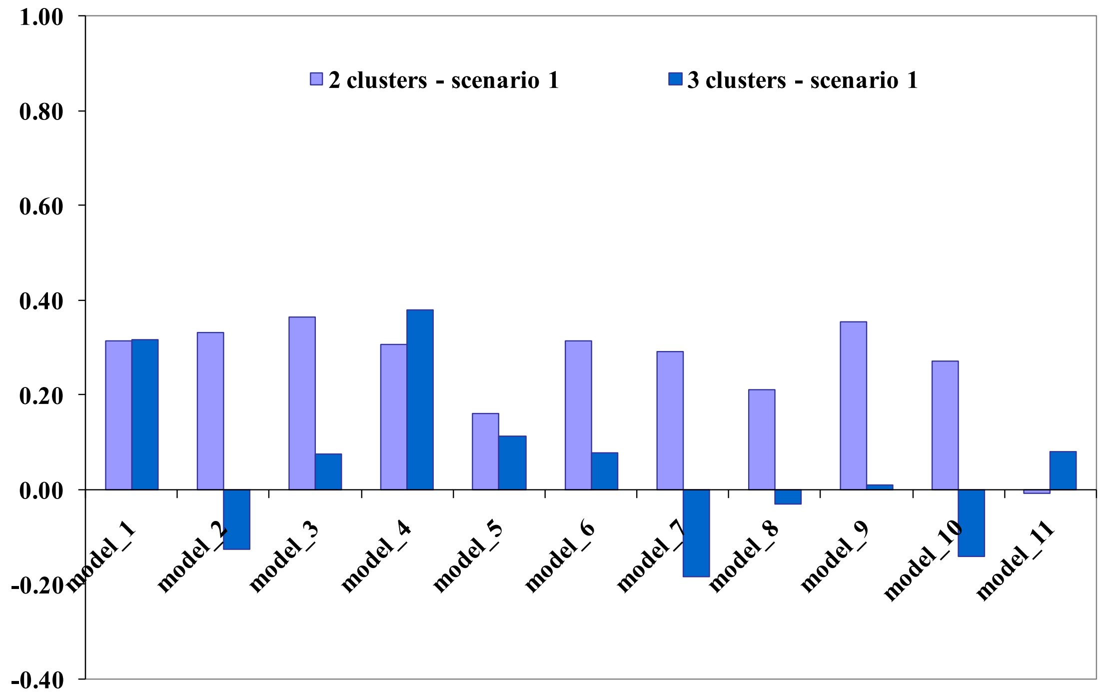

Figure 4.5. ***R*²** **results during validation – Scenario 1.**

4.9.2 Split-Sample Scenario 2

Fig. 4.6 **(Calibration)**: The results for Scenario 2 are similar to those of Scenario 1 except for model_1, model_3 and model_6 in which the R^2 values for the case of two clusters are better than those for the three clusters. Model_11 for the case of three clusters outperformed all other models in terms of R^2.

Fig. 4.7 **(Validation)**: The R^2 values for the two-clusters case are in general better than the values for the three-clusters case with the exception of model_4, model_7, and model_9. Also for the case of three clusters there is an obvious deterioration in the R^2 values for all models compared to the value of model_1. On the other hand, in the case of two clusters the only model which was able to outperform model_1 is model_3. The R^2 for the latter is the best among all other models.

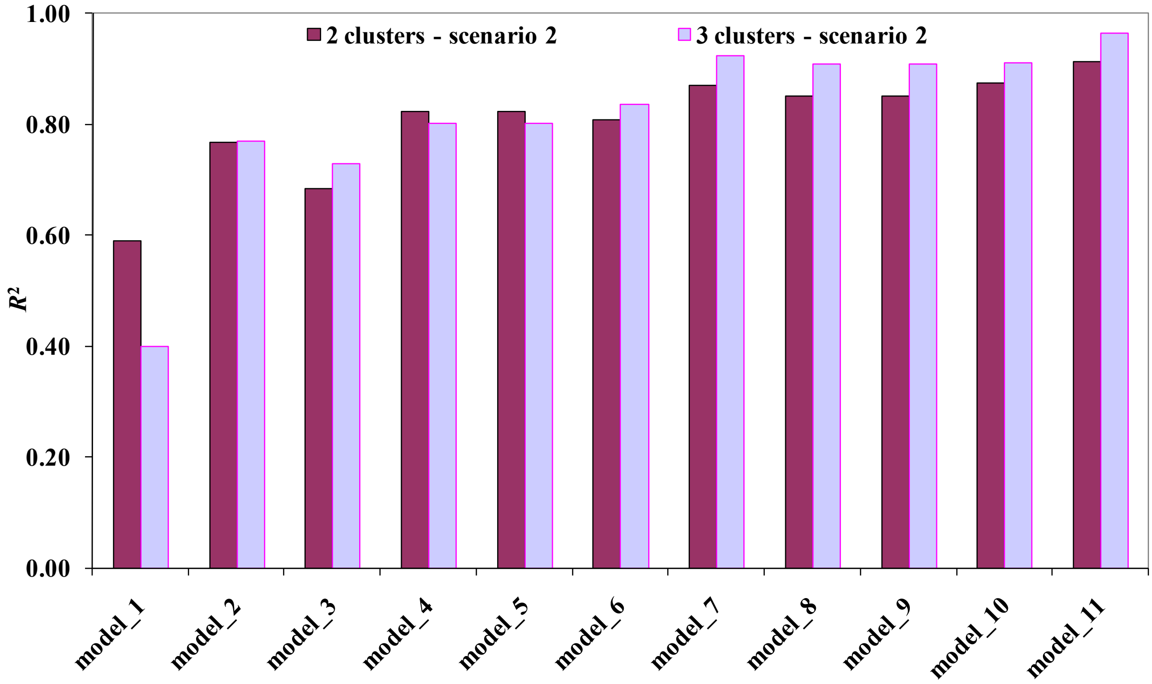

Figure 4.6. R^2 results during calibration – Scenario 2.

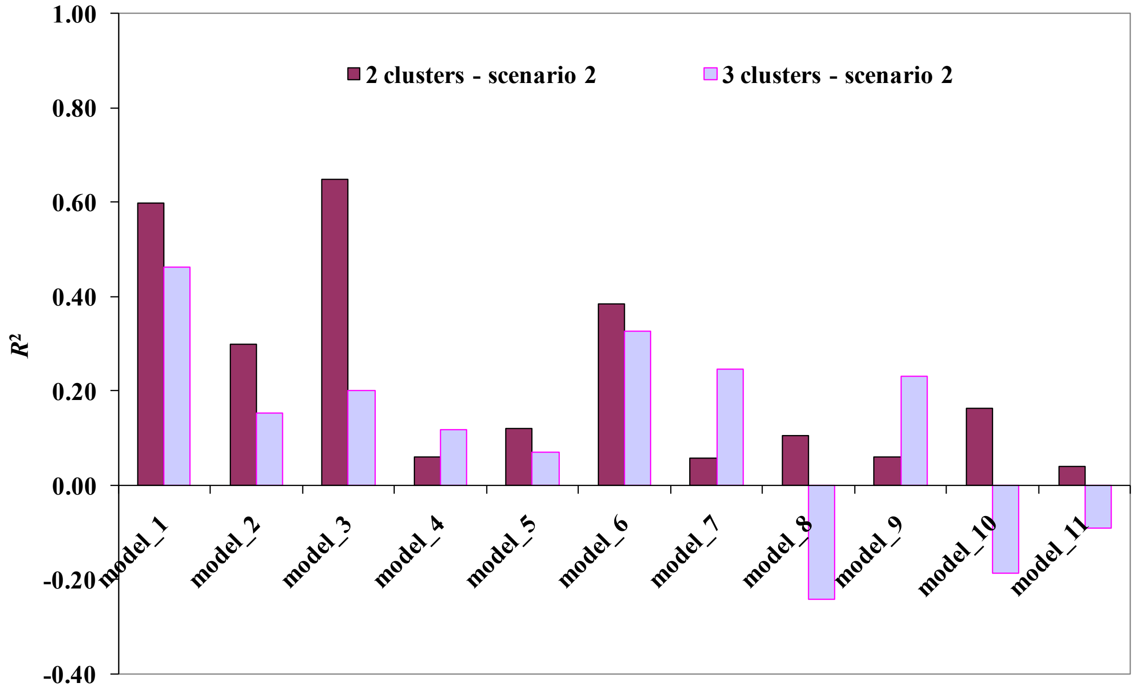

Figure 4.7. R^2 results during validation – Scenario 2.

4.9.3 Split-Sample Scenario 3

Fig. 4.8 **(Calibration)**: The three-clusters case consistently improved over the two-clusters case. Also in both cases none of the models produced an R^2 value below the value of model_1. The best R^2 value was achieved by model_10 of the three-clusters case.

Fig. 4.9 **(Validation)**: In contrast to the validation results of the previous scenarios, no negative values were found for any of the modes and the R^2 coefficient was much better than for the previous scenarios. The results for the three-clusters case were better than for the two-clusters case, except for model_4, model_5, model_8, and model_11. Model_9 with 3 clusters generated the best R^2 value. Some of the models including model_2, model_3, model_6, model_7, model_9, and model_10 in the two-cluster case and model_5, model_8, and model_11 in the three-clusters case were not able to perform better than model_1.

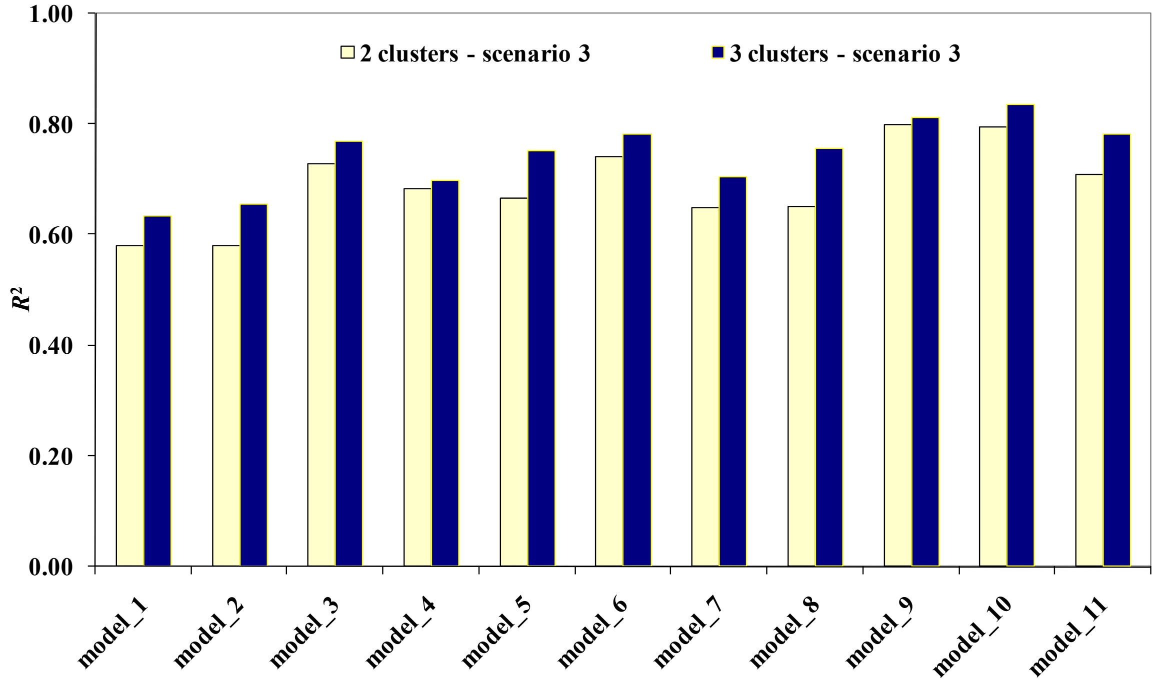

Figure 4.8. R^2 results during calibration – Scenario 3.

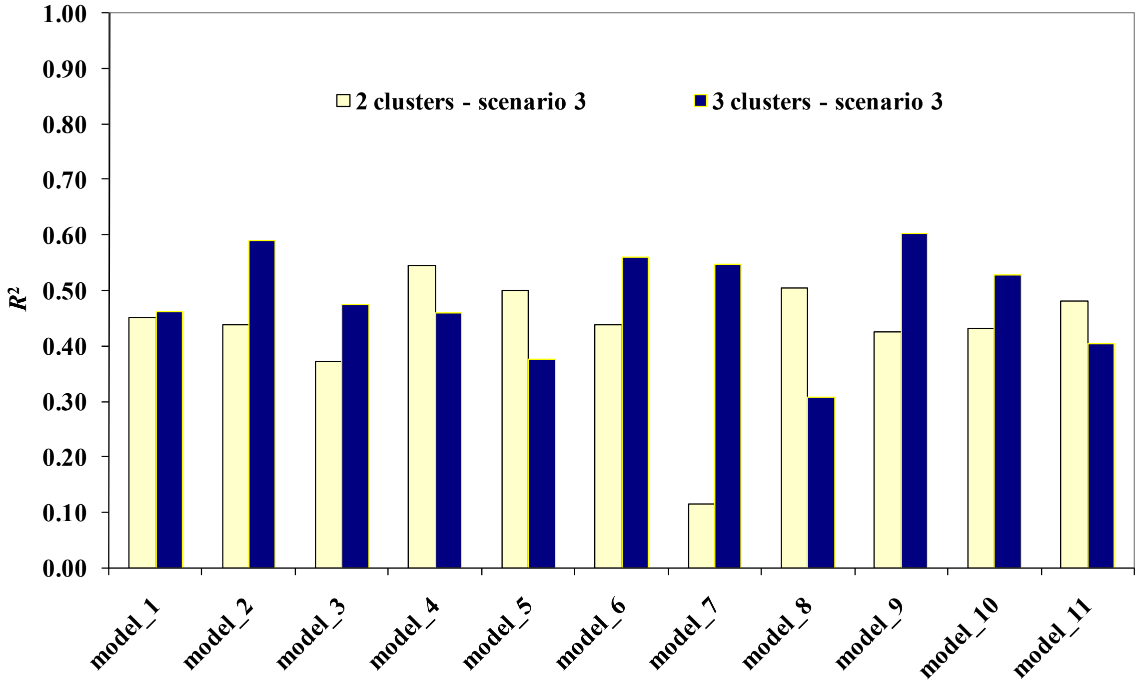

Figure 4.9. R^2 results during validation – Scenario 3.

4.9.4 Split-Sample Scenario 4

Fig. 4.10 **(Calibration)**: The trend of the results for this scenario is similar to Scenario 3. This is expected because only a small number of data points used in Scenario 3 have been replaced with different data points in this scenario. In addition, here the R^2 value for model_10 of the three-clusters case was the best. Model_1 of both clusters cases has R^2 value less than all other models.

Fig. 4.11 **(Validation)**: Among all models, only model_3 and model_7 of the two-clusters case were able to produce R^2 better than their counterparts in the three-clusters case. However, two models, namely model_8 and model_10, of the three-clusters case have the same R^2 value which represents the best among all other models. Model_2, model_5, and model_8 in the two-clusters case and model_2, and model_3 in the three-clusters case had R^2 values less than model_1.

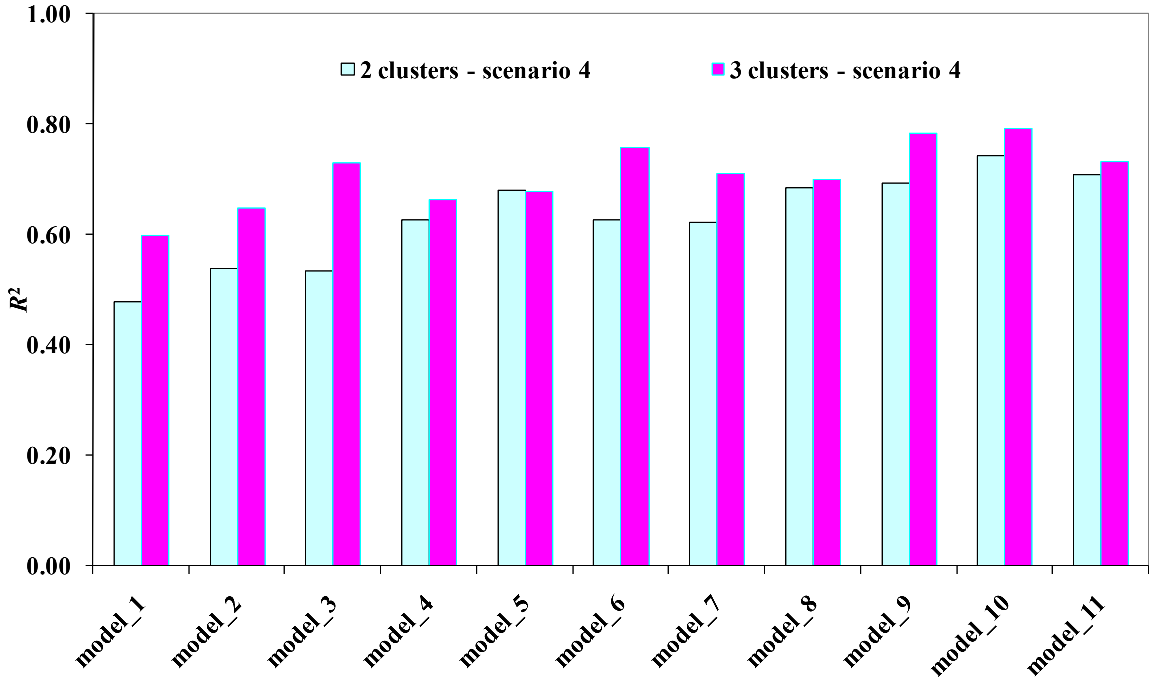

Figure 4.10. R^2 results during calibration – Scenario 4.

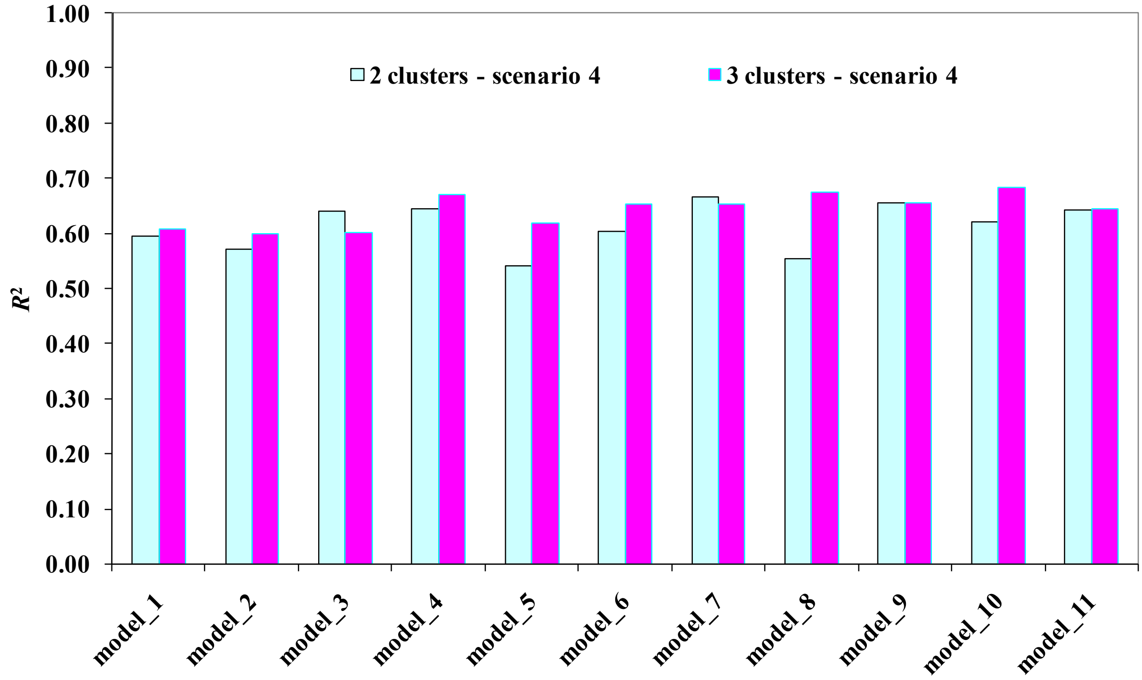

Figure 4.11. R^2 results during validation – Scenario 4.

4.9.5 Split-Sample Scenario 5

Fig. 4.12 **(Calibration)**: All models for the three-clusters case showed a significant improvement in terms of R^2 when compared with the two-clusters case and all other models were better than model_1. Model_8 in the three-clusters case has the best R^2 value among all.

Fig. 4.13 **(Validation)**: In contrast to the calibration results, the three-clusters case does not consistently outperform the two-clusters case except for model_9 and model_11. Moreover, all other models in both clusters cases produced R^2 values less than the value of model_1. However, the only exception is model_3 in the two-clusters case which also succeeded in achieving the best R^2 value.

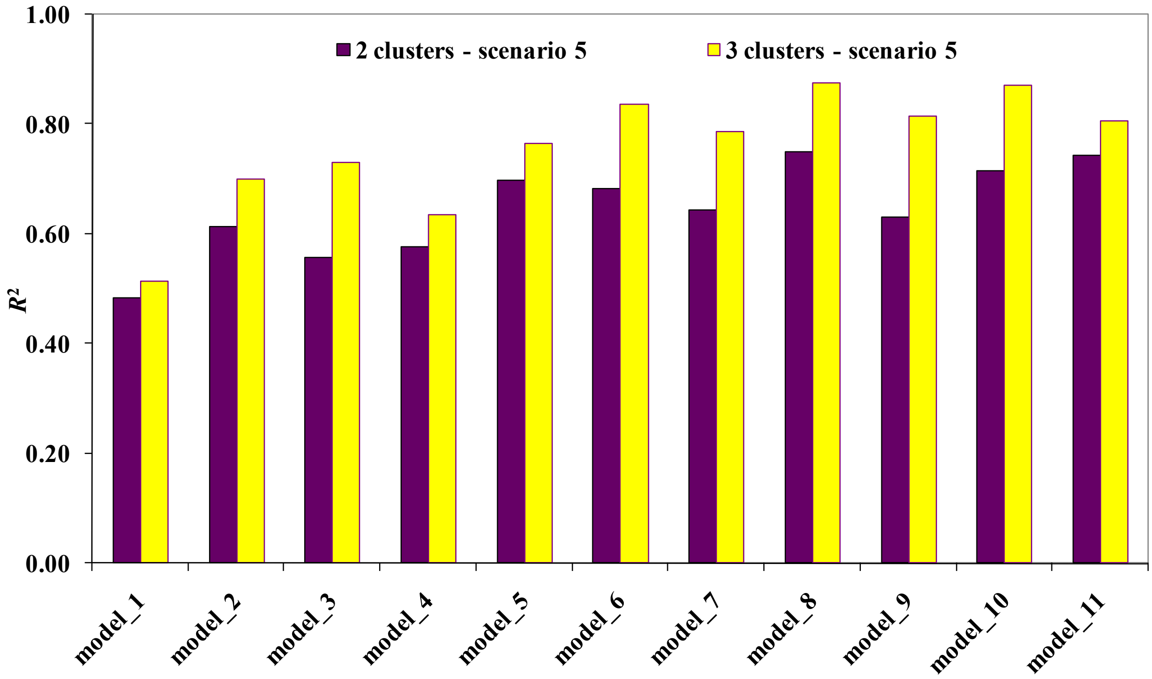

Figure 4.12. R^2 results during calibration – Scenario 5.

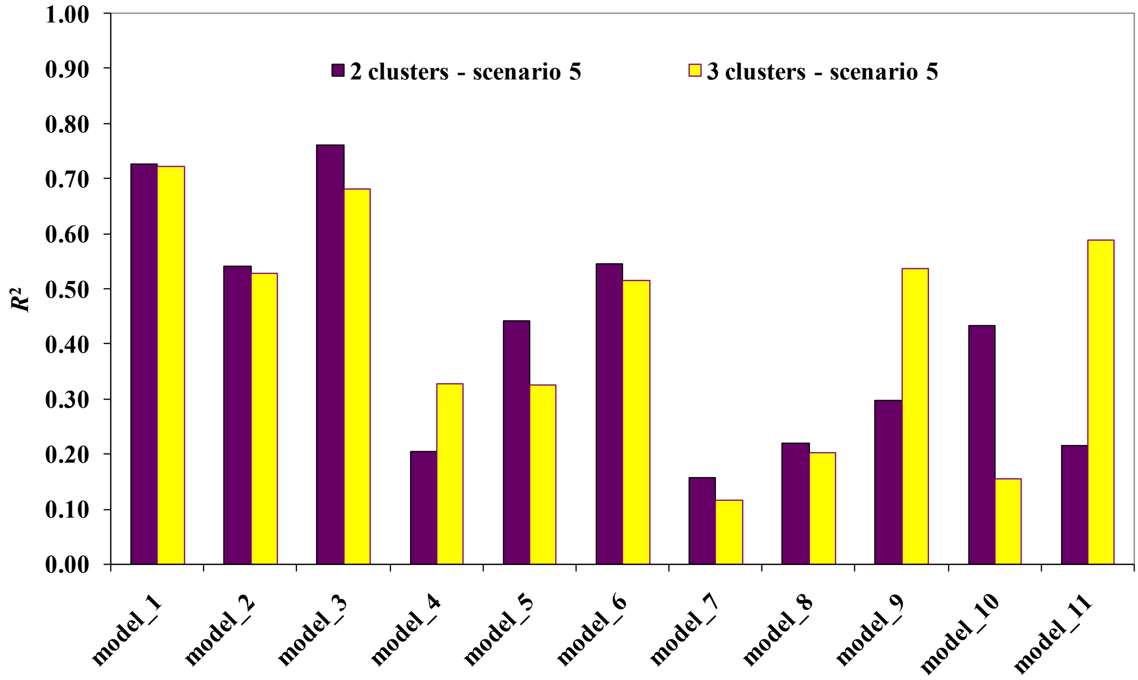

Figure 4.13. R^2 results during validation – Scenario 5.

4.9.6 Split-Sample Scenario 6

[Fig. 4.14](#) **(Calibration)**: Unlike the results of Scenario 5, the models in the three-clusters case do not show a significant improvement in their R^2 values over those in the two-clusters case. Model_1 in both the two- and three-clusters cases did not generate an R^2 value larger than the other models. Model_9 in the three-clusters case is the best model among all in terms of R^2.

[Fig. 4.15](#) **(Validation)**: The noticeable observation about the results in this scenario is that model_1 has the best R^2 value among all models in both the two- and three-clusters cases. This means that no benefit would be gained when adding more spatial variables to the PDI and RRI in a model. Generally, the results for the three-clusters case are better than those for the two-clusters case.

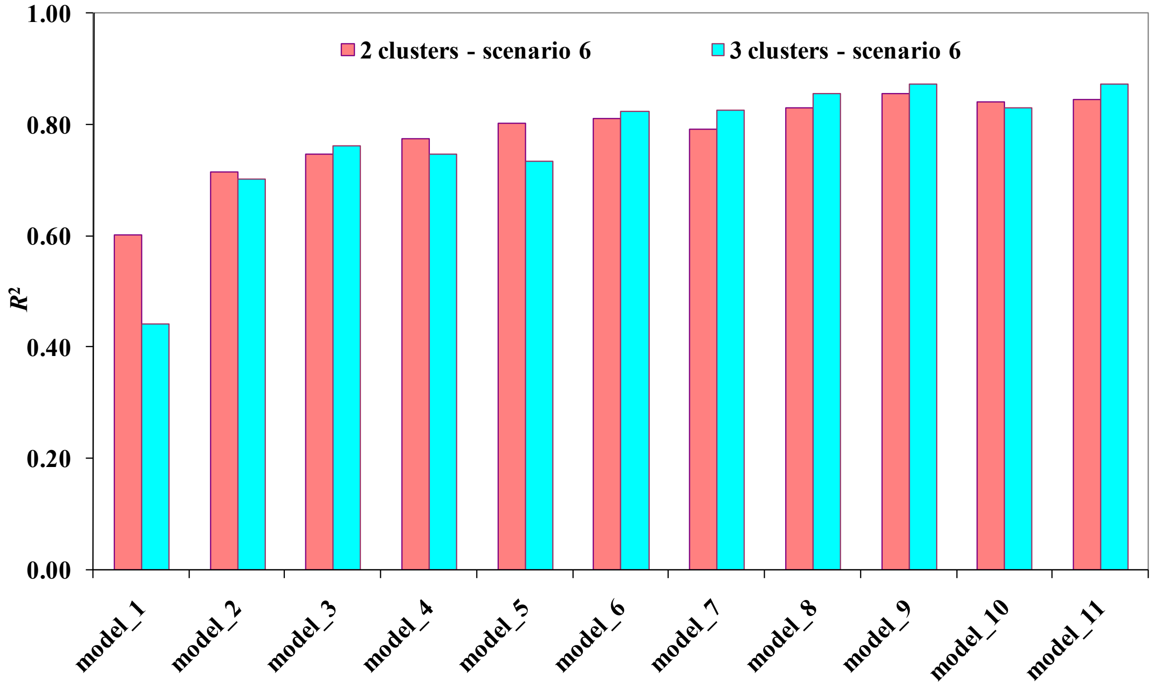

Figure 4.14. R^2 results during calibration – Scenario 6.

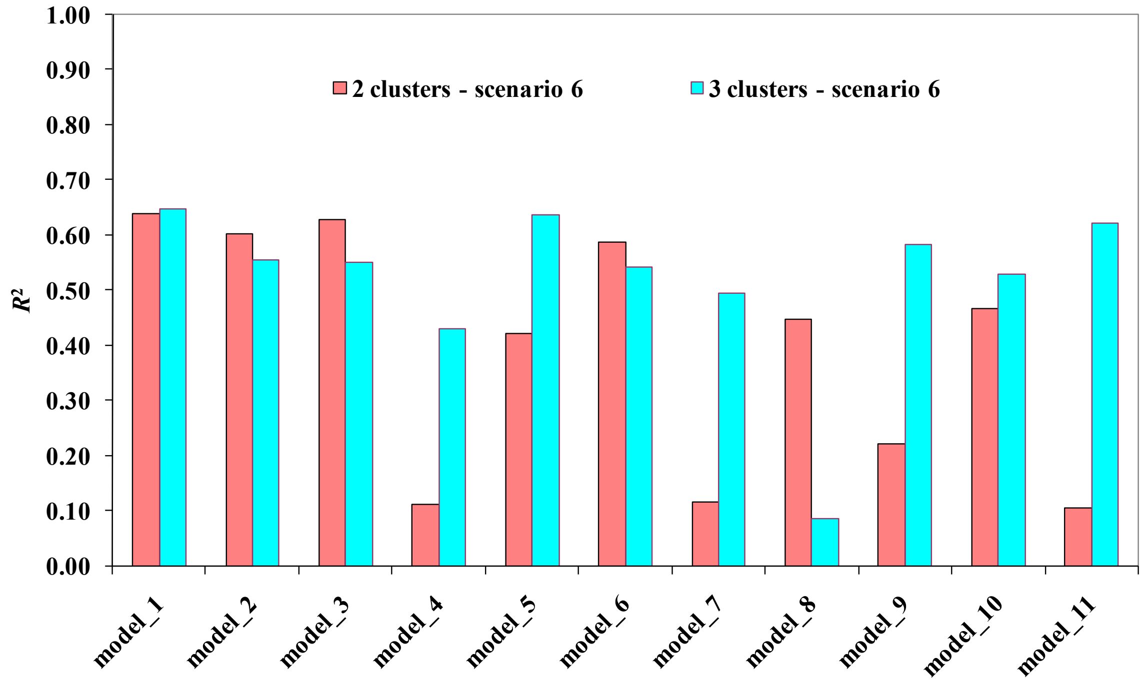

Figure 4.15. R^2 results during validation – Scenario 6.

4.10 Discussion

4.10.1 Model set up

The neuro-fuzzy national phosphorus model is expected to provide a powerful tool that can facilitate the prediction of the annual amounts of diffuse-source P from a catchment using only the catchment characteristics as inputs. Such predication is required during the design of any management plan to reduce the amount of P loss from land to water. The model has been calibrated using data from 84 catchments from different regions in Ireland. A split-sample technique was employed, in which some catchments were used to calibrate the model and the remainder to validate the calibrated model. This independent validation result was important for judging the possibility of generalising the use of the model for predictions in other catchments not included in the calibration.

Calibration of the models was performed for six different random groupings of the available catchments. The remaining catchments in each scenario were left for model validation. Using the *k*-means clustering algorithm, the catchments of each sample were clustered into two and three groups respectively. The inputs to the algorithm were the six spatial variables (PDI, RRI, GEO, GW, LU and SO) with centre vectors obtained for each cluster in the two- and three-clusters cases. In addition, standard deviation vectors were calculated for the same cases. For each of the six calibration–validation scenarios, 11 different models were formulated to determine from among the six spatial variables (PDI, RRI, GEO, GW, LU and SO) those appropriate for using as predictors to the annual orthoP concentrations. All models were run for the cases of two and three clusters or sub-models.

4.10.2 R^2 Results

Generally, the results of R^2, which were used to assess the model's performances during calibration indicated that for all models the use of three clusters is better than two clusters. This finding is expected in general since the use of three clusters or sub-models increases the number of parameters in the model and this in turn increases the degree of freedom in the model; hence, better calibration results can generally be expected. Nevertheless, the use of many parameters may not result in a good performance during validation if the model has been over-parameterised. This phenomenon occurred for most models in Scenarios 1, 2 and 5 where the results of two-clusters case were better than the three-clusters case. Note that in Scenarios 1 and 2, half of the data was used to calibrate and the other half to validate the models. In the other scenarios, 2/3 of the data was used for calibration and the remaining 1/3 of the data for validation.

Using spatial variables other than the PDI and RRI as predictors was examined by comparing the value of R^2 for model_1 with the values of the other models for the two- and three-clusters cases. The calibration results proved that there is a benefit for the model in additional spatial variables as well as PDI and RRI. However, the validation results do not always show the same trend except for few models, and this suggests that adding more variables to the PDI and RRI in a model may result in only a slight improvement. More models outperformed model_1 for both the two- and the three-clusters cases in Scenarios 3 and 4 than in the other scenarios. The variety in performance in the validation results emphasises the variability in the degree by which the spatial variables influence the processes that affect the mobilisation and transportation of P from land to water. Physically, the orthoP concentration is influenced by the six spatial variables (PDI, RRI, GEO, GW, LU and SO), and hence they should be represented in the model. However, some of these variables may not be linearly related with the orthoP, and hence their use in the linear form of the neuro-fuzzy model may degrade the results. In addition, it is worth mentioning that Daly and Mills (2006) calculated PDI and RRI from the soil map and used both variables as indicators for the hydrological and the hydro-chemical characteristics of the catchment. This indeed explains why PDI and RRI dominate the other spatial variables in their influence on the orthoP concentration.

In terms of the R^2 magnitude, for each of the six scenarios a model from the three-clusters case achieved the best value during calibration (Table 4.9). On the other hand, during validation, a model from the three-clusters case was the best in Scenarios 1, 3, 4 and 6 while a model from the two-clusters case was the best in the other scenarios (Table 4.9). To investigate the usefulness of the neuro-fuzzy national phosphorous model, the best model for each scenario was compared with a model that used same input variables and had a structure similar to the Daly and Mills (2006) model.

Table 4.9. Summary of the neuro-fuzzy national phosphorus models which achieved the best R^2 values vs the Daly and Mills model.

Scenario	Calibration				Validation			
	Neuro-fuzzy national phosphorus model			Daly and Mills model	Neuro-fuzzy national phosphorus model			Daly and Mills model
	Cluster case	Best model	R^2	R^2	Cluster case	Best model	R^2	R^2
1	3	Model_8	0.90	0.73	3	Model_4	0.38	0.32
2	3	Model_11	0.97	0.63	2	Model_3	0.65	0.50
3	3	Model_10	0.84	0.72	3	Model_9	0.60	0.38
4	3	Model_10	0.79	0.63	3	Model_8, Model_10	0.68	0.52, 0.49
5	3	Model_8, Model_10	0.87	0.41, 0.45	2	Model_3	0.76	0.66
6	3	Model_9	0.87	0.70	3	Model_1	0.65	0.56

The comparison of the models was based on the R^2 values (shown in Table 4.9). It is obvious from the table that in all scenarios none of the Daly and Mills model (2006) type was able to produce R^2 better than its correspondence in the neuro-fuzzy national phosphorus model. This observation indicates the superiority of the neuro-fuzzy national phosphorus model over the simple structure model of Daly and Mills (2006). However, Table 4.9 also shows that in all scenarios, except for Scenario 4, no single model was found to be the best during both calibration and validation.

4.10.3 Visual Assessment

To provide a visual assessment of the results, a plot of the observed annual orthoP concentration against the best estimates by the neuro-fuzzy national phosphorous model is given for three scenarios. Figures 4.16, 4.17 and 4.18 show these plots during validation for Scenarios 1, 2 and 5 respectively. The three figures illustrate a good scatter of the values around the 1:1 line, which means a reasonable matching between the observed and the estimated values. However, there is an obvious underestimation of all values larger than 0.08 mgP/l by the models.

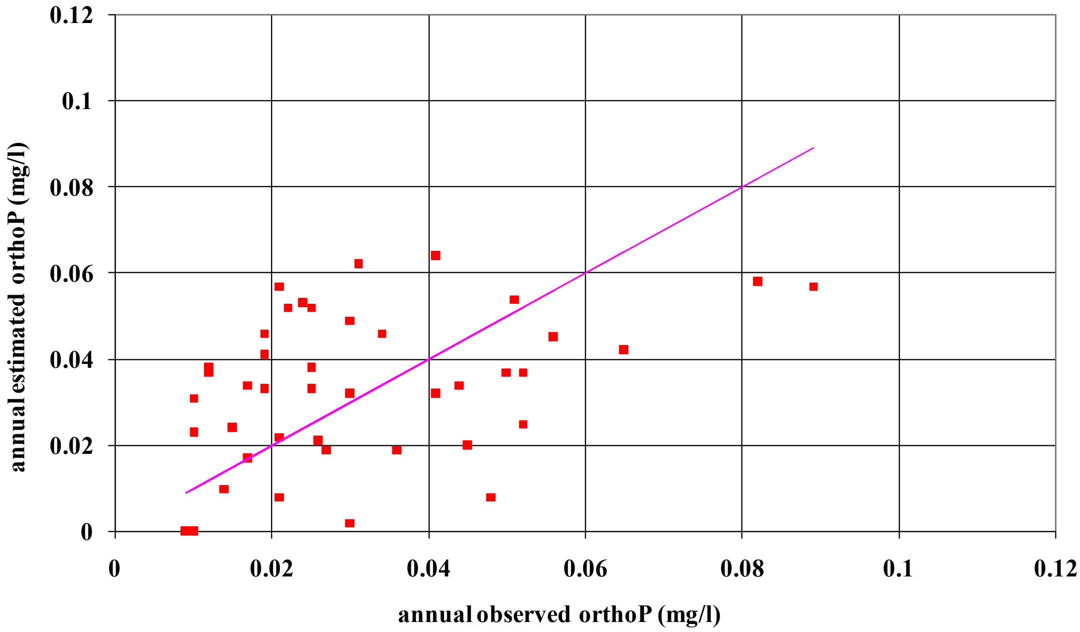

Figure 4.16. Observed vs estimated annual orthoP concentrations during validation – Scenario 1 – model_4 of the three-clusters case.

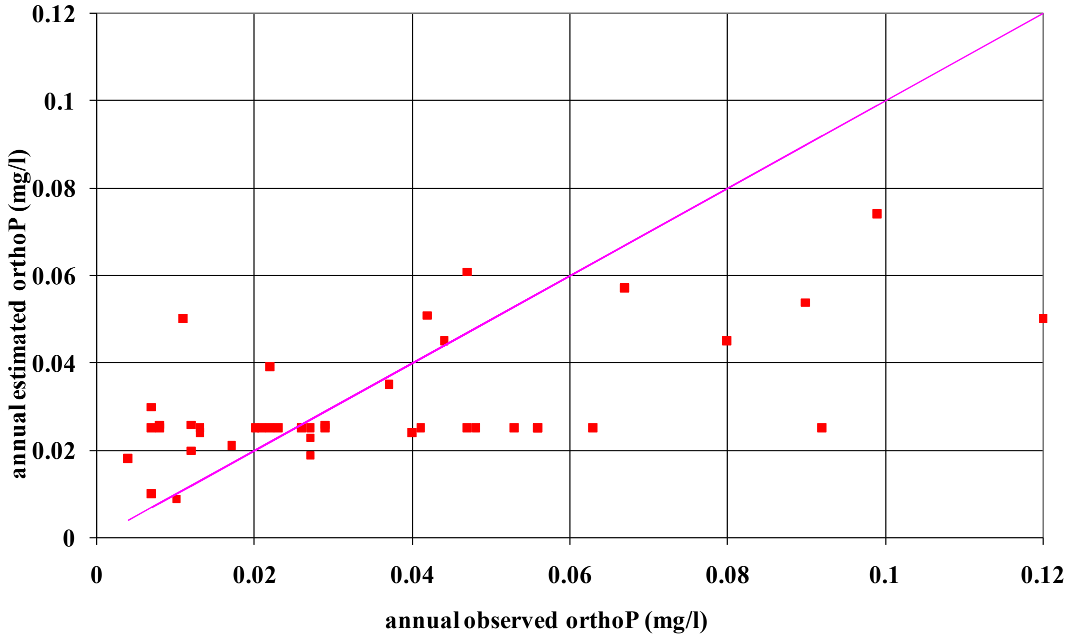

Figure 4.17. Observed vs estimated annual orthoP concentrations during validation – Scenario 2 – model_3 of the two-clusters case.

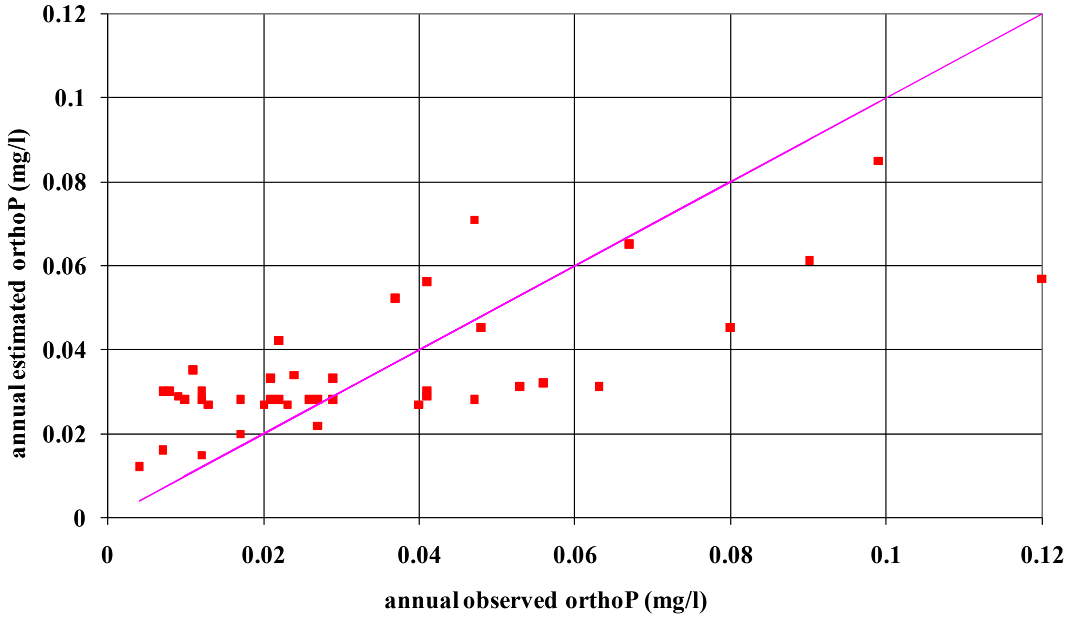

Figure 4.18. Observed vs estimated annual orthoP concentrations during validation – Scenario 5 – model_3 of the three-clusters case.

4.11 Conclusions

In the current study, the concept of fuzzy modelling was utilised to develop a national model to predict annual average orthoP concentrations using the catchment characteristics as independent variables. Data from 84 catchments from Ireland were used in testing the new model. Six different split-sample scenarios was applied to partition the data into two parts used to calibrate and validate the model. The *k*-means clustering algorithm was used to determine two and three clusters of catchments respectively. Then for each scenario and for each cluster case, 11 different models were formulated by using different input variables selected from among six spatial variables (PDI, RRI, GEO, GW, LU and SO). Generally, the results demonstrated the ability of the new modelling approach to produce good estimates to the annual average orthoP concentrations. This study has also found that the PDI and an RRI are the most important input variables to the model. Finally, the validation results confirmed that using two clusters that comprise of few spatial variables can result in the best neuro-fuzzy national P model.

5 Conclusions and Recommendations

5.1 Overview

The need for computer models as predictive tools to guide the implementation of the WFD in Ireland was the main motive behind this study. A state-of-the-art ANFIS modelling approach was employed to construct a suite of two models to simulate diffuse-source phosphorus pollution at a catchment scale. The first model – the ANFISP model – was designed to simulate continuous discharges and TP loads at a daily time step. The SMAR hydrological model was used for modelling the processes involved in the discharges simulation while the GOPC model was used for estimating the TP loads. The second model is intended to be used as a national phosphorus model (for unmonitored catchments), which estimates the average annual orthoP concentrations, and uses some catchments characteristics as sole inputs. Both models were applied in different study cases and their performance assessed.

5.2 ANFISP Model

The development of the ANFISP model was in two stages. First the performance of the model in simulating the discharges from the catchment was investigated thoroughly. The suitability of the SMAR catchment model as a component of the ANFISP model to transform the rainfall and evaporation into discharge was tested by comparing its performance against an alternative catchment model, the SLR model. Two separate variations of the model, the ANFISP_T and the ANFISP_S, were formulated to examine the ability of the model to account for the effects of the temporal and the spatial variations respectively.

In the ANFISP_T scenario, the rainfall and evaporation are treated as fuzzy numbers with a varying number of fuzzy subsets. The performance of the model was assessed for ten different cases, each with different numbers of fuzzy subsets for the rainfall and evaporation (Table 3.1) by applying it to 11 different catchments from around the world, including the Brosna catchment in Ireland (Table 3.2). Assessment of the models was based on two criteria: the Nash–Sutcliffe efficiency index (NSR^2) and the average relative errors (*ARE*) of the estimated discharge peaks over a threshold. A split-sample approach was used in which the available data in each catchment were split into two parts according to the ratio of 2:1. The first part was used to calibrate the models while the second was used in validating the model. The following conclusions emerged:

- Using more than one fuzzy subset for either or both of the rainfall and evaporation always improves the results. This improvement certainly occurs as a result of using different sub-models to address the effect of the temporal variation on the catchment behaviour. It is worth noting that the number of sub-models in each case was determined by multiplying the number of fuzzy subsets for the rainfall by the number for the evaporation.

- In all cases, the performance of the model with the SMAR catchment model was notably better than using the SLR model. Although the SLR model is a very simple model, it was used as a baseline to assess the more substantive SMAR model.

The ANFISP_S scenario was tested with data from the Brosna catchment only. In this scenario, the spatial variation in the response of this catchment was addressed through defining groups of spatial units called HHCUs. Each group represented a number of homogenous areas which were assumed to respond similarly to rainfall and evaporation and hence a separate model was used for each of them. The HHCUs were determined by using the subtractive clustering algorithm. The input variables to the algorithm included elevation, slope index, generalised land-use types and soil types, all generated from the DEM, the land-use and the soil maps of the catchment. All possible combination alternatives involving the four input variables (Table 3.3) were tested For each combination alternative, only the cases with a number of HHCUs less than 40 (chosen arbitrarily) were used to construct the models tested in this scenario. Each model comprised a number of sub-models, each representing a specific HHCU to account for the different spatial variation patterns in the catchment. The same criteria and data-splitting schemes used in the ANFISP_T scenario were also applied in the ANFISP_S scenario. The results indicated that:

- Using one HHCU is not enough to obtain a good discharge simulation. Nevertheless, using a large number of HHCUs will not always significantly improve the model performance.
- The suitability of the SMAR model for simulating the hydrological processes related to the discharge estimation is supported by the outstanding results obtained from this model compared with the results from the SLR model.

A comparison between the best results obtained from the ANFISP_T and ANFISP_S scenarios in the Brosna catchment highlighted the differences and similarities in performance in simulating discharge between the two scenarios. Therefore, because of its simplicity, the ANFISP_T scenario has been chosen to be extended for modelling diffuse phosphorus loss in the second stage of the ANFISP model application. The GOPC model has been added to the ANFISP to model the TP loads. The ability of the resulting model in simulating both the discharge and the TP loads was tested by applying it to the Oona Water catchment in Northern Ireland. The assessment in this case was based on the NSR^2 criterion alone during the calibration and validation periods. In addition to the rainfall and evaporation, the estimated amount of applied fertilisers (Nasr and Bruen, 2006) was used as an input to the model. However, only the rainfall and evaporation were assumed to be fuzzy numbers, and the performance of the models corresponding to different cases of the number of the rainfall and evaporation fuzzy subsets (Table 3.7) have been investigated. The results of these models suggested that:

- The best simulation for the discharge was achieved when using two fuzzy subsets for the rainfall and a single subset for the evaporation, whereas a combination of four rainfall subsets and three evaporation subsets was the best case for the TP loads simulation.
- The best case of the ANFISP, which resulted on the best TP loads results, was compared against the fully distributed physically based SWAT model. The comparison showed that the ANFISP performance was not significantly worse than the complex distributed SWAT model and this underpins the potential of the ANFISP model for simulating diffuse phosphorus loss.

5.3 The Neuro-Fuzzy National Phosphorus Model

The hypothesis of this model has its origin in the national phosphorus model developed by Daly and Mills (2006) where the average annual orthoP concentrations is linearly related with some catchment characteristics, and a single linear model is used to describe this relationship. Here, the ANFIS modelling approach was adapted to obtain a neuro-fuzzy national phosphorus model, which coupled a number of linear models, each of which described the relationship between the annual average orthoP concentrations and the catchment characteristics for a specific cluster of catchments. The catchments in any cluster were assumed to have a homogenous pattern of spatial data and thus should respond in a similar manner. The same 84 catchments used by Daly and Mills (2006) were employed here to test the new model. Six different split-sample scenarios were applied to partition the total number of the catchments into two parts used to calibrate and validate the model. The *k*-means clustering algorithm was used to determine two and three clusters of catchments respectively. Then for each scenario and for each clusters case, 11 different models were formulated by using different input variables selected from among six spatial variables (PDI, RRI, GEO, GW, LU and SO). The results of these models supported the following findings:

- In comparison to Daly and Mills' 2006 simple empirical model, the newly developed neuro-fuzzy national phosphorus model showed an improved capability in predicting the orthoP concentrations at a catchment level. This qualifies the neuro-fuzzy national phosphorus model for use in a wide range of applications related to implementing the WFD in Ireland.
- The PDI and an RRI were found to have the most significant influence in predicting the orthoP concentrations. Although including other spatial variables may produce a marginal improvement in the prediction, their use is important to produce a model suitable for studying the effect of these variables and through them, the effect of various catchment management options.
- The best calibration results were obtained for the models that use three clusters or sub-models and

have many spatial variables included. However, in validation the best models mostly have two clusters and few spatial variables. This demonstrates the phenomenon of model over-parameterisation, which occurs when using more parameters in the model than required to fit the data.

- The variation between the results for the six calibration–validation scenarios revealed that the performance of the model was affected directly by the random sample of catchments data selected for model calibration. Therefore, to ensure the generality of the model a more formal uncertainty analysis is recommended for future work.

5.4 Future Work

This work has shown that combinations of relative simple models as in the ANFISP_S model can extend their ability to model diffuse phosphorus loss for a range of catchment behaviour without requiring fully distributed time-varying, physically based models. While here it is shown to be useful in the Brosna catchment, it should be applied to other catchments with a wider range of climatic variation and conditions to test its generality. In addition, it should be possible to extend the approach to model other water-quality variables (e.g. nitrate), where the output at a single point is all that is required. In such cases, the effort to generate and calibrate a physically based distributed model may not be justified and a calibrated combination of simple models may suffice.

An uncertainty analysis is highly recommended for the neuro-fuzzy national phosphorus model. This will allow the determination of a set of catchments which results in the best calibration and validation. Moreover, the uncertainty analysis should include an investigation of the best way of splitting the available data into two parts used in the calibration and validation.

The key role of GIS in processing the data used in the ANFISP and the neuro-fuzzy national phosphorus models requires a smooth link between the GIS and the FORTRAN codes of the models. This can be achieved by developing a user-friendly interface for the models to be used from within the GIS. A trial version for this user-friendly interface has already been developed as part of this project. This version is still under test, and some improvements are needed in order to produce a robust version which will be released to the RBDs for free use.

The ANFIS modelling approach can be used in all investigations that compare time series or model the relationship between two time series, such as investigating teleconnections between climate variables at different locations.

References

Abbott, M.B., Bathurst, J.C., Cunge, J.A., O'Connell, P.E., and Rasmussen, J., 1986a. An introduction to the European Hydrological System – Système Hydrologique Européen, 'SHE' 1: History and philosophy of a physically-based, distributed modelling system. Journal of Hydrology 87, 45–59.

Abbott, M.B., Bathurst, J.C., Cunge, J.A., O'Connell, P.E., and Rasmussen, J., 1986b. An introduction to the European Hydrological System – Système Hydrologique Européen, 'SHE' 2: Structure of a physically-based, distributed modelling system. Journal of Hydrology 87, 61–77.

Abraham, A., 2001. Neuro-Fuzzy Systems: State-of-the-Art Modeling Techniques. In: Connectionist Models of Neurons, Learning Processes, and Artificial Intelligence, Lecture Notes in Computer Science, Ed. by: J. Mira and A. Prieto, Springer-Verlag GmbH, Germany, vol. 2084, pp. 269–276.

Ahsan, M., and O'Connor, K.M., 1994. A simple non-linear rainfall–runoff model with a variable gain factor. Journal of Hydrology 155, 151–183.

Ajami, N.K., Gupta, H., Wagener, T., and Sorooshiam, S., 2004. Calibration of a semi-distributed hydrologic model for streamflow estimation along a river system. Journal of Hydrology 298, 112–135.

Alvisi, S., Mascellani, G., Franchini, M., and Bardossy, A., 2006. Water level forecasting through fuzzy logic and artificial neural network approaches. Hydrology and Earth System Science 10, 1–17.

Arnold, J.G., Srinivasan, R., Muttiah, R.S., and Williams, J.R., 1998. Large area hydrological modelling and assessment Part I: Model development. Journal of the American Water Resources Association (JAWRA) 34(1), 73–89.

Arnold, J.G., Williams, J.R., and Maidment, D., 1995. Continuous time water and sediment – routing model for large basins. Journal of Hydraulics Engineering 121(2), 171–183.

Arnold, J.G., and Williams, J.R., 1987. Validation of SWRRB – Simulator for water resources in rural basins. Journal of Water Resources Planning and Management 113(2), 243–246.

Bazartseren, B., Hildebrandt, G., and Holz, K.-P., 2003. Short-term water level prediction using neural networks and neuro-fuzzy approach. Neurocomputing 55, 439–450.

Becker, A., and Kundzewicz, Z.W., 1987. Nonlinear flood routing with multilinear models. Water Resources Research 23(6), 1043–1048.

Behrendt, H., 1996. Inventories of point and diffuse sources and estimated nutrient loads – A comparison for different river basins in Central Europe. Water Science and Technology 3(4–5), 99–107.

Berankova, D., and Ungerman, J., 1996. Non-point sources pollution in the Morava River Basin. Water Science and Technology 33(4–5), 127–135.

Beven, K., 2000. Uniqueness of place and process representations in hydrological modeling. Hydrology and Earth System Sciences 4(2), 203–213.

Beven, K., 1993. Prophecy, reality and uncertainty in distributed hydrological modelling. Advances in Water Resources 16(1), 41–51.

Beven, K., and Binley, A.M., 1992.The future of distributed models: Model calibration and predictive uncertainty. Hydrological Processes 6, 279–298.

Bicknell, B.R., Imhoff, J.C., Donigian, A.S., and Johanson, R.C., 1997. Hydrological Simulation Program – FORTRAN (HSPF), User's Manual for release 11. Environmental Protection Agency – 600/R-97/080. United States EPA, Athens, GA., USA.

Bruen, M., and Dooge, J.C.I., 1992. Unit hydrograph estimation with multiple events and prior information: I. Theory and a computer program. Hydrological Sciences Journal 37(5), 429–443.

Bruen, M., 1985. Black box modelling of catchment behaviour. Ph.D. thesis submitted to National University of Ireland, Dublin.

Chang, F.J., and Chen, Y.C., 2001. A counterpropagation fuzzy-neural network modelling approach to real time streamflow prediction. Journal of Hydrology 245, 153–164.

Chen, J., and Adams, B.J., 2006. Integration of artificial neural networks with conceptual models in rainfall–runoff modelling. Journal of Hydrology 318, 232–249.

Chen, S.H., Lin, Y.H., Chang, L.C., and Chang, F.J., 2006. The strategy of building a flood forecast model by neuro-fuzzy network. Hydrological Processes 7, 1525–1540.

Chiu, S.L., 1994. Fuzzy model identification based on cluster estimation. Journal of Intelligent Fuzzy system 2, 267–278.

Clabby, K.J., Bradley, C., Craig, M., Daly, D., Lucey, J., McGarrigle, M., O'Boyle, S., Tierney, D., and Bowman, J., 2008. Water quality in Ireland 2004–2006. Environmental Protection Agency (EPA), PO Box 3000, Johnstown Castle Estate, County Wexford, Ireland.

CORINE (Co-ORdination of INformation on the Environment), 1989. Land Cover Project, The Nomenclature. Commission of the European Communities, Directorate-General Environment Nuclear Safety and Civil Protection, Rue de la Loi 200, B-1049 Brussels, Belgium.

Daly, K., and Mills, P., 2006. Eutrophication from agricultural sources: Relating catchment characteristics to phosphorus concentrations in Irish Rivers –Final Report. Environmental Protection, Wexford, Ireland.

Daly, K., and Coulter, B., 2000. National phosphorus model. In: Quantification of phosphorus loss from soil to water. Ed. by: H. Tunney, B. Coulter, K. Daly, I. Kurz, C. Coxon, D. Jeffrey, P. Mills, G. Kiely, and G. Morgan, Synthesis Report, R&D Report Series no. 6, EPA, Wexford, Ireland.

Davies, H., and Neal, C., 2007. Estimating nutrient concentrations from catchment characteristics across the UK. Hydrology and Earth System Sciences 11(1), 550–558.

Dixon, B., 2005. Applicability of neuro-fuzzy techniques in predicting groundwater vulnerability: a GIS-based sensitivity analysis. Journal of Hydrology 309, 17–38.

Dixon, B., 2004. Prediction of groundwater vulnerability using an integrated GIS-based neuro-fuzzy techniques. Journal of Spatial Hydrology 4(2), 1–38.

EEC (European Economic Community), 2000. The council of 23 October 2000 establishing a framework for Community action in the field of water policy (2000/60/EC). Official Journal of the European Communities, L327, 1–72.

Ewen, J., Parkin, G., and O'Connell, E., 2000. SHETRAN: Distributed basin flow and transport modelling system. Journal of Hydrologic Engineering, 5(3), 250–258.

Fortin, V., Perreault, L., and Salas, J.D., 2004. Retrospective analysis and forecasting of streamflows using a shifting level model. Journal of Hydrology 296, 135–163.

Gardiner, M.J., and Radford, T., 1980. Soil Associations of Ireland and their land use potential (Explanatory Bulletin to Soil Map of Ireland 1980). Published by An Foras Taluntais, 19 Sandymount Avenue, Dublin 4, Ireland.

Gupta, V.J., and Sorooshian, S., 1983. Uniqueness and observability of conceptual rainfall–runoff model parameters: the percolation process examined. Water Resources Research 19(1), 269–276.

Hartigan, J.A., and Wong, M.A., 1979. Algorithm AS 139: A k-means clustering algorithm. Applied Statistics 28, 100–108.

Holland, J.H., 1975. Adaptation in natural and artificial systems. University Michigan Press, Ann Arbor.

Ganoulis, J.G., 1994. Engineering risk analysis of water pollution: Probabilities and fuzzy sets. VCH Verlagsgesellschaft mbH, Weinheim (Germany) and VCH Publishers Inc. (USA).

Gustafson, D., and Kessel, W., 1979. Fuzzy clustering with a fuzzy covariance matrix. Proceedings of the IEEE CDC, San Diego, CA, USA, pp. 761–766.

Haberlandt, U., Krysanova, V., and Bardossy, A., 2002. Assessment of nitrogen leaching from arable land in large river basins: Part II. Regionalisation using fuzzy rule based modelling. Ecological Modelling 150, 277–294.

Irvine, K., Mills, P., Bruen, M., Walley, W., Hartnett, M., Black, A., Tynan, S., Duck, R., Bragg, O., Rowen, J., Wilson, J., Johnston, P., and O'Toole, C., 2005. Water Framework Directive: An assessment of mathematical modelling in its implementation in Ireland – Final Report. EPA, Wexford, Ireland.

Jacquin, A.P., and Shamseldin, A.Y., 2006. Development of rainfall–runoff models using Takagi–Sugeno fuzzy inference systems. Journal of Hydrology 329, 154–173.

Jang, J.S.R., 1993. ANFIS architecture. In: Neuro-fuzzy and Soft Computing, Ed. by: J.S.R. Jang, C.-T. Sun, and E. Mizutani, Prentice Hall, New Jersey.

Jantzen, J., 1998. Neuro-fuzzy modelling. Tech. report no 98-H-874 (nfmod), Department of Automation, Technical University of Denmark, Denmark.

Kachroo, R.K., and Natale, L., 1992. Non-linear modelling of the rainfall–runoff transformation. Journal of Hydrology 133, 341–369.

Kaufmann, A., and Gupta, M.M., 1991. Introduction to fuzzy arithmetic: Theory and applications. Van Nostrand Reinhaold, New York, USA.

Khan, H., 1986. Conceptual modelling of rainfall–runoff systems, Unpublished Master thesis submitted to the Department of Engineering Hydrology, National University of Ireland, Galway.

KMMP (Kirk McClure Morton and EG Pettits), 2001. Lough Leane Catchment Monitoring and Management System: Final Report. Kirk McClure Morton, Consulting Engineers, Dublin, Ireland.

Krysanova, V., Muller-Wohlfeil, D.-I., and Becker, A., 1998. Development and test of a spatially distributed hydrological/water quality model for mesoscale watersheds. Ecological Modelling 106 (1–2), 261–289.

Lek, S., Guiresse, M., and Giraudel, J., 1999. Predicting stream nitrogen concentration from watershed features using neural networks. Water Research 33(16), 3469–3478.

Liang, G.C., 1992. A note on the revised SMAR model. Memorandum to the River Flow Forecasting Workshop Group, Department of Engineering Hydrology, National University of Ireland, Galway. (Unpublished).

Lindenschmidt, K.-E., Hattermann, F., Mohaupt, V., Merz, B., Kundzewicz, Z.W., and Bronstert, A., 2007. Large-scale hydrological modelling and the Water Framework Directive and Floods Directive of the European Union – 10th Workshop on Large-Scale Hydrological Modelling. Advances in Geosciences 11, 1–6.

Lucey, J., 2009. Water quality in Ireland 2007 – 2008 - Key Indicators of the Aquatic Environment. EPA, Wexford, Ireland.

Mainstone, C.P., and Parr, W., 2002. Phosphorus in rivers: Ecology and management. The Science of the Total Environment, 282–283, 25–47.

Mamdani, E.H., and Assilian, S., 1975. An experimental in linguistic synthesis with a fuzzy logic controller. International Journal of Man-Machine Studies 7(1), 299–321.

Marce, R., Comerma, M., Garcia, J.C., and Armengol, J., 2004. A neuro-fuzzy modelling tool to estimate fluvial nutrients loads in watershed under time-varying human impact. Limnology and Oceanography: Methods 2, 342–255.

Marechal, D., and Holman, I.P., 2005. Development and application of a soil classification-based conceptual catchment-scale hydrological model. Journal of Hydrology 312, 277–293.

McGuckin, S.O., Jordan, C., and Smith, R.V., 1999. Deriving phosphorus export coefficients for CORINE land cover types. Water Science and Technology 39(12), 47–53.

McIntyre, N.R., and Wheater, H.S., 2004. Calibration of an in-river phosphorus model: prior evaluation of data needs and model uncertainty. Journal of Hydrology 290, 100–116.

MCOS (M.C. O'Sullivan and Company Ltd.), 2002. Three Rivers Project: Final Report. Consulting Engineers, Dublin, Ireland.

Meynendonckx, J., Heuvelmans, G., Muys, B., and Feyen, J., 2006. Effects of watershed and riparian zone characteristics on nutrient concentrations in the River Scheldt Basin. Hydrology and Earth System Sciences 10, 913–922.

Mizagalewics, P.J., 1996. Modelling agrichemical transport in Midwest Rivers using geographic information systems. PhD thesis submitted to the Faculty of the Graduate School of the University of Texas at Austin, USA.

Nash, J.E., and Foley, J.J., 1982. Linear models of rainfall–runoff systems. In: Rainfall runoff relationship, Proceedings of the International Symposium on Rainfall–runoff modelling, Ed. by V.P. Singh, Mississippi State University, Water Resources Publications, USA, pp. 51–66.

Nash, J.E., and Sutcliffe, J.V., 1970. River flow forecasting through conceptual models. Part 1. A discussion of principles. Journal Hydrology 10, 282–290.

Nash, J.E., 1957. The form of the instantaneous unit hydrograph. IHAS Publication 45(3), 114–118.

Nasr, A., and Bruen, M., 2006. Eutrophication from agricultural sources: A comparison of SWAT, HSP and SHETRAN/GOPC phosphorus models for three Irish catchments – Final Report. EPA, Wexford, Ireland.

Nasr, A., Taskinein, A., and Bruen, M., 2005. Developing an independent, generic, phosphorus modelling component for use with grid-oriented, physically based distributed catchment models. Water Science and Technology 51(3–4), 135–142.

Nasr, A., 2004. Modelling of phosphorus loss from land to water: a comparison of SWAT, HSPF and SHETRAN/GOPC for three Irish catchments. PhD thesis submitted to the Department of Civil Engineering, University College Dublin, Ireland.

Nauck, U., and Kruze, R., 1999. Design and implementation of a neuro-fuzzy data analysis tool in JAVA: User's Manual. Technical University of Braunschweig, Germany.

Nayak, P.C., Sudheer, K.P., Rangan, D.M., and Ramasastri, K.S., 2004. A neuro-fuzzy computing technique for modelling hydrological time series. Journal of Hydrology 291, 52–66.

Neitsch, S.L., Arnold, J.G., Kiniry, J.R., and Williams, J.R., 2001. Soil and Water Assessment Tool User's Manual – version 2000. Grassland, Soil and Water Research Laboratory, Agricultural Research Service, 808 East Blackland Road, Temple, Texas 76502. Blackland Research Centre, Texas Agricultural Experiment Station, 702 East Blackland Road, Temple, Texas 76502.

Norton, M.M., and Fisher, T.R., 2000. The effect of forest on stream water quality in two coastal plain watersheds of the Chesapeake Bay. Ecological Engineering 14, 337–362.

O'Connell, P.E., Nash, J.E., and Farrell, J.P., 1970. River flow forecasting through conceptual models: Part 1. A discussion principles. Journal of Hydrology 10, 282–290.

Ozelkan, E.C., and Duckstein, L., 2001. Fuzzy conceptual rainfall–runoff model. Journal of Hydrology 253, 41–68.

Pekarova, P., and Pekar, J., 1996. The impact of land use on stream water quality in Slovakia. Journal of Hydrology 180, 333-350.

Quiroga, C.A., Singh, V.P., and Lam, N., 1996. Land-use hydrology. In: Geographical Information Systems in Hydrology, Ed. by: V.P. Singh, and M. Fiorentino, Kluwer Academic Publishers, The Netherlands, pp. 389–414.

Reis Jr., D.S., and Stedinger, J.R., 2005. Bayesian MCMC flood frequency analysis with historical information. Journal of Hydrology 313, 97–116.

Saloranta, T.M., Kamari, J., Rekolainen, S., and Malve, O., 2003. Benchmark Criteria: A tool for selecting appropriate models in the field of water management. Environmental Management 32(3), 322–33.

Scholten, H., van Waveren, R.H., Groot, S., van Geer, F.C., Wosten, J.H.M., Koeze, R.D., and Noort, J.J., 2000. Good modelling practice in water management. Paper presented in HydroInformatics 2000, Cedar Rapids, IA, USA.

Schulz, K., and Huwe, B., 1997. Water flow modelling in the unsaturated zone with imprecise parameters using a fuzzy approach. Journal of Hydrology 201, 211–229.

See, L., and Abrahart, R.J., 2001. Multi-model data fusion for hydrological forecasting. Computers and Geosciences 27, 987–994.

Shamseldin, A.Y., O'Conner, K.M., and Liang, G.C., 1997. Methods for combining the outputs of different rainfall–runoff models. Journal of Hydrology 197, 203–229.

Shamseldin, A.Y., and O'Connor, K.M., 1996. A nearest neighbour linear perturbation model for river flow forecasting. Journal of Hydrology 179, 353–375.

Sriti, M., Thibaud, R., and Claramunt, C., 2005. A fuzzy identity-based temporal GIS for the analysis of geomorphometry changes. In: Semantic-based geographical information systems, Lecture Notes in Computer Science, Ed. by: S. Saccapietra and E. Zimanyi, Journal of Data Semantic 3, Springer-Verlag GmbH, Germany, vol. 3534, pp. 81–99.

Su, B., Kazama, S., Katayama, S., and Sawamoto, M., 2006. Influence of catchment characteristics on nitrogen concentration in largely forested streams during the base flow period. Hydrological Processes 20, 4391–4403.

Takagi, T., and Sugeno, M., 1985. Fuzzy identification systems and its application to modelling and control. IEEE Transactions on Systems, Man, and Cybernetics 15, 116–132.

Tan, B.Q., and O'Connor, K.M., 1996. Application of an empirical infiltration equation in the SMAR conceptual model. Journal of Hydrology 185, 275–295.

Todini, E., and Wallis, J.R., 1977. Using CLS for daily or longer period rainfall–runoff modelling. In Mathematical models for surface water hydrology. (Proceedings of the 1974 Workshop held at the IBM Centre, Pisa, Italy): Ed. by: T.A. Ciriani, U. Maione, and J.R. Wallis, John Wiley & Sons, London, pp. 149–168.

Vernieuwe, H., Georgieva, O., De Baets, B., Pauwels, V.R.N., Verhoest, N.E.C., and De Troch, F.P., 2005. Comparison of data-driven Takagi–Sugeno models of rainfall-discharge dynamics. Journal of Hydrology 302,173–186.

Viney, N.R., Sivapalan, M., and Deeley, D., 2000. A conceptual model of nutrient mobilisation and transport applicable at large catchment scales. Journal of Hydrology, 240, 23–44.

Wade, A.J., Whitehead, P.G., and Butterfield, D., 2002. The integrated catchments model of phosphorus dynamics (INCA-P), a new approach for multiple source assessment in heterogeneous river systems: model structure and equations. Hydrology and Earth System Science 6(3), 583–606.

Wagener, T., and Wheater, H.S., 2002. A generic framework for the identification of parsimonious rainfall–runoff models. In: Integrated assessment and decision support, proceedings of the first Biennial Meeting of the International Environmental Modelling and Software Society, Ed. by: A.E. Rizzoli, and A.J. Jakeman, vol. 1, pp. 434–439.

Williams, J.R., Nicks, A.D., and Arnold, J.G., 1985. Simulator for water resources in rural basins. Journal of Hydraulic Engineering (ASCE) 111(6), 970–986.

Xiong, L., Shamseldin A.Y., and O'Connor, K.M., 2001. A non-linear combination of the forecasts of rainfall–runoff models by the first-order Takagi–Sugeno fuzzy system. Journal of Hydrology 245, 196–217.

Yu, P.-S., and Yang, T.-C., 2000. Fuzzy multi-objective function for rainfall–runoff model calibration. Journal of Hydrology 238, 1–14.

Zadeh, L.A., 1965. Fuzzy sets. Information and Control 8, 338–353.

Zhang, X., and Lindstorm, G., 1997. Development of an automatic calibration scheme of the HBV model. Hydrological Processes 11, 1671–1682.

Zimmermann, H.J., 1985. Fuzzy set theory and its application. Martinus Njhoff, Dordrecht, 363 pp.

Acronyms and Annotations

ANFIS	Adaptive neuro-fuzzy inference system
ANFISP	Adaptive neuro-fuzzy inference system phosphorus [model]
ANN	Artificial neural network [model]
ARMA	Auto-regressive moving average [model]
ARE	Average relative error
DEM	Digital elevation model
DP	Dissolved phosphorus
DSPIR	Drivers, Pressures, State, Impact and Response [conceptual framework]
EU	European Union
EPA	Environmental Protection Agency
FIS	Fuzzy inference system
FL	Fuzzy logic
GA	Genetic algorithm
GEO	Geology
GIS	Geographic information system
GOPC	Grid Oriented Phosphorus Component [Model]
GW	Groundwater
HBV	Hydrologiska Byråns Vattenbalansavdelning [model]
HHCU	Homogenous hydrologic characteristics unit
HRU	Hydrologic response unit
HSPF	Hydrological simulation programme – FORTRAN [model]
INCA-P	Integrated catchment model – phosphorus [model]
LASCAM	Large scale catchment model
LU	Land use
MCMM	Markov chain Monte Carlo [method]
MUSLE	Modified universal soil loss equation [model]
NF	Neuro-fuzzy
NSR^2	Nash–Sutcliffe index
P	Phosphorus
PDI	Phosphorus desorption index
RBD	River basin district
ROTO	Routing outputs to the outlet [model]

RR	Reject ratio
RRI	Runoff risk index
SCA	Subtractive clustering algorithm
SLR	Simple linear reservoir [model]
SMAR	Soil moisture accounting and routing [model]
SO	Soil
SWAT	Soil water and assessment tool [model]
SWIM	Soil and water integrated model
SWRRB	Simulator for water resources in rural basins [model]
TP	Total phosphorus
WFD	Water Framework Directive

Appendix: Published Papers or in Preparation

Nasr, A., and Bruen, M., 2008. Development of neuro-fuzzy models to account for temporal and spatial variations in a lumped rainfall–runoff model. Journal of Hydrology 349, 277–290.

Nasr, A., and Bruen, M., 2007. Coupling system model with fuzzy logic rules for use in runoff and total phosphorus load prediction in a catchment. Proc. of the 7th International Water Association Symposium on Systems Analysis and Integrated Assessment in Water Management (May 7–9, 2007), Washington DC – USA.

Bruen, M., and Nasr, A., 2006. Multi-criteria and Decision Support Systems in support of the Water Framework Directive. Proc. of the 3rd Harmoni-CA Forum and Conference, 5–7 April 2006, Osnabrück, Germany.

Nasr, A., Bruen, M., and Daly, K. Derivation of neuro-fuzzy national phosphorus export model using 84 Irish catchments. (Under preparation).

An Ghníomhaireacht um Chaomhnú Comhshaoil

Is í an Gníomhaireacht um Chaomhnú Comhshaoil (EPA) comhlachta reachtúil a chosnaíonn an comhshaol do mhuintir na tíre go léir. Rialaímid agus déanaimid maoirsiú ar ghníomhaíochtaí a d'fhéadfadh truailliú a chruthú murach sin. Cinntímid go bhfuil eolas cruinn ann ar threochtaí comhshaoil ionas go nglactar aon chéim is gá. Is iad na príomh-nithe a bhfuilimid gníomhach leo ná comhshaol na hÉireann a chosaint agus cinntiú go bhfuil forbairt inbhuanaithe.

Is comhlacht poiblí neamhspleách í an Ghníomhaireacht um Chaomhnú Comhshaoil (EPA) a bunaíodh i mí Iúil 1993 faoin Acht fán nGníomhaireacht um Chaomhnú Comhshaoil 1992. Ó thaobh an Rialtais, is í an Roinn Comhshaoil agus Rialtais Áitiúil a dhéanann urraíocht uirthi.

ÁR bhFREAGRACHTAÍ

CEADÚNÚ

Bíonn ceadúnais á n-eisiúint againn i gcomhair na nithe seo a leanas chun a chinntiú nach mbíonn astuithe uathu ag cur sláinte an phobail ná an comhshaol i mbaol:

- áiseanna dramhaíola (m.sh., líonadh talún, loisceoirí, stáisiúin aistrithe dramhaíola);
- gníomhaíochtaí tionsclaíocha ar scála mór (m.sh., déantúsaíocht cógaisíochta, déantúsaíocht stroighne, stáisiúin chumhachta);
- diantalmhaíocht;
- úsáid faoi shrian agus scaoileadh smachtaithe Orgánach Géinathraithe (GMO);
- mór-áiseanna stórais peitreail.
- Scardadh dramhuisce

FEIDHMIÚ COMHSHAOIL NÁISIÚNTA

- Stiúradh os cionn 2,000 iniúchadh agus cigireacht de áiseanna a fuair ceadúnas ón nGníomhaireacht gach bliain.
- Maoirsiú freagrachtaí cosanta comhshaoil údarás áitiúla thar sé earnáil - aer, fuaim, dramhaíl, dramhuisce agus caighdeán uisce.
- Obair le húdaráis áitiúla agus leis na Gardaí chun stop a chur le gníomhaíocht mhídhleathach dramhaíola trí comhordú a dhéanamh ar líonra forfheidhmithe náisiúnta, díriú isteach ar chiontóirí, stiúradh fiosrúcháin agus maoirsiú leigheas na bhfadhbanna.
- An dlí a chur orthu siúd a bhriseann dlí comhshaoil agus a dhéanann dochar don chomhshaol mar thoradh ar a ngníomhaíochtaí.

MONATÓIREACHT, ANAILÍS AGUS TUAIRISCIÚ AR AN GCOMHSHAOL

- Monatóireacht ar chaighdeán aeir agus caighdeáin aibhneacha, locha, uiscí taoide agus uiscí talaimh; leibhéil agus sruth aibhneacha a thomhas.
- Tuairisciú neamhspleách chun cabhrú le rialtais náisiúnta agus áitiúla cinntí a dhéanamh.

RIALÚ ASTUITHE GÁIS CEAPTHA TEASA NA HÉIREANN

- Cainníochtú astuithe gáis ceaptha teasa na hÉireann i gcomhthéacs ár dtiomantas Kyoto.
- Cur i bhfeidhm na Treorach um Thrádáil Astuithe, a bhfuil baint aige le hos cionn 100 cuideachta atá ina mór-ghineadóirí dé-ocsaíd charbóin in Éirinn.

TAIGHDE AGUS FORBAIRT COMHSHAOIL

- Taighde ar shaincheisteanna comhshaoil a chomhordú (cosúil le caighdéan aeir agus uisce, athrú aeráide, bithéagsúlacht, teicneolaíochtaí comhshaoil).

MEASÚNÚ STRAITÉISEACH COMHSHAOIL

- Ag déanamh measúnú ar thionchar phleananna agus chláracha ar chomhshaol na hÉireann (cosúil le pleananna bainistíochta dramhaíola agus forbartha).

PLEANÁIL, OIDEACHAS AGUS TREOIR CHOMHSHAOIL

- Treoir a thabhairt don phobal agus do thionscal ar cheisteanna comhshaoil éagsúla (m.sh., iarratais ar cheadúnais, seachaint dramhaíola agus rialacháin chomhshaoil).
- Eolas níos fearr ar an gcomhshaol a scaipeadh (trí cláracha teilifíse comhshaoil agus pacáistí acmhainne do bhunscoileanna agus do mheánscoileanna).

BAINISTÍOCHT DRAMHAÍOLA FHORGHNÍOMHACH

- Cur chun cinn seachaint agus laghdú dramhaíola trí chomhordú An Chláir Náisiúnta um Chosc Dramhaíola, lena n-áirítear cur i bhfeidhm na dTionscnamh Freagrachta Táirgeoirí.
- Cur i bhfeidhm Rialachán ar nós na treoracha maidir le Trealamh Leictreach agus Leictreonach Caite agus le Srianadh Substaintí Guaiseacha agus substaintí a dhéanann ídiú ar an gcrios ózóin.
- Plean Náisiúnta Bainistíochta um Dramhaíl Ghuaiseach a fhorbairt chun dramhaíl ghuaiseach a sheachaint agus a bhainistiú.

STRUCHTÚR NA GNÍOMHAIREACHTA

Bunaíodh an Ghníomhaireacht i 1993 chun comhshaol na hÉireann a chosaint. Tá an eagraíocht á bhainistiú ag Bord lánaimseartha, ar a bhfuil Príomhstiúrthóir agus ceithre Stiúrthóir.

Tá obair na Gníomhaireachta ar siúl trí ceithre Oifig:

- An Oifig Aeráide, Ceadúnaithe agus Úsáide Acmhainní
- An Oifig um Fhorfheidhmiúchán Comhshaoil
- An Oifig um Measúnacht Comhshaoil
- An Oifig Cumarsáide agus Seirbhísí Corparáide

Tá Coiste Comhairleach ag an nGníomhaireacht le cabhrú léi. Tá dáréag ball air agus tagann siad le chéile cúpla uair in aghaidh na bliana le plé a dhéanamh ar cheisteanna ar ábhar imní iad agus le comhairle a thabhairt don Bhord.

National Development Plan 2007 - 2013

The EPA's Environmental Research Centre (ERC) was established as a centre of excellence under the National Development Plan (NDP) to build capacity in environmental data handling, modelling, assessment and guidance. The objective of the ERC is to allow for a more structured approach to environmental research, through the development of advanced innovative techniques and systems to address priority environmental issues and thereby support environmentally sustainable development.

Environmental Protection Agency
An Ghníomhaireacht um Chaomhnú Comhshaoil

ENVIRONMENTAL PROTECTION AGENCY
PO Box 3000, Johnstown Castle Estate, Co. Wexford, Ireland
t 053 916 0600 f 053 916 0699
LoCall 1890 33 55 99
e info@epa.ie w http://www.epa.ie

SSTI Strategy for Science, Technology and Innovation

Comhshaol, Oidhreacht agus Rialtas Áitiúil
Environment, Heritage and Local Government